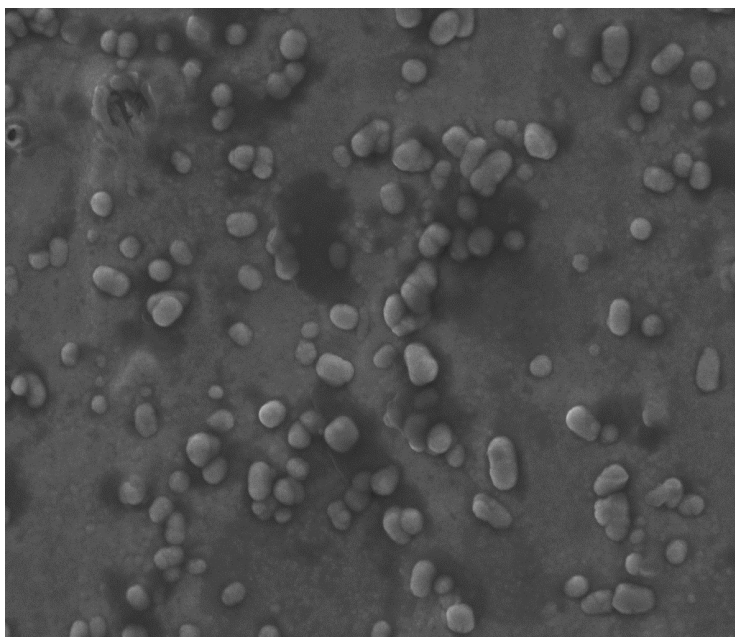
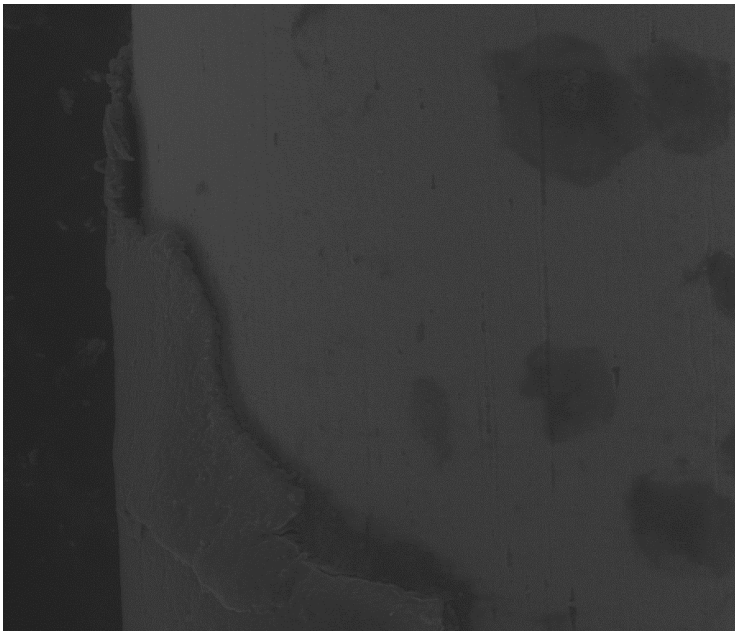


2011-
2014

Aesthetic orthodontic archwires:
Progress in their knowledge



Roberto Rongo

SCHOOL OF DOCTORAL
PROGRAMS IN CLINICAL
AND EXPERIMENTAL
MEDICINE

PhD in Oral Sciences

UNIVERSITA' DEGLI STUDI DI NAPOLI
FEDERICO II



Dipartimento di Neuroscienze e Scienze Riproduttive
ed Odontostomatologiche

SCUOLA DI DOTTORATO IN MEDICINA
CLINICA E SPERIMENTALE

Dottorato di Ricerca in Scienze
Odontostomatologiche

Coordinatore: Prof. Sandro Rengo

TESI DI DOTTORATO IN ORTODONZIA

**Aesthetic orthodontic archwires:
Progress in their knowledge**

RELATORE

Chiar.mo Prof.
Roberto Martina

CANDIDATO

Dott. Roberto Rongo

ANNI ACCADEMICI 2011-2014

Promotor:

Prof. Roberto Martina

Copromotors:

Prof. Rosa Valletta

Prof. Ambrosina Michelotti

Dr. Vincenzo D'Antò

Dr. Gianluca Ametrano

Eng. Antonio Gloria

Department of Neurosciences, Reproductive Sciences and Oral Sciences, Section of Orthodontics and Temporomandibular Disorders, University of Naples “Federico II”, Italy

Department of Material and Production Engineering, University of Naples “Federico II”, Italy

This thesis was the result of a PhD program attended at the Department of Neurosciences, Reproductive Sciences and Oral Sciences, Section of Orthodontics and Temporomandibular Disorders, University of Naples “Federico II”.

The studies included in this thesis are part of articles published or submitted for publication, and are covered by copyrights.

Ciò che sappiamo è una goccia, ciò che ignoriamo è un oceano

Isaac Newton (1643-1727)

Abstract

Introduction: In orthodontics, is quickly increasing the demand for treatments with a very low aesthetic impact in the social life. More and more adult patients want satisfy their necessity to have a beautiful smile, with “invisible” appliances. Numerous are the opportunities to perform an aesthetic orthodontic treatment such as lingual orthodontics, clear aligners or clear labial orthodontics. Aesthetic orthodontic archwires are a component of clear labial orthodontics together with aesthetic brackets, but unlike the latter, they have not been extensively studied in literature. Hence the aim of this thesis was to understand more the physical and mechanical properties of the aesthetic orthodontic archwires.

Materials and Methods: a literature review was done to collect information on this field. By means of an Atomic Force Microscope (AFM), the surface roughness of 8 aesthetic and metallic orthodontic archwires was assessed to verify the effect of the surface treatments on the wires' roughness. Four nickel-titanium (NiTi) wires (Sentalloy, Sentalloy High Aesthetic, Titanium Memory ThermaTi Lite, and Titanium Memory Esthetic), three β -titanium (β -Ti) wires (TMA, Colored TMA, and Beta Titanium), and one stainless steel (SS) wire (Stainless Steel) were considered for this study. Successively, a retrieved analysis of NiTi aesthetic archwires was done to evaluate the effect of the clinical use on the mechanical and physical properties of these wires, by means of AFM, Scanning Electron Microscope and Universal Testing Machine Instron. Five NiTi wires were considered for this study (Sentalloy, Sentalloy High Aesthetic, Superelastic Titanium Memory Wire, Esthetic Superelastic Titanium Memory Wire, and EverWhite).

Results: The first experimental study highlights how the surface roughness of the wire was affected by the surface treatment but in different way according to the

alloys and the technique. Coated NiTi wires were less rough than metallic and ion implanted wires, while β -Ti ion implanted wires were less rough of normal wire. The AFM was a useful tool to assess surface roughness. The second experimental study showed that the clinical use and the oral cavity altered the physical and mechanical properties of the wires, especially for the aesthetic archwires that worsened considerably. After clinical use at AFM, surface roughness increased significantly. The SEM images showed homogeneity for the as-received control wires; however, after clinical use aesthetic wires exhibited a heterogeneous surface with craters and bumps. All the wires, except Sentalloy, showed a statistically significant increase in friction between the as-received and retrieved wires.

Conclusion: Aesthetic orthodontic archwires are improving their properties since their introduction in orthodontics but still they do not have the same physical and mechanical properties of the metallic archwires.

Table of Contents

Overview	1
Chapter I: Aesthetic Orthodontic Archwires	3
I.1 Archwires Alloys	4
I.1.1 Stainless Steel Alloys (SS)	4
I.1.2 Cobalt-Chromium Alloys (Co-Cr)	6
I.1.3 Nickel-Titanium Alloys (NiTi)	7
I.1.4 Beta-Titanium (β -Ti)	11
I.2 Aesthetic Archwires Characteristics	12
I.2.1 Ion Implantation	14
I.2.2 Surface Coating	16
I.2.2.i PTFE	16
I.2.2.ii Epoxy-resin	17
I.2.3 Composite Archwires	18
I.3 Aesthetic Archwires: Literature Review	19
Chapter II: Relationship between Surface Roughness and Friction	31
II.1 Surface Roughness	31
II.2 Friction	36
II.2.1 Sliding Resistance in Orthodontics	41
Chapter III: Experimental Tools and Techniques	47
III.1 Atomic Force Microscope (AFM)	47
III.1.1 Working Principle	49
III.1.2 Methods of Use	51
III.1.2.i Contact mode	51
III.1.2.ii Non-contact mode	52
III.1.2.iii Tapping mode	53
III.2 Scanning Electron Microscope (SEM)	54
III.1.1 Working Principle	55
III.3 Universal Testing Machine Instron	58
III.3.1 Working Principle	60
III.4 Retrieval Analysis	61

Chapter IV: Evaluation of Surface Roughness of Orthodontic Wires by means of Atomic Force Microscopy	62
IV.1 Abstract	62
IV.2 Introduction	64
IV.3 Materials and Methods	67
IV.4 Results	68
IV.5 Discussion	73
IV.6 Conclusions	76
Chapter V: Effects of Intraoral Aging on Surface Properties of Coated Nickel-Titanium Archwires	77
V.1 Abstract	77
V.2 Introduction	79
V.3 Materials and Methods	81
V.4 Results	88
V.5 Discussion	101
V.6 Conclusions	105
Chapter VI: General Conclusions	106
References	108
Curriculum Vitae	119

List of Figures

Figure I.1: Shape Memory Effect. If mechanical load is applied to the material in the state of twinned martensite (at low temperature) it is possible to detwin the martensite. Upon releasing of the load, the material remains deformed. A subsequent heating of the material to a temperature above A_0f will result in reverse phase transformation (martensite to austenite) and will lead to complete shape recovery 8

Figure I.2: Stress-Strain curve pseudo elastic NiTi: this curve stress-strain shows the superelasticity, due to the transformation from the austenite phase to the martensite by the action of a stress. The distance AB represents the elastic deformation of the austenitic phase. The point B corresponds to the stress required to induce the transformation to the martensitic phase. At point C the transformation is complete. When the conversion is completed, the martensitic structure continues to deform in an elastic way if stressed, as is represented by the segment CD (orthodontic arches are almost never stressed up to this point). In point D reaches the yield strength of the martensitic form and the material begins to deform plastically until rupture occurs at point E. If the sollicitation is suspended before reaching the point D (as in point C' in the diagram), the elastic curve of discharge takes place along the line C'-F. At this point begins the reverse transformation to austenite, which continues to point G, where the austenitic structure is completely restored. GH represents the discharge curve of the austenitic phase. A small portion of the overall stress is not recovered because of the irreversible changes that occur during the loading and unloading. 9

Figure I.3: Example of aesthetic orthodontic wires on ceramic brackets. 13

Figure II.1: Surface roughness. 32

Figure II.2: Average Roughness. 32

Figure II.3: Friction force. F_p weight force; F_{\perp} perpendicular component of F_p ; $F_{//}$ parallel component of F_p ; F_r friction. 37

Figure II.4: Binding. 43

Figure II.5: Notching pattern (Articolo et al., 2000). 45

Figure III.1: SPM family tree. 47

Figure III.2: Atomic force microscope (AFM) diagram of operation: The AFM consists of a cantilever, the end of which is fitted with a tip, typically composed of silicon or silicon nitride, which has a radius of curvature on the order of nanometers. Attraction and repulsion forces between the tip and the sample depend on Van der Waals forces, which cause a deflection of the cantilever (the elastic constant of which is known), in accordance with Hooke's Law. The deflection is measured using a laser light reflected from the top of the micro-lever, which will be detected by a four-quadrant photodiode. A feedback loop adjusts the distance between the tip and the sample in order to keep the force acting between them constant, which in turn allows for perfect scanning of all the surface asperities. The sample is placed on a piezo-electric tube that can move it perpendicularly (z direction) to maintain a constant force in the plane (x and y directions) to analyze the surface. The resulting map (x, y) represents the topography of the surface sample.

48

Figure III.3: SEM layout. The SEM uses a beam of high energy electrons generated by an electron gun, processed by magnetic lenses, focused at the specimen surface and systematically scanned (rastered) across the surface of a specimen. Unlike the light in a light microscope (LM), the electrons in a scanning electron microscope (SEM) never form a real image of the sample. The SEM image is in the form of a serial data stream i.e. it is an electronic image. It is a result of the beam probe illuminating the sample one point at a time in a rectangular scanning pattern (raster), with the strength of the signal generated from each point being a reflection of differences (e.g. topographical or compositional) in the sample. The screen is scanned in synchrony with the beam on the specimen in a one-to-one relationship between points on the specimen and points on the image viewing screen i.e. a point-by-point translation. Increased magnification is produced by decreasing the size of the area scanned.

55

Figure III.4: UTM Instron. The specimen is fixed in special clamps for tensile testing, or is placed on plates for compression tests. Special devices are available for individual applications, such as bending tests and peel. If you require strain measurement, an optional extensometer is attached to the specimen.

59

Figure IV.1: Representative three-dimensional AFM topography images (15x15 μm) of the eight samples of orthodontic archwires: Stainless Steel (A), Beta-Titanium (B), Titanium Memory Esthetic (C), Titanium Memory ThermoTi Lite (D), Sentalloy High Aesthetic (E), Sentalloy (F), TMA (G), and Colored TMA (H).

69

Figure IV.2: Representative AFM topography images (15x15 μm) of the eight samples of orthodontic archwires: Stainless Steel (A), Beta- Titanium (B), Titanium Memory Esthetic (C), Titanium Memory ThermoTi Lite (D), Sentalloy High Aesthetic (E), Sentalloy (F), TMA (G), and Colored TMA (H).

70

Figure V.1: Representative Time-Friction graphs for Sentalloy on metal brackets (left column) and ceramic brackets (right column), before (upper row) and after (lower row) the clinical use. In evidence the maximum peak. 83

Figure V.2: Representative Time-Friction graphs for Sentalloy High Aesthetic on metal brackets (left column) and ceramic brackets (right column), before (upper row) and after (lower row) the clinical use. In evidence the maximum peak. 84

Figure V.3: Representative Time-Friction graphs for Superelastic Titanium Memory Wire on metal brackets (left column) and ceramic brackets (right column), before (upper row) and after (lower row) the clinical use. In evidence the maximum peak. 85

Figure V.4: Representative Time-Friction graphs for Esthetic Superelastic Titanium Memory Wire on metal brackets (left column) and ceramic brackets (right column), before (upper row) and after (lower row) the clinical use. In evidence the maximum peak. 86

Figure V.5: Representative Time-Friction graphs for EverWhite on metal brackets (left column) and ceramic brackets (right column), before (upper row) and after (lower row) the clinical use. In evidence the maximum peak. 87

Figure V.6: Sentalloy SEM images at three magnifications x200, x500, x1000, before (left column) and after (right column) the clinical use. 89

Figure V.7: Sentalloy High Aesthetic SEM images at three magnifications x200, x500, x1000, before (left column) and after (right column) the clinical use . 90

Figure V.8: Superelastic Titanium Memory Wire SEM images at three magnifications x200, x500, x1000, before (left column) and after (right column) the clinical use. 91

Figure V.9: Esthetic Superelastic Titanium Memory Wire SEM images at three magnifications x200, x500, x1000, before (left column) and after (right column) the clinical use. 92

Figure V.10: EverWhite SEM images at three magnifications x200, x500, x1000, before (left column) and after (right column) the clinical use. 93

Figure V.11: Representative AFM images of Sentalloy and Sentalloy High Aesthetic before (left column) and after (right column) the clinical use. 94

Figure V.12: Representative AFM images of Superelastic Titanium Memory Wire, Esthetic Superelastic Titanium Memory Wire and EverWhite before (left column) and after (right column) the clinical use.

List of Tables

Table I.1: Research strategy and results.	19
Table I.2: Aesthetic orthodontic archwires.	26
Table II.1: Physical, mechanical and biological factors that affect friction (Kusy and Whitley, 1997).	42
Table IV.1: R_a , R_{ms} and M_h of AFM topography images.	71
Table IV.2: P-values from statistical analysis of archwires roughness parameters (ANOVA with Tukey's post hoc test). * ($P<0.05$), ** ($P<0.01$) and * ($P<0.001$) indicate significant statistically differences between the two archwires.	72
Table V.1: Roughness Average (R_a), Root Mean Square (R_{ms}), and Maximum Height (M_h) values (mean \pm SD) of Atomic Force Microscope (AFM) images of orthodontic archwires before (As-received) and after (Retrieved) the clinical use. ns (not significant) * ($P<0.05$), ** ($P<0.01$) and *** ($P<0.001$) indicate significant statistically differences between As-received and Retrieved (Student's t test for unpaired data).	97
Table V.2: P-values from statistical analysis of archwires roughness parameters (ANOVA with post hoc Tukey's test). ns indicates not significant. * $P<0.05$; ** $P<0.01$; and *** $P<0.001$ indicate statistically significant differences between two archwires.	98
Table V.3: Friction (N) values (mean \pm SD) on metallic and ceramic brackets of orthodontic archwires before (As-received) and after (Retrieved) the clinical use. ns (not significant) * ($P<0.05$), ** ($P<0.01$) and *** ($P<0.001$) indicate significant statistically differences between As-received and Retrieved (Student's T test for unpaired data). a ($P<0.05$), b ($P<0.001$), c (not significant) indicate significant statistically differences between ceramic brackets and metallic brackets (Student's t-test for paired data).	99
Table V.4: P-values from statistical analysis of archwires friction parameters (ANOVA with post hoc Tukey's test): ns (not significant) * ($P<0.05$), ** ($P<0.01$) and *** ($P<0.001$) indicate significant statistically differences between the archwires on the two brackets typology.	100

Overview

Patients' expectations about a low aesthetic impact of the appliance during the orthodontic treatment are increasing and then, several are the attempts to combine adequate appliance aesthetics with satisfactory treatment efficiency and efficacy. Numerous solutions are available for example the lingual orthodontics is almost invisible but requires additional skills and chair time to the orthodontist. Orthodontic clear aligners are having a great spread in the last ten years but they are still use above all for simple treatments. However, complex cases still require fixed appliance treatment and hence, clear labial brackets associated with aesthetic archwires are available for those clinicians and patients that are aesthetically orientated (Russell, 2005). In orthodontics, the availability of different alloys for archwires has been one of the main breakthroughs in orthodontic materials research, leading to key improvements in the field of mechanotherapy (Eliades, 2007). Nevertheless, new materials are constantly being proposed to the orthodontists, and this sometimes increases confusion about the actual characteristics of the wires. In fact, the ubiquitous claims of improved performance are not always supported by accurate scientific information. Thus, the characterization of archwire alloys can be considered an initial step in understanding wire behaviour in the clinical context (Krishnan and Kumar, 2004). The properties to consider when looking for an ideal orthodontic wire for a given clinical use are: biocompatibility, aesthetics, moldability, weldability, toughness, strength, stiffness, springback and friction (Kusy, 1997). Friction is a force that opposes the motion of two surfaces in contact with each other. Friction is not a major force because it is derived from electromagnetic forces between atoms and is

enhanced by surface roughness (Jastrebski, 1987) and the force with which the surfaces are kept in contact. Friction is affected by numerous factors like the alloy composition of the archwire, the wire size, the elasticity, and the surface roughness that can be modified by surface treatments useful to improve some archwires characteristics. Surface roughness is one of the most considerable archwires characteristics because has a substantial influence of many other archwires aspects such as biocompatibility, corrosion and aesthetic. Hence, due to the little information on aesthetic archwires the aim of this thesis was to describe the properties of this kind of wires.

In chapter 1 an accurate review on current archwires and on aesthetic archwires was reported. In chapter 2 the fundamental role of the surface roughness and of the sliding resistance were summarized. Chapter 3 presents a brief description of the tools used during the performed experiment. In chapter 4 the use of the Atomic Force Microscopy to analyse surface roughness and to compare it among different archwires materials was described. In chapter 5 the effects of the oral environment on different archwires properties were evaluated. Chapter 6 includes a general discussion of the study's design and findings.

The work contained in this thesis has led to the following publications:

D'Antò V, Rongo R, Ametrano G, et al. Evaluation of surface roughness of orthodontic wires by means of atomic force microscopy. *Angle Orthod.* 2012;82:922-8.

Rongo R, Ametrano G, Gloria A, Spagnuolo G, Galeotti A, Paduano S, Valletta R, D'Antò V. Effects of intraoral aging on surface properties of coated nickel-titanium archwires. *Angle Orthod.* 2013. doi: 10.2319/081213-593.1

Chapter I

Aesthetic Orthodontic Archwires

The archwire are the engine of the orthodontic appliance, brackets do not move teeth, wires do. When banding and bonding is complete, an archwire is placed into the bracket slots and retained in position using ligatures and elastic modules. The archwire interacting with the bracket slots provides a force necessary to move the teeth and to determine the overall shape of the dental arch (Williams et al, 1995). The most used materials for metallic archwires are stainless steel alloys, cobalt-chromium alloys, nickel-titanium alloys and β -titanium alloys. Each alloy has some peculiarities and is used in different phases of orthodontic treatment even if their use depends also by the ingrained philosophy of treatment of each clinician. The behaviour and performance of an archwire depend on a variety of factors such as different alloy types, shapes, sizes and stage of treatment. During the interaction between archwire and bracket a force is produced. At the present stage, thanks to bone biology research, the ideal orthodontics force has to be light and continuous to create minimal hyalinised tissue and to create continuous effects without hurts the periodontal ligament vascular microcirculation (Proffit et al., 2012).

I.1 Archwires Alloys

The archwires available in orthodontics are almost all in metal alloys: Stainless Steel (SS), Cobalt-Chromium (CoCr), Nickel-Titanium (NiTi) and Beta-Titanium (β -Ti).

I.1.1 Stainless Steel Alloys (SS)

SS was introduced as an orthodontic wire in 1929 (Kapila and Sachdeva, 1989). The Austenitic form had a great strength and a high Young's Modulus (E) associate with a good resistance to corrosion with a more accessible cost than gold alloy. Nowadays, SS is a very popular wire thanks to its mechanical characteristics and physical properties. The most commonly SS types are the 302 and the 304 used to form bands and wires. A typical formulation for orthodontic use has 18% chromium and 8% nickel (thus the material is often referred to as an 18-8 stainless steel). The properties of these wires can be controlled by varying the amount of cold working and annealing during manufacture. SS is softened by annealing and hardened by cold working. Fully annealed SS wires are soft and highly formable and are used, for example, in form of ligatures to tie orthodontic archwires into brackets. SS archwire are offered in a range of partially annealed states, in which yield strength is progressively enhanced at the cost of formability. The SS wires with the most impressive yield strength ("super" grades) are almost brittle and will break if bent sharply. The "regular" grade of orthodontic steel wire can be bent to almost any desired shape without breaking. If sharp bends are not needed, the super wires can be useful, but it is difficult to show improved clinical performance that justifies either their higher cost or limited formability. The SS wires have a higher E and

stiffness but a lower springback as compared to the other alloys used in orthodontics. Hence, to align moderate or severe displaced teeth the SS is not suggested, or has to be used with small dimensions wires that are more prone to loss three-dimensional control during teeth movement (Kusy, 1997). On the other hand, the high stiffness is an advantage during the use of large dimensions wires (0.019x0.025 or larger) for the resistance to deformation caused by extra- and intra-oral tractional forces (Drake et al, 1982). Another drawback of this alloy is the lower springback in fact the wires produce high forces dissipated over a short period of time, thus requiring frequent activations or archwire changes. Hence, its characteristics make the SS wires ideal for the final stage of the treatment where stability and small amount of movement.

I.1.2 Cobalt-Chromium Alloys (Co-Cr)

The Co-Cr alloy was mainly composed by 39-41% cobalt, 19-21% chromium, 14-16% nickel, 11.3-20.5% iron. These alloys were originally named Elgiloy and their properties were also useful for orthodontic applications. This alloy presents a similar stiffness to SS but its formability and strength can be modified by heat treatment. The wires are available in four tempers: soft, ductile, semiresilient and resilient. After heat treatment, the softest Elgiloy becomes equivalent to regular stainless steel, while harder initial grades are equivalent to the “super” steels. Soft-temper wires were popular with clinicians because they are easily deformed and shaped; then heat treated to increase its yield strength and resilience. This effect is called precipitation hardening heat treatment that increases the ultimate strength and the resilience of the wire without changing its stiffness (Fillmore and Tomlinson, 1979). The improvements in resilience and strength provide to the wire a greater resistance to fatigue and distortion and above all a longer function. It was recommended for use when considerable bending, soldering or welding is required. This material, however, had almost disappeared by the end of the twentieth century because of its additional cost relative to stainless steel and the extra step of heat treatment to obtain optimal properties (Proffit, 2012).

I.1.3 Nickel-Titanium Alloys (NiTi)

NiTi alloys archwires are useful during the initial phase of the orthodontic treatment (alignment) due to their intrinsic ability to apply light force over a large range of activations and long time. The first NiTi alloy was developed for the space program and named NiTiNOL (Ni, nickel; Ti, titanium; NOL, Naval Ordnance Laboratory) was first introduced in 1971 and it was based upon the intermetallic compound NiTi, which has weight percentages of 55% Ni and 45% Ti. However this alloy did not present the two main characteristics that make this alloy so special: shape memory and superelasticity (Andersen and Morrow, 1978). These two properties are strictly linked and depend on the equilibrium between the two metallic forms present in the NiTi alloy, the martensitic form and the austenitic form. At lower temperatures and higher stress, the martensitic form is more stable, while at higher temperatures and lower stress, the austenitic form is more stable (Figure I.1).

The transition between the two structure forms occurs, for all the other metallic alloys at high temperature around hundreds Celsius degrees, instead for the NiTi alloys the temperature of transition is low and it is fully reversible. The shape memory is the ability of NiTi alloys to remember the form in the austenitic structure after undergoing plastic deformation in the martensitic phase. The alloy could be plastically modified in the martensitic phase and when heated it will be return to the original shape, this phenomenon it is called also thermoelasticity.

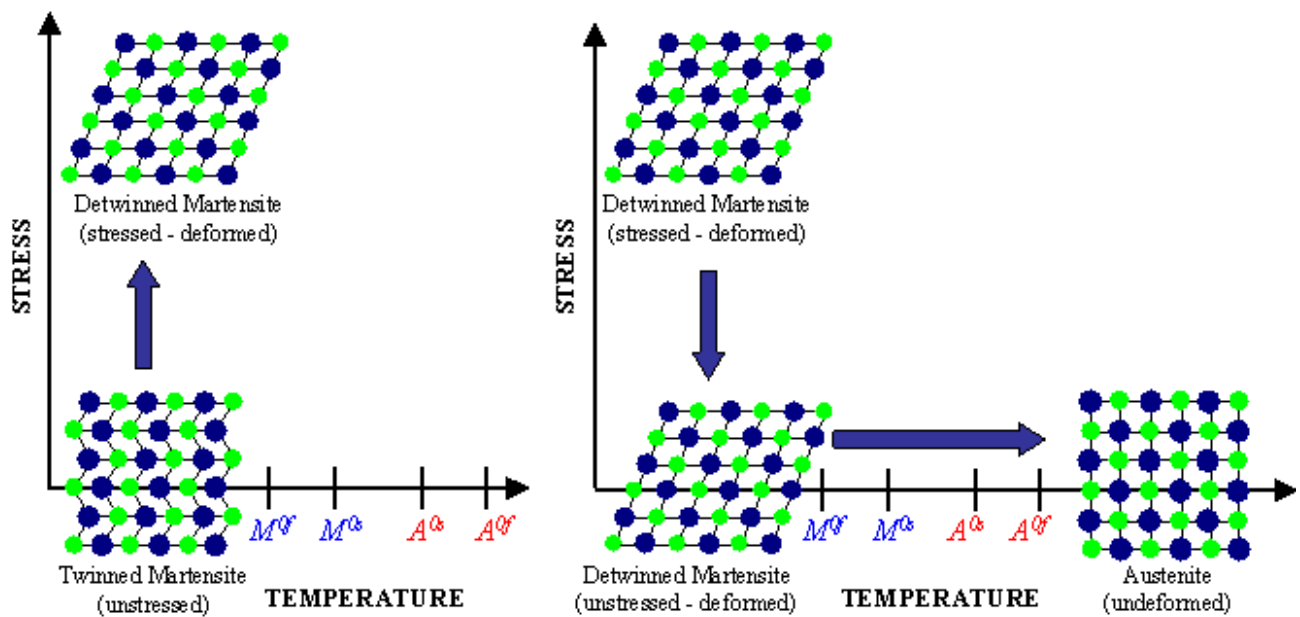


Figure I.1: Shape Memory Effect. If mechanical load is applied to the material in the state of twinned martensite (at low temperature) it is possible to detwin the martensite. Upon releasing of the load, the material remains deformed. A subsequent heating of the material to a temperature above A_0f will result in reverse phase transformation (martensite to austenite) and will lead to complete shape recovery.

Andersen and Morrow (1978) described the shape memory phenomenon as the capability of the wire to return to a previously manufactured shape when it is heated through its transitional temperature range (TTR). Typically, a certain shape such as dental arch is set to the austenitic NiTi at high temperature above the TTR, after the alloy is cooled and deformed, when the wire reach another time the TTR it returns to the dental arch shape, this is the principle of function of Thermal active NiTi alloy. The superelasticity (Figure I.2) allows the alloy to totally recover large deformation with a constant delivered force until to the complete return to the original shape. This phenomenon is due to the formation of stress induced martensite (SIM).

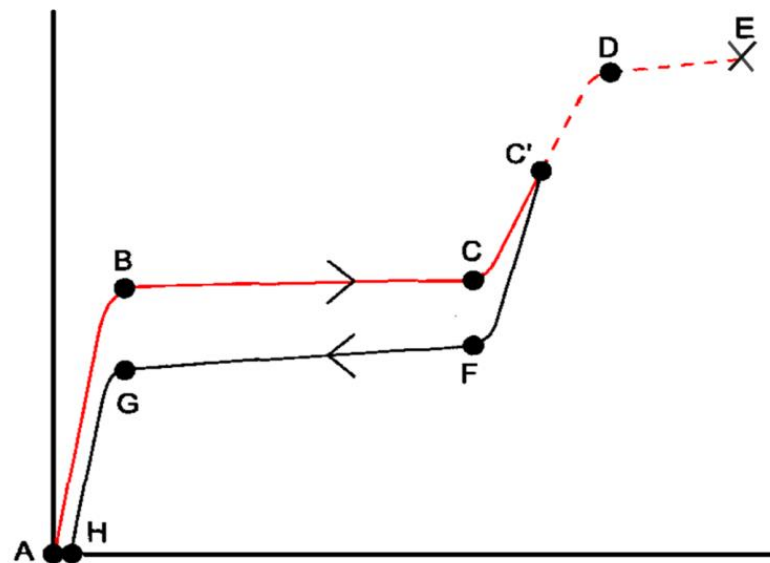


Figure I.2: Stress-Strain curve pseudo elastic NiTi: this curve stress-strain shows the superelasticity, due to the transformation from the austenite phase to the martensite by the action of a stress. The distance AB represents the elastic deformation of the austenitic phase. The point B corresponds to the stress required to induce the transformation to the martensitic phase. At point C the transformation is complete. When the conversion is completed, the martensitic structure continues to deform in an elastic way if stressed, as is represented by the segment CD (orthodontic arches are almost never stressed up to this point). In point D reaches the yield strength of the martensitic form and the material begins to deform plastically until rupture occurs at point E. If the sollicitation is suspended before reaching the point D (as in point C' in the diagram), the elastic curve of discharge takes place along the line C'-F. At this point begins the reverse transformation to austenite, which continues to point G, where the austenitic structure is completely restored. GH represents the discharge curve of the austenitic phase. A small portion of the overall stress is not recovered because of the irreversible changes that occur during the loading and unloading.

This is possible because the TTR is very close to room temperature. Most archwire materials can be reversibly deformed only by stretching interatomic bonds (which creates the linear region of the stress-strain curve), while superelastic materials can undergo a reversible change in internal structure after a certain amount of deformation. The SIM starts when a force modifies an austenitic sample beyond the elastic threshold (1-2%), producing at an initial phase, and an elastic behaviour of the sample. After this initial phase the stress/strain curve shows a plateau phase indicating the transformation in martensite of the sample. At the end of the plateau the material is totally martensitic and the stress/strain curve shows an increased slope due to a new elastic behaviour of the sample. Removing the force, the curve

shows the same trend of the previous one returning minus force until the total recovering of the initial shape. This phenomenon is due to hysteresis, i.e. a part of the energy stored by the sample during its modification is lost and dispersed; hence the unloading curve is different from the loading one.

Although shape memory is a thermal reaction and superelasticity is a mechanical one, they are inherently linked. Superelastic materials must exhibit a reversible phase change at a close transition temperature, which must be lower than room temperature for the austenite phase to exist clinically. Shape memory alloys only have exceptional range clinically if stress-induced transformation also occurs.

In orthodontics, low stiffness of NiTi does not make this alloy ideal for completion of treatment, due to an inadequate stability respect to SS alloys. Moreover, this alloy is more expensive than the others (Baldwin et al., 1999; Nakano et al., 1999). Another drawback of NiTi is the nickel hypersensitivity reactions to nickel-titanium wires, even if also the brackets and other device contain nickel (Bass et al., 1993). It is also difficult to place permanent bends and the wire cannot be bent over sharp edges or into a complete loop. Furthermore, it cannot be soldered and must be joined by mechanical crimping process (Kusy, 1997). The wires also have a high bracket/wire friction (Kusy et al., 1988). However, the properties of the superelastic or thermoactive NiTi have made it the first choice alloy for the initial stage of treatment, in which is needed low and constant forces for a long periods without required several activations.

I.1.4 Beta-Titanium Alloys (β -Ti)

The β -Ti was introduced in 1980 (Burstone and Goldberg, 1980). It was firstly produced as titanium-molybdenum alloy (TMA, Ormco, Orange, CA). The nominal composition of TMA is 77.8% titanium, 11.3% molybdenum, 6.6% zirconium and 4.3% tin. The molybdenum causes a series of change crystalline structure of the alloy, resulting in an excellent formability for permanent deformation. It is also the only orthodontic wire alloy that possesses true weldability (Nelson et al., 1987). β -Ti has a Young's Modulus less than that of stainless steel and about twice that of nickel-titanium (Kusy, 1997). These characteristics make the β -Ti ideal in situations in which there is a need of an alloy able to return forces less intense than those of SS and easier moldable than NiTi to obtain accurate shape such as a cantilever (Burstone and Goldberg, 1980). This makes it an excellent choice also for intermediate and finishing archwires, especially rectangular wires for the late stages of edgewise treatment. Moreover, the β -Ti is more elastic than SS with comparable corrosion resistance (Goldberg and Burstone, 1982) but this alloy shows the highest friction coefficient among all the alloys probably due to the adhesive and abrasive wear produced with the slot of the bracket as a result of the high reactivity of the wire's surface (Kusy et al., 1991; Kusy et al., 2004) This drawback excludes the use of β -Ti wires during orthodontic sliding mechanics (Kusy and Whitley, 1990).

I.2 Aesthetic Archwires Characteristics

The aesthetic perception of the orthodontics appliances is an issue that is becoming constantly more important in the modern time above all due to the increasing treatment demands by adult patients (Ziuchkovski et al., 2008). Nowadays, several are the tools available for an orthodontist to satisfy the patients' requests, such as the lingual orthodontics, the clear aligners or the clear labial orthodontics. Recently, some studies discuss about the attractiveness and the acceptability of orthodontic appliances at different age. The study of Ziuchkovski and coll. (2008) showed that the preferred appliances, by a group of 200 adult patients, were the alternative appliances (lingual or clear aligners) followed by the clear labial appliances and at the end the metallic ones. Moreover, orthodontic appliance attractiveness can vary with wire and tie selection in ceramic bracket appliances. Another work looked at the preferences of children and adolescents found that children accepted positively metallic brackets with colored ligatures while adolescents preferred clear aligners and metallic brackets with colored ligatures (Walton, 2010). Therefore, the perception of the orthodontics appliances significantly differs between adults and young people. Clear labial orthodontics is still well accepted by the patients and it is a good compromise between efficiency and efficacy of the appliance, orthodontist's skills and aesthetic impact. In fact the clear labial orthodontics does not require furthers skills as like as the lingual orthodontics and can be used to treat every kinds of malocclusions unlike clear aligners (Russell, 2005).

The production of clear brackets is reaching very high standard with the creation of ceramic brackets totally clear, with colour stability, resistant to the fracture and adequate bond strength (Filho et al., 2013). On the other hand, although aesthetic brackets have brought a dramatic improvement in the appearance of appliances,

metal archwires are still visible and several were the attempts to create an adequate aesthetic archwire to associate to the ceramic brackets. These wires have to be visually imperceptible and at the same time keep the same performance of the metallic ones. Polymer-coated archwires were introduced during the 70s but their coatings were not stable enough and peeled off during the treatment.

Nowadays, two are the main surfaces treatment to try to improve the aesthetic characteristics of an orthodontic archwires: the ion implantation and the surface coating: ion implantation and surface coating.



Figure I.3: Example of aesthetic orthodontic wires on ceramic brackets.

I.2.1 Ion Implantation

Ion implantation is a process based on the acceleration, in an electrical field, of the ions of a material that are implanted into a solid. This process is used to change the physical, chemical, or electrical properties of the solid.

Ion implantation is used in semiconductor device fabrication and in metal finishing, as well as various applications in materials science research. The ions alter the elemental composition of the target, if the ions differ in composition from the target, stop in the target and stay there. They also cause much chemical and physical change in the target by transferring their energy and momentum to the electrons and atomic nuclei of the target material. This causes a structural change, in that the crystal structure of the target can be damaged or even destroyed by the energetic collision cascades.

Ion implantation equipment typically consists of an ion source, where ions of the desired element are produced, an accelerator, where the ions are electrostatically accelerated to a high energy, and a target chamber, where the ions impinge on a target, which is the material to be implanted. Thus ion implantation is a special case of particle radiation. In orthodontics to create aesthetic archwires is used a specific ion implantation process the plasma-immersion ion implantation (PIII) introduced by Adler and Conrad around 1980 (Adler and Picraux, 1980; Conrad et al., 1987) and describe by Sridharan and coll. in 2000. In case of PIII process, the target is directly immersed in a chamber of plasma of ion species to be implanted and is biased with a pulse of high negative potential of the order of kV with respect to the ground potential of chamber walls. The applied negative potential drifts the electrons away from the target to form a positive ions sheath around the target. With time, the positive ions present in the sheath are being dragged towards the target due to its negative potential and get implanted onto the target surface from

all sides. Thus PIII, being a non-line-of sight technique, completely eliminates the complicated and sophisticated mechanisms of conventional ion implantation and proves to be a comparatively simple and cost competitive process technology. The wires undergoing different processes of ion implantation for aesthetic reasons are the Bioforce and the Sentalloy (GAC International) and the TMA (Ormco).

I.2.2 Surface Coating

The first attempt to make aesthetic wires was to camouflage the archwire by covering it with a plastic layer. Polymer-coated metallic wires (Rocky Mountain Teflon-coated stainless steel wires) were introduced in the 1970s. Although the appearance of the wires was greatly improved, experience with the initial Teflon-coated archwires showed that the coating tend to stain and split with usage, revealing the underlying metal. Another alternative is using a spray-coat, which has the advantage of adding only a thin layer to the archwire, but the coat tends to have a rather grey tinge and often chips off with use (Postlethwaite, 1992). NiTi and SS are usually coated with a polytetrafluoroethylene (PTFE), epoxyresin, parylene-polymer, or rarely palladium covering to obtain a similar colour to the enamel. To get excellent aesthetic, flake resistance and maximum efficiency, the coating material and thickness of the coating, and steps within the application process can vary for different manufacturers.

Currently, the two most common coating for the aesthetic archwires are PTFE or epoxy-resin.

I.2.2.i PTFE

Teflon PTFE, commonly recognized by the DuPont Co brand name Teflon, is a synthetic polymer consisting wholly of carbon and fluorine. PTFE has the third lowest coefficient of friction of any known solid, making it ideal for use as a non-stick coating and sliding mechanics PTFE coating is applied to an orthodontic wire by thermal spraying, a process in which finely heated materials are sprayed in a molten condition onto a surface to form a coating. Thermal spraying of PTFE onto an orthodontic archwire entails: (1) surface treatment of the wire by sandblasting (50-micron alumina) to support coating adhesion, (2) “masking” or covering with

tape areas that are not be treated, (3) air-spraying atomized PTFE particles with clean compressed air to coat the wire, (4) baking in a chamber furnace to cure the coating onto the wire, and (5) removal of the masking tape. The PTFE layer adds a minimal thickness (.0008 to .001 inch) to the archwire. Though PTFE has an extremely low coefficient of friction, it is used primarily for aesthetic purposes.

1.2.2.ii Epoxy-resin

Epoxy is a synthetic resin made by combining epoxide with another compound. They are widely used in orthodontic materials, including composite resins, molds, and polyurethane aligners. Epoxy-resin coating is applied to an orthodontic archwire by electrostatic coating, or E-coating. Electrostatic coating is a process that uses electrostatically charged particles to more efficiently coat a work piece. Electrostatic coating of epoxy resin onto an archwire entails: (1) applying a high-voltage electrostatic charge to the archwire, (2) applying an opposing electrostatic charge to the epoxy, (3) air-spraying atomized liquid epoxy particles to the wire, and (4) baking in a chamber furnace to cure the coating onto the wire. The epoxy coating does add a more significant thickness (.002 inch) to the archwire. Therefore, a .0180-inch NiTi wire becomes .020-inch diameter with an epoxy coating, or alternatively, the manufacturer may choose to use a smaller diameter wire to compensate for the thickness of the coating.

I.2.3 Composite Archwires

Within the past 20 years, significant advancements have been made to create non-metallic arches whose properties resemble metal alloys. Flexible non-metallic arches are typically made from glass spindles embedded in a polymeric matrix. The first, completely non-metallic archwire was introduced into the orthodontic market, called a “totally aesthetic labial archwire”. The commercial name is Optiflex (Ormco/Sybron). The wire comprises of three layers: a silica core, which is surrounded by a moisture protection silicone resin middle layer and a stain-resistant nylon outer layer. The outer layer has the dual purpose of preventing damage to the archwire and further increase the strength of the archwire. This wire was aesthetically very pleasing. However, its orthodontic force is too light for clinical use (Lim et al., 1994).

It has been recognized that an optimal and aesthetic archwire can be developed using composite technology from continuous fibres and polymer matrix to suit the varying degree of stiffness required for each stage of orthodontic treatment (Goldberg and Burstone, 1992). Some examples of non-metallic arches include fibre-reinforced polymer or self-reinforced polymer. These arches allow for a few millimetres of deformation and may be suitable for levelling and aligning in patients with Class I malocclusions with mild to moderate crowding. More importantly, they display the translucency and transparency ideal for ceramic brackets. Non-metallic arches are not readily available. The manufacturing process for non-metallic arches will vary depending on the type of polymer.

I.3 Aesthetic Archwires: Literature Review

Aesthetic archwires were not widely discussed in literature. A literature research was done in Web of Knowledge and Medline by PubMed (Table I.1). Of the 106 suitable papers only 33 articles were resulting discussing physical, chemical and clinical characteristics of aesthetic archwires.

Database	Research strategy	Results	Selected
Medline via PubMed	(ion implantation AND archwires) OR (coated archwires) OR (aesthetic archwires) OR (composite archwires)	56	21
Web of Science	TOPIC: (((aesthetic archwires) OR (coated archwires) OR (ion implantation AND archwires) OR (composite archwires)))	103	30
Total after duplicate removal=106 selected=33			

Table I.1: Research strategy and results.

Firstly, Lim et al. (1994) started to assess the springback and stiffness of two aesthetic archwires a Teflon coated SS round wire and a round Optiflex, a wire composed by a silicon dioxide core, a silicon resin middle layer and a nylon outer layer. Optiflex was found to have low stiffness and resilience and poor springback and the archwire remained bent upon deactivation. The stiffness for the Teflon-coated archwire was found to be higher and more in line with the stiffness for the control. Both the Teflon-coated and stainless steel archwires displayed good springback property. Hence the authors rejected the clinical efficacy of the Optiflex due to the poor springback and the low stiffness. Properties of SS aesthetic archwires have been little investigated; it was showed that as-received coated SS archwires produce less friction of uncoated ones, independently by cross section

(Husmann et al., 2002; Farronato et al., 2012, Hiroce et al., 2012) and that suffered of less corrosion processes (Neumann et al., 2002).

Differently, NiTi archwires have been deeply studied; in fact more investigations have been done on coated and ion implanted wires.

Coated and ion-implanted as-received NiTi wires showed lower friction than the uncoated wires for round and rectangular sizes (Husmann et al., 2002, Farronato et al., 2012, Bandeira et al., 2012, Bravo et al., 2013; Krishnan et al., 2013) even if some authors found no differences using small round coated wires (Murayama et al., 2013) or even highest friction for coated archwires (Jang et al., 2011). Nevertheless, there are no studies that test this property after the clinical use.

Most of coated NiTi wires present a minor dimensional section respect to the nominal one to compensate for the thickness of the coating layer (da Silva et al., 2013^b) and this leads to a reduction in delivery forces of NiTi wires. As matter of fact, several studies reported that both for round and rectangular wires, the coated NiTi wires usually deliver less force of the similar nominal dimensions uncoated archwires (Elayyan et al., 2010; Alavi and Hosseini, 2012; Kaphoor and Sundareswaran, 2012; Bradley et al., 2013; da Silva et al., 2013^b) and the same was found for ion implanted NiTi (Iijima et al., 2012). However, some other interesting studies have discordant results. Iijima et al. (2012) studied Woowa (Dany Harvest, Seoul, South Korea) a double-layered coating structured wire (inner layer: silver and platinum coating; outer layer: special polymer coating); this innovative composition wire was able to produce higher mean unloading force than the uncoated Woowa; while Murayama and coll. (2013) found that for small diameter round wires there were not significant differences in delivered forces between coated and uncoated wires. Another notable wire was the TP orthodontics[™] aesthetic wire, this wire is coated just on the labial surface and has a very thin coating indeed, it did not show

any significant difference between the uncoated and coated cross-section dimensions (da Silva et al., 2013^b). Thanks to the stable cross-section dimensions the TP orthodontics™ aesthetic wire displayed no significant differences in modulus of elasticity and maximum deflection force values between the uncoated and coated wires (Kaphoor and Sundareswaran, 2012; da Silva et al., 2013^b).

Finally, the loading and unloading forces of retrieved archwires were also tested, and the results depend extremely by the wires analysed. Bradley and coll. (2013) stated that after the clinical use the coated wires reached higher loading and unloading force than respective uncoated retrieved wires, hence the coating has an effect on the force levels. As more of the coating was lost the wire began to behave more like the uncoated wires, which have greater stiffness and force values as-received, on the other hand other studies revealed that retrieved coated archwires produce lower unloading force values than as-received coated archwires with conventional ligation (Elayyan et al., 2008; da Silva et al., 2013^b) and the same forces on self-ligating brackets (Elayyan et al., 2008).

Coating has been suggested to reduce nickel release in mouth and to improve corrosion resistance of the wires (Kim and Johnson, 1999). The authors found that epoxy resin coating decreased corrosion, reducing the corrosion potential of the wire. Similar results were found by Neumann and coll. (2002) and Krishnan and coll. (2014) that found that Teflon coating prevented the corrosion of the wires. On the other hand, rhodium ion implantation reduced corrosion resistance and pronounced susceptibility to pitting corrosion in artificial saliva (Katić et al., 2014) Bradley and coll. (2013) stressed that statistical significant differences were found in thermal properties between coated and uncoated as-received wires while this differences disappeared after the clinical use. This indicates that coated wires may behave differently in the mouth than the uncoated ones, and probably during the

clinical use the loss of the coating transform the coated archwires more likely the uncoated versions. The authors supposed that the coating dramatically alters the thermal properties of the wire because it might work as insulator for the heat transfer.

The main drawback of coated archwires is the loss of the coating that affects the aesthetic impact of the wires. The retrieved analysis of this kind of wires underlines constantly a considerable exposition of the underlying metal (Elayyan et al., 2008, Bradley et al., 2013; da Silva et al., 2013^a; da Silva et al., 2013^b; da Silva et al., 2013^c). In most cases, the coated archwires showed discolouration, ditching, and cracking, and the amounts of deterioration was highly variable. On average 25-44% of the coating was lost (Elayyan et al., 2008; Bradley et al., 2013). Obviously, the loss of the coating is noted by patients, in fact from a survey it was clear that about half of the patients were aware of colour and texture change over time (Bradley et al., 2013).

Finally the surface roughness of aesthetic coated archwires was assessed, with different techniques, for new and retrieved samples. Typically, epoxy-resin, Teflon coated or ion-implanted as-received archwires showed lower surface roughness respect to the respective metal wires (Elayyan et al., 2008, da Silva et al., 2013^c; Bravo et al., 2013; Krishnan et al., 2013; Krishnan et al., 2014); however, Iijima and coll. (2012) found higher surface roughness in coated and ion implanted archwires than in no-treated archwires. At scanning electron microscope (SEM) analysis coated archwires might present an inhomogeneous protective coating that creates internal tensions between the layer and the substrate, which is favourable for the exfoliation process (Zegan et al., 2012, Krishnan et al., 2014). Moreover, after the clinical use the surface roughness of the wires increases, in some cases dramatically, and it can reach or even exceed the roughness of the metallic wires

(Elayyan et al., 2008; Iijima et al., 2012; da Silva et al., 2013).

The elective treatment to make aesthetic the β -Ti alloy was ion implantation; the ion-implanted TMA was firstly described by Burstone and Fazin-Nia in 1995. This wire presented an higher friction coefficient respect to SS but frankly lower than untreated TMA (both static and kinetic); no differences in elasticity modulus respect to untreated TMA similarly the loading and unloading forces were similar between these two wires. In conclusion, Burstone showed that the resistance to fracture, the ductility and the recovery rate of the surface treated TMA were better than the classic TMA. Other few studies were performed on this wire, Husmann and coll. (2002) confirmed that aesthetic TMA had a lower friction coefficient, again more recently Cash and coll. (2004) and Krishnan and coll. (2013) found the same results. Moreover, has been observed that ion implantation reduced the surface roughness of the TMA (Krishnan et al., 2013).

After the first attempt of Lim and coll. (1994) to introduce a composite aesthetic wire, several were the investigators that tried to create a clear and efficacious composite archwires. Firstly, in 1998 Zufall and coll. started analysing the friction coefficient of a prototype of composite fibre reinforcement wires, and found that the friction produced by this wire was higher than the one produced by SS wire but similar to NiTi and TMA friction, with different bracket materials and different bracket angulations. Successively, the viscoelastic behaviour of this wire was assessed (Zufall and Kusy, 2000) and they stated that the stress relaxation behaviour was strongly correlated with the archwire reinforcement level while archwire recovery was not correlated with reinforcement level. The relaxed elastic moduli in bending of the composite wires were similar to the elastic moduli in bending of several conventional orthodontic archwire materials. Stiffness losses associated with the viscoelastic behaviour, varied with decreasing reinforcement level from 1.2 to 1.7

GPa. Because these modulus losses were minimal, each archwire retained sufficient resilience to be applicable to the early and intermediate stages of orthodontic treatment. Further test were done on this kind of wire, in fact, a tribological (friction and wear) study was also designed to determine the effect of coating on the composite wires (Zufall and Kusy, 2000^b). It was observed that although the coating did increase the frictional and binding coefficients of the wires, it was still within the limits outlined by conventional wire-bracket couples. In addition, it reduced the risk of glass fibre release into the oral cavity. In the 2003, Huang and coll. introduced a new technique based on tube shrinkage for the fabrication of composite archwires. Compared with the traditional pultrusion method, this new technique can avoid any fibre damage during the fabrication and can provide the archwire with a required curvature in its final clinical usage.

In 2011 Goldberg and coll. evaluated another composite wire based on a recently developed translucent polyphenylene thermoplastic. Firstly, they evaluated the viscoelastic properties and it was evident that polyphenylene-based orthodontic wires exhibit viscoelastic properties typical for an amorphous polymer. Hence, due to this viscoelastic behaviour forces that are applied below the yield strength can produce both stress relaxation (loss of force) and deformation, large deflections approaching the yield strength can produce significant time-dependent force loss and deformation, indeed aesthetic translucent polyphenylene arch requires the orthodontist to understand and apply important viscoelastic concepts to optimize its clinical use. Secondly, Burstone and coll. (2011) studied the physical and mechanical properties of this wire suggesting that polyphenylene polymers could serve as aesthetic orthodontic archwires. In fact, the wires, analysed by SEM, were visually smooth and the cross-sectional dimensions were consistent with well-defined profile. Mechanical properties were comparable to NiTi and β -Ti wires

with somewhat smaller cross sections, but did experience some stress relaxation. These findings were confirmed also by other recent studies (Ballard et al., 2012). Nonetheless, composite archwires are very aesthetic but their use in orthodontics is very limited and still need to be developed. For example water exposure is detrimental to translucent wires that were more likely to crack/craze during bending and to change their mechanical properties (Chang et al., 2013; Ohtonen et al., 2013) and also fluoride exposure can have negative effects such as a statistically significant reduction in modulus of elasticity (E), yield strength (YS) and springback ratio (YS/E), in association with corrosion process (Hammad et al., 2012).

Name	Producer	Material	Dimension	Characteristics
Orthoform Tooth Coated NiTi	3M http://solutions.3m.com	NiTi SS	014-016-018-020 016x022 018x025 019x025 020x020 021x025	Orthoform tooth coated archwires are epoxy coated for maximum aesthetics and wear resistance
EverWhite	American Orthodontics www.americanortho.com	NiTi		Reduced visibility with remarkable performance. Proprietary Micro-Layering process provides the most durable cosmetic coating available.
Translucent Arch Wire	BioMers www.biomersbraces.com	Composites		The BioMers arch wires are translucent and, therefore, nearly invisible. As they function in the same way as metal wires, orthodontists do not have to undergo special training to use them. These wires have the necessary mechanical properties to straighten teeth effectively by means of the company's patented fabrication technology and appropriate material selection. Round only
Regecency-Confidential Archwire	ClassOne www.classoneorthodontics.com	NiTi SS	012-014-016-018-020 016x022 017x025 018x018 018x025 019x025 020x020 021x025	Coated with thin epoxy outer layer for smooth surface B2 shading most like natural tooth colouring

<u>Archwire - Aesthetic Micro Coated</u>	DBORTHO www.dbortho.com	NiTi SS	012-014-016-018-020 016x016 016x022 017x025 018x025 019x025 021x025	The arch wire is only coated on labial surface. -a huge advancement in coated archwires provides an optimum cosmetic appearance.-. -achieve a true archwire size as the PTFE coating is only .0005”. - micro-coated labial surface provides an Optimum cosmetic Appearance.
Titanol Cosmetic Archwires	Forestadent www.forestadent.com	NiTi	014-016-018-020 018x018 018x024 (coated)	Tooth-coloured archwires
BioCosmetic archwires	Forestadent www.forestadent.com	NiTi	017-019 016x016 016x012 018x025 (coated)	Tooth-coloured archwires
<i>G4 NiTi</i> ULTRAESTHETIC TOOTH COLORED ARCHWIRES	G&H corporation www:ghwire.com	NiTi	012-014-016-018-020 016x022 017x025 018x018 018x025 019x025 020x020 021x025	Epoxy Coating - Tooth-Colored Polymer Coated

Sentalloy® High Aesthetic Archwire	GAC www.gacintl.com	NiTi	016x022 018x018 018x025 020x020	Sentalloy® wires feature thermally activated shape memory and IonGuard® coatings that dramatically reduce friction Rhodium Ion implantation.
BioForce High Aesthetic Archwire	GAC www.gacintl.com	NiTi	016x016 016x022 018x018 018x025 019x025 020x020 021x028 022x018	BioForce® High Aesthetic is part of the first and only family of biologically correct archwires. Rhodium Ion implantation.
Orthocosmetic Elastinol	Masel www.maselortho.com	NiTi	014-016-018	The tooth-colored nickel titanium archwire has a special aesthetic coating that blends exceptionally well with ceramic or plastic brackets.
Coated Aesthetic NiTi Arches Natural Form	O.S.E. Co., INC. www.osecompany.com	NiTi	014-016-018-020 018x018 016x022 018x025	Coated with a polymeric plastic composite.
Micro-coated super elastic NiTi	O.S.E.Co.,INC. www.osecompany.com	NiTi	012-014-016-018-020 016x022 017x025 018x025 019x025 021x025	Aesthetically pleasing, this tooth colored NiTi archwire is only coated on the front surface allowing the wire to slide into bracket smoothly
ProFlex Micro-Coated	ODP http://www.odpinc.com/	NiTi SS	014-016-018 016x016 016x022 017x025 018x025	Micro-coated

Low-Friction and Colored TMA	Ormco www.ormco.com	TMA	016-018-020 0175x0175 016x022 017x025 019x025 021x025	Through Ion beam implantation we created Low-Friction and Colored Low-Friction TMA (on average 1/3 less friction).
Orthocharger	ORTHOBYTE www.ortho-byte.com	NiTi	014-016-018 016x022 018x025 019x025	The new Orthocharger™ cosmetic nickel titanium arch wires are coated with a synthetic thermosetting epoxy resin utilizing a cutting edge technology.
NITI Tooth Colored Archwire-RECTANGULAR	ORTHODIRECT www.ortho-direct.com	NiTi	016x022 018x018 018x025 019x025 020x020 021x025	Super Elastic Tooth colored archwires have ink midline for symmetrical identification. After archwire placement, rub midline gently with a cotton swab dipped in isopropyl alcohol. This will remove the majority of ink.
NITI Tooth Colored Archwire-ROUND	ORTHODIRECT www.ortho-direct.com	NiTi	012-014-016-018-020	Tooth colored archwires have ink midline for symmetrical identification. After archwire placement, rub midline gently with a cotton swab dipped in isopropyl alcohol. This will remove the majority of ink.
Uni-Coat	OrthoSpecialties www.orthospecialties.com	NiTi SS	012-014-016-018 016x016 016x022 017x025 019x025	Uni-Coat archwires have an almond colour coating on the labial and buccal surfaces of the archwire for patient aesthetics and acceptance. The lingual surfaces (facing the archwire slot) are not coated and retain their full sliding properties for maximum treatment efficiency.

Tooth Tone Coated Archwire	OrthoTecnology www.orthotechnology.com	NiTi SS	014-016-018-020 016x022 017x025 018x018 018x024 019x027 020x020	The same great features as our TruFlex Nickel Titanium and stainless steel archwires with a durable tooth coloured overcoat which offers superior aesthetics, stain resistance and low friction.
Aesthetic Wire	TP Orthodontics www.tportho.com	NiTi SS	014-016-018-020 016x022 017x025 018x025 019x025 021x025	TP Orthodontics applies a very thin .0005” tooth-colored coating only to the labial surface of aesthetic archwires, leaving the remaining three critical wire dimensions unchanged.
OPTIS	TP Orthodontics www.tportho.com	Composite	0.14 0.16 0.18	High-strength composites in a patented process that produces superior elasticity and mechanical performance. Only OPTIS Preformed Archwires use an advanced fibre-reinforced polymer composite for strength and flexibility. The excellent surface finish and uniform reinforcement distribution of OPTIS Preformed Archwires are the keys to their performance.

Table I.2: Aesthetic orthodontic archwires.

Chapter II

Relationship between Surface Roughness and Friction

II.1 Surface Roughness

Surface roughness represents all the surface irregularities that occur with relatively small step left by the manufacturing process and/or other influential factors. All the surfaces are characterised by a roughness, which is substantially the deviation of a real surface from an ideal form. It is very difficult to produce a really flat surface, even with carefully polished surfaces, hills and valleys are large compare with the size of molecule. Although the techniques of grinding and polishing have advanced recently, it remains difficult to prepare surfaces of appreciable size that are flat. Irregularities may show randomly, and usually are represented by a series of grooves, more or less ordered and regular with variable depth, disposed on a surface. If two solids are placed in contact, the upper the upper surface will be supported on the summits of the irregularities, and large areas of the surfaces will be separated by a distance which is great compared with the molecular range of action (Persson, 2000; Bowden and Tabor 2001).

Surface roughness is defined and measured imaging to dissect the surface with an orthogonal plane; this plane intersects the surface defining the real profile of the surface as the intersection in the space between the two surfaces (Figure II.1).

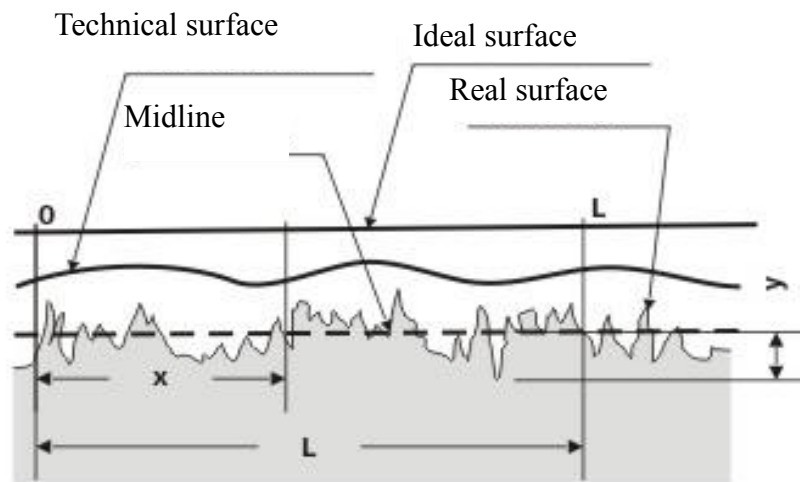


Figure II.1: Surface roughness.

There are several parameters to objectively measure the roughness, the most used was R_a , the average roughness (μm or nm). The evaluation of the surface roughness is performed on a certain length L_n said length of evaluation; it is 5 times the base length L which in turn depends on the expected value of the roughness. For the determination of the roughness R_a is taken as reference the midline of the profile, which is the line for which there is the minimum sum of distances of the square of the contour points from the same line (Figure II.2).

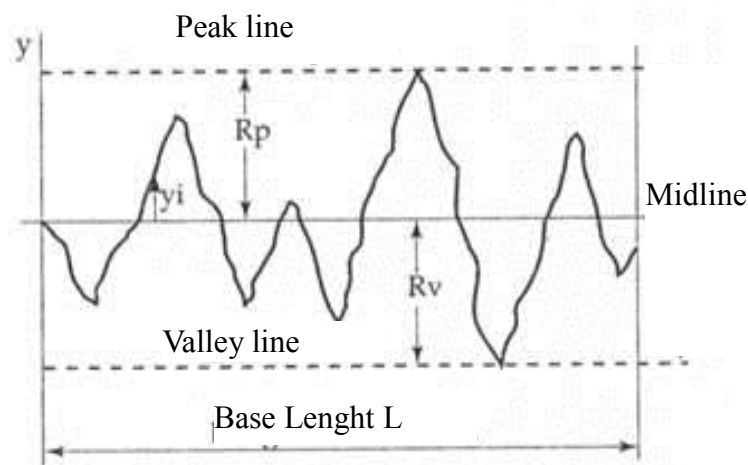


Figure II.2: Average Roughness.

Assuming the median line as x-axis, it is defined R_a the mean value of the profile ordinate y (as absolute value). Hence, R_a is the arithmetical mean of the distance between the profile points and the median line of the profile. In the discrete set the R_a formula is:

$$Ra = \frac{1}{n} \sum_{i=1}^n |yi|$$

Nevertheless, this parameter is just a mean and does not provide clear information about the quality of the surface. In fact R_a can have similar values for a surface with few high peaks or several little hills, hence is not able to clearly discriminate the surface roughness. For this reason several other parameters were inserted to describe surface roughness, the roughness R_z is the distance between two straight lines parallel to the midline drawn at a distance equal to the mean of the five highest peaks and the mean of the five lowest valleys in the range of the length of the base; R_{max} is the distance between two lines parallel to the midline, the first tangent to the highest peak and the second tangent to the lower valley; R_t also used to define the quality of the surfaces, it is defined as the maximum distance between the highest peak and the deepest valley in the base length L . Indeed, R_a is not sufficient to precisely shows surfaces characteristics and together with the previous data, another very interesting values is the R_{ms} (Root-mean-square) it is the mean square deviations of the profile points from the midline this parameter, being a quadratic mean is more sensitive to abrupt deviations of the profile to a regular pattern and it is in general greater than the R_a value.

So, R_{ms} in the discrete set will be:

$$RMS = \sqrt{\frac{1}{n} \sum_{i=1}^n yi^2}$$

These parameters return a numeric value, thus providing an indisputable value on the evaluation and comparison of the surfaces.

Surface roughness has a huge influence on many important physical phenomena such as contact mechanics, sealing, adhesion and friction (Yang et al., 2006)

In orthodontics surface topography can critically affect aesthetics, performance and biocompatibility of working orthodontic components (Kusy et al., 1988; Bourauel et al., 1998; Chern et al., 1996; Drescher et al., 1989; Kusy and Whitley 1990; Prosocki et al., 1991; Saunders and Kusy 1994; Hunt et al., 1999; Es-Souni et al., 2002; Husmann et al., 2002; Kim and Johnson, 1999; Thierry et al., 2000; Vaughan et al., 1995; Wichelhaus et al., 1997; Watanabe and Watanabe, 2003; Wichelhaus et al., 2005; Huang, 2007; Doshi and Bhad-Patil, 2011; Amini et al., 2012; Normando et al., 2013). Moreover, plaque accumulation is affected by the surface roughness and this in turn affects the properties described above (Wichelhaus et al., 2005). Hence, the surface roughness of the orthodontic archwires is considered fundamental for the evaluation of a performant wire, due to the several properties strongly linked to it. It was shown that SS alloy is the less rough wire among the commercially orthodontic wires alloy, followed by β -Ti and NiTi (Kusy et al., 1988; Bourauel et al., 1998; Hunt et al., 1999). Moreover, it is still under debate the association between high values of roughness and high values of friction. Opposite opinions exist about the influence of surface quality of wires and bracket slots on the production of friction. Frictional force between wires and brackets is considered a harmful factor that influences the normal movement of the

teeth during sliding mechanics (Frank and Nikolai, 1980) Many studies confirm that a correlation exists between surface roughness and friction (Tselepis et al., 1994; Downing et al., 1994; Bazakidou et al., 1997), but tooth orthodontic movement is a very complex process, correlated with a number of critical factors. In fact, Kusy and coll. (1988), Prosski and coll. (1991) and Ghafari (1992) found that low wire-surface roughness is not a sufficient condition for low frictional coefficients. β -Ti generally exhibits maximum frictional force, probably as a result of the adhesive and abrasive wear produced with the slot of the bracket as a result of the high reactivity of the wire's surface (Kusy et al., 1991; Kusy et al., 2004). The NiTi wire, on the other hand, creates lower friction than β -Ti wires; in fact, its stiffness and flexibility improve the performance of the archwire (Kusy et al., 1988; Matarese et al., 2008).

II.2 Friction

Friction is a complex multiscale phenomenon that depends both on the atomic interactions inside the contacts and on the macroscopic elastic and plastic deformation and on the unavoidable, stochastic roughness characterizing real surfaces that determine the morphology and stress distribution within these contacts (Rabinowicz, 1995).

Friction is a dissipative force, which impedes the relative motion of two surfaces in contact and always acts in the direction opposite to that of the movement (Jastrebski, 1987).

Several kinds of friction exist: dry friction produced by the two solid surfaces in contact; or viscous when it is relative to the contact of a solid and a fluid or to the internal movement of a liquid. Hence, friction, therefore, opposes the motion of two bodies (Kusy and Whitley, 1997). The dry friction is divided in two components, the static friction that is the force to be overcome to start a movement between two surfaces still between them, and the dynamic or kinetic friction that takes over when the phase of relative motion begins, usually the dynamic friction is less than static friction, and it is the force that must be overcome in order to continue the motion in a uniform manner. The dynamic friction opposes the direction of motion (Rossouw, 2003).

According to Amontons-Coulomb Laws, friction is equal to

$$F_r = \mu_r \times F_{\perp}$$

where μ_r represents the friction coefficient and F_{\perp} the force applied on the surfaces (Figure II.3).

On a horizontal plane F_{\perp} is equal to the weight force, on inclined plane, instead, is due to:

$$F_{\perp} = \cos\alpha \times F_p$$

The friction coefficient μ_r is dimensionless and depends by the two surfaces material in contact and by the way were processed; from the microscopic point of view the coefficient of friction μ_r is given by the forces of interaction between the atoms of the materials in contact.

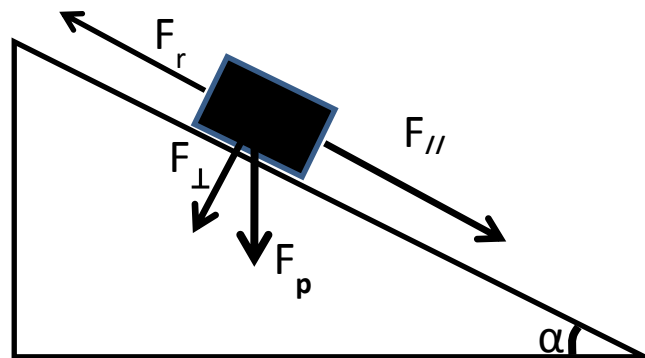


Figure II.3: Friction force. F_p weight force; F_{\perp} perpendicular component of F_p ; $F_{//}$ parallel component of F_p ; F_r friction.

Friction follows three fundamental laws (Jastrebski, 1987; Kusy et al., 1991), which however are not respected by all the materials: the first law says that the frictional force is proportional to the load applied through a constant which is the coefficient of friction μ_r ; in fact in the graph F_r / F_{\perp} the line passes through the origin and has a constant slope equal to the coefficient of friction μ_r .

The second law states that the friction coefficient μ_r is independent of the apparent contact surfaces, and this is true if the surface can be deformed plastically (Saunders and Kusy, 1994).

The third law states that the coefficient of friction μ_r of a pair of surfaces is independent of the sliding speed; however this is not always true since there are materials that are influenced by the speed of sliding (Kusy and Whitley, 1989).

Friction is formed basically of three components dependent on the characteristics of the material (Jastrebski, 1987). The causes of this resistive force are molecular adhesion (SH_{fr}), surface roughness (IN_{fr}) and the so-called effect plowed (PL_{fr}).

The molecular adhesion occurs between two surfaces in close contact made through the electromagnetic interactions between the surface components. The cutting force needed to break these bonds is a component of friction (SH_{fr}); plowed effect is when a material substantially harder than the other exceeds the yield strength of the softer material and removes it, causing abrasive damage (PL_{fr}), the surface roughness is represented by the microscopic roughness of the surface which may block to each other, interlocking, by slowing down the relative motion of the surfaces (IN_{fr}) (Zufall and Kusy, 2000^b).

Hence, friction is due to the interlocking of the surface asperities and represents in the main work of lifting the load over the summits of these asperities. When one surface slides on the other at low speed, first there is a loading phase during which the actual configuration stores elastic energy. Then, when the stored energy is large enough, instability arises: the system jumps abruptly to another configuration and releases elastic energy into irregular heat motion (Persson and Tosatti, 1996; Persson and Tosatti, 1999).

There are many possible origins of elastic instabilities, e.g., they may involve individual molecules or, more likely, groups of molecules or “patches” at the interface, which have been named stress domains (Caroli and Nozieres, 1998). As a result the overall motion may not exhibit any stick and slip behavior at macroscopic level, since the local rearrangements can occur at different times in an incoherent manner.

When the two contacting surfaces do not match, the formation of a stable state is hindered: some groups of atoms are interfaced with the other surface, occupying a

local energy minimum while some other groups of atoms cannot adjust to the local energy-minimum configuration without a deformation of the solids. In this case there is a competition between two energies: the force produced by the atoms in the local energy minimum, and the elastic energy to deform the solid so that every surface patch adjusts into a local minimum. If the latter prevails, static friction appears. Otherwise, if the solid is sufficiently stiff, local domains do not show any instability and can overcome reversibly the local barriers (Yang et al., 2006). The overall effect is a motion with no static friction, since when some domains move uphill some other regions move downhill, so that the total energy is constant. This absence of instabilities due to a mismatch of the two surfaces' structures has been named superlubricity (Shinjo and Hirano, 1993)

Friction is significantly link to other physical characteristics; in fact a strong dependence of sliding friction on the elastic modulus and surface roughness exists. Peculiarly, for stiff solids with planar surfaces extremely low friction (superlubricity) has been observed, and friction increases very abruptly as the elastic modulus of the solids decreases. Thus, a light increase in the elastic modulus results in the decrease in the frictional shear stress. Moreover, a relatively small surface roughness may kill the superlubricity state and at same time increased surface roughness, in less stiff materials, results in more instability and enhanced friction (Yang et al., 2006).

Most surfaces of solids have roughness on many different length scales (Krim et al., 1993), and it is usually necessary to consider many decades in length scale when describing the contact between solids (Persson et al., 2005).

The two most important properties are the area of real contact and the interfacial separation between the solid surfaces.

The area of real contact, and the space between two solids has a tremendous influence on many important processes heat transfer (Volokitin and Persson, 2007)

contact resistivity (Rabinowicz, 2005), lubrication (Persson, 2000), sealing (Patir and Cheng, 1978) and optical interference (Benz et al., 2006).

For small load the contact area varies linearly with the load, and the interfacial separation depends logarithmically on the load. For high load the contact area approaches the nominal contact area (i.e., complete contact), and the interfacial separation approaches zero. For the same squeezing pressure, the stronger is the adhesion the smaller is the interfacial separation.

II.2.1 Sliding Resistance in Orthodontics

Friction in orthodontics blocks or retards the relative motion of two objects in contact, the wire and the bracket, which do not slip between them. The direction of the friction is tangent to the common boundary of the two surfaces in contact. It has been verified that the portion of the strength lost due to the resistance to slipping is between 12% and 60% (Kusy and Whitley, 1997) If the frictional forces are high, the efficiency of the system is altered and the treatment time may increase, even the results of treatment can be compromised due to unwanted movement, lack of movement and anchorage loss. 1 In the oral cavity we talk about dynamic friction, although at low speeds, because the static and kinetic friction are dynamically linked (Rossouw et al., 2003). Friction occurs primarily in the processes of gain or space closure, because, if we could close a diastema with a total movement of the tooth, in the absence of friction, the whole force applied would be spent to move the element, in the presence of friction, however, our strength will decrease, then we will not have the desired movement of the tooth, to make up for this reduction we need to increase the force applied. Unfortunately, we are not always able to calculate the correct value of the friction, so often we may encounter unwanted movement (Kusy and Whitley, 1997).

Essential for proper orthodontic treatment is to evaluate some parameters that go to influence this dissipative force, each material has a different behaviour with respect to friction. The nature of friction in orthodontics is multifactorial, and stems from various biological and mechanical factors (Table II.1).

Physical and mechanical factors
Archwires properties: <i>material, shape and size of the section, surface roughness and stiffness</i>
Ligature properties: <i>materials and ligation method</i>
Bracket properties: <i>material, surface treatment, manufacturing process, width and depth of the slot, bracket design, bracket prescription</i>
Device properties: <i>interbracket distance, retraction force</i>
Biological factors
<i>saliva, plaque, acquired film corrosion and food particles</i>

Table II.1: Physical, mechanical and biological factors that affect friction (Kusy and Whitley, 1997).

Other parameters depends by the interface bracket/wire relationship, these two elements have to be compatible each other moreover in order to not compromise the sliding should not damage each other.

The oral cavity plays a key role in the friction production, in fact it was showed that the daily micro motions, presented in the mouth due to the mastication, reduce friction because minimize the normal force applied on the wire (Braun et al., 1999). During the mastication process the wire is moved within the slot, in this way the normal force, which pushes down the wire into the slot, decreases, and, as a consequence, the friction reduces (Picton, 1964; Proffit et al., 2012).

These findings suggest the absence of interferences between friction and orthodontic treatment. In this regard, it was found that factors such as the inclination of the tooth, the clearance between the bracket and the wire, the ligation methods do not have a measurable effect on the frictional resistance in a simulated oral environment, because of the continuous movement of wire and teeth (Braun et al., 1999).

In a study by Braun and coll. (1999) it was seen that each perturbation yields a

decline of friction by reducing the normal force. From this study we can notice how the oral environment decreases the friction and how this reduction depends on the intensity of the perturbation. This thesis would need more information as the perturbations used in this study are a replica inaccurate, intraoral of the dynamics.

Iwasaky and coll. (2003) belies in part what is stated by the previous study (Braun et al., 1999). They have performed experiments to measure the static friction coefficient during the sliding of an archwire in vivo. This test measured the intra-oral friction associated to sliding of a stainless steel band of 4 mm and 8 mm along an auxiliary stainless steel archwire. It has been verified that the friction coefficient was higher for the longer bands and that, although the intra-oral vibrations would decrease the friction coefficient, the frictional resistances were not totally eliminated. Furthermore, in a second experiment, claimed that the vibrations introduced by the chewing of a gum do not completely eliminate the friction although a decrease was evident.

The sliding resistance between wire and bracket are not given only by the friction classic but there are two other factors that hinder or, in some cases, help the orthodontist's work: the binding and the notching (Kusy and Whitley, 1999; Articolo and Kusy, 1999).

The binding occurs when a tooth bends or a wire flexes, practically, when a contact between the wire and the bracket wings is created.

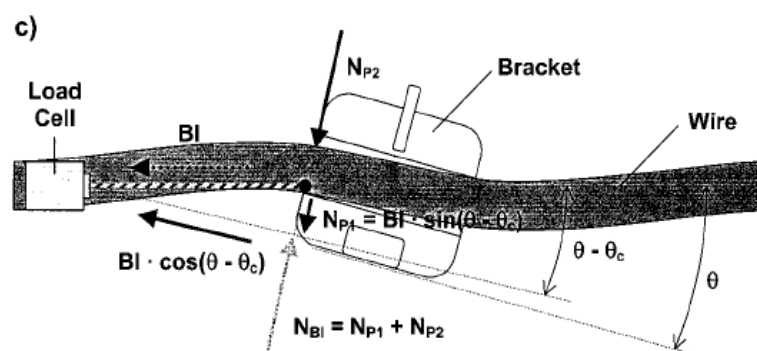


Figure II.4: Binding.

This contact between the bracket and the wire, activates forces acting perpendicular to the extremes of the bracket which increase the sliding resistance (Kusy and Whitley, 1999; Articolo and Kusy, 1999).

The notching, instead, is a real permanent deformation of the wire which causes the block of the movement of the tooth until the notch do not "relaxes" (Kusy and Whitley, 1999; Articolo and Kusy, 1999, Articolo et al., 2000). Both these parts of the sliding resistance are totally independent from the ligatures as demonstrated by various studies (Beer and Johnston, 1981; Thorstenson and Kusy, 2003). The binding has a value variable and its incidence increases with angle θ increasing. The angle θ is the angle that is formed between the wire and the edge of the slot and can have variable amplitude. In passive configuration $\theta=0$, and then the binding is absent $RS=FR$. In active configuration $\theta>0$, binding is added to the normal friction $RS=FR+BI$, when $\theta> \theta_c$ the binding has the greatest influence $RS=BI$ (Kusy and Whitley, 1999).

θ_c is the critical angle after which the friction loses its importance and if sharply exceeded involves notching, which completely prevents sliding $RS=NO$.

θ_c is an angle that depends only on the geometrical characteristics of the bracket and of the wire and it is independent from the material and the surface characteristics. The geometric parameters to be evaluated are SLOT: the width of the slot of the bracket; WIDHT: the width of the bracket; SIZE: the thickness of the wire. Through an easy demonstration is shown that:

$$\theta_c = \cos^{-1} \frac{(Size)^2 - (Width)^2}{(Size) \cdot (Slot) \pm (((Width)^2(- (Size)^2 + (Slot)^2 + (Width)^2))^{0,5}}$$

This equation is valid for all types of orthodontic brackets and wires, and in general it was found that for the value of the wires in trade in orthodontics θ_c must be between 0° and 4° to allow the sliding (Kusy and Whitley, 1999).

Brackets self ligating develop substantially lower levels of friction when compared with the conventional brackets, even if they behave in the same way of the conventional brackets against the binding (Kusy and Whitley, 2000; Whitley and Kusy, 2007).

Finally, for high values of θ , the wire is permanently deformed and the sliding may stop for the appearance of notching which is the other component of the resistive force.

The notching is an elastic deformation of the wire, it can be defined as a mechanical damage evident on an archwire and it appears during the latter stages of the binding. The release of the notch is given by a bone remodelling (Articolo et al., 2000). The notching is manifested as a defect classifiable in number, type and severity. The notch causes slow or no sliding and prevents all the movements of the tooth causing a block of the wire in the bracket. There are 14 identified notch pattern 7 for the rectangular wires and 7 for round wires plus a 10% pattern do not recognized (Figure II.5).

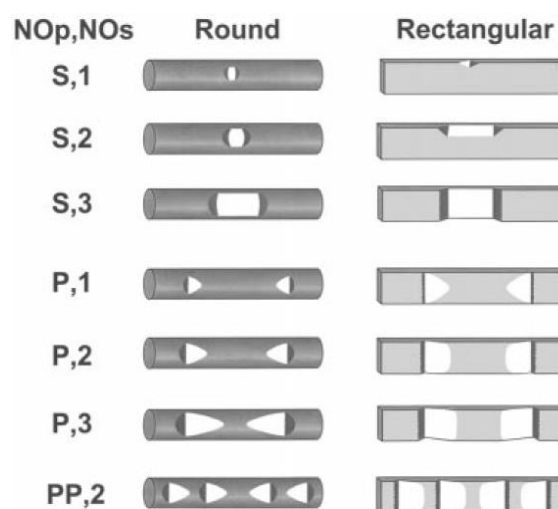


Figure II.5: Notching pattern (Articolo et al., 2000).

The notching presents some peculiarity; usually wires appear damaged more lingually than buccally and more on the canines, where there is the greater curvature of the archwires. It is clear also that wires, with higher hardness and wider, should easily meet notching; moreover, the ceramic brackets create more number of notch and of greater intensity due, probably, to the hardness and rigidity of the material (Articolo et al., 2000).

The notch is caused by mechanical damage due to the contact force between bracket and arch, and the amount and direction of movements determine the type of damage, the quality of the pattern, the severity and the frequency of notch.

There are two types of damage, the fretting wear caused by the vertical movement of the tooth with respect to the periodontal ligament, which can lead to the consumption of the wire surface, the sliding wear caused by the horizontal movement or translation of the teeth, during orthodontic treatments useful to close or open spaces, which cause erosion of the surface. The number of notch is not dependent on the time spent in the mouth or the duration of treatment. It is seen, in fact, that the greatest number of notch occurs in the first month of treatment, the period in which the wire is subjected to greater stress to realign the teeth. However, there are factors that increase the incidence of notch as: the patient's anatomic factors and parafunctional habits (Articolo et al., 2000).

Chapter III

Experimental Tools and Techniques

III.1 Atomic Force Microscope (AFM)

The AFM is a member of the family of microscopes generally indicated by the acronym SPM (Scanning Probe Microscope) (Figure III.1). The SPM construct an image of the sample under observation through the interaction of a probe with the surface atomic layers, in analogy with what is “the tip of a record player on the disk”. In both cases, an appropriate sensor converts the variations of the properties of the sample surface into an electrical signal. While in the record player the stylus touches the disk surface, in SPM, a distance of the order of a few nm always exists between the surface to be studied and the probe. The final image is obtained in response to a complex processing of the electrical signals collected by the probe. The geometry of the tip is the main limiting factor in the resolution of the SPM.

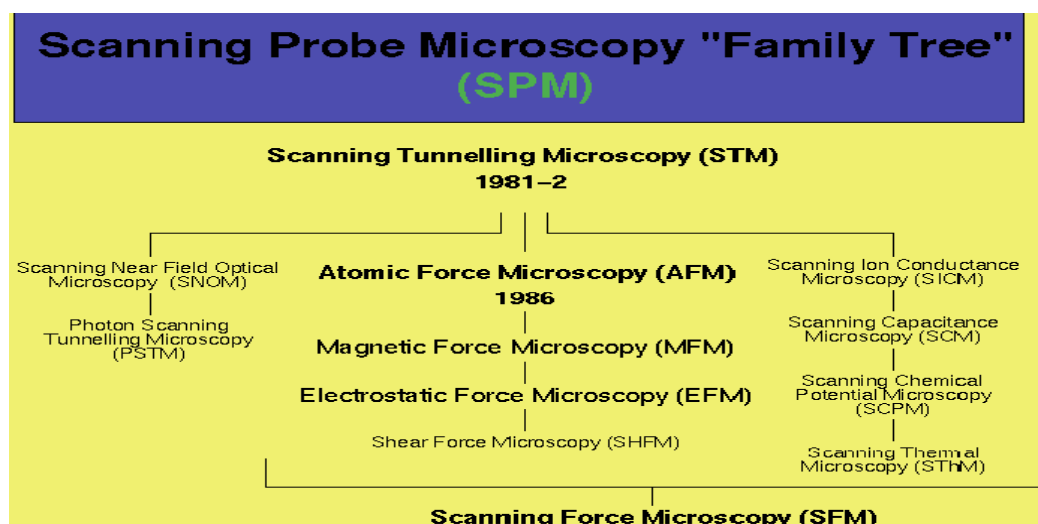


Figure III.1: SPM family tree.

In the AFM, a small tip of conductive very stiff material (in the early models was used a diamond tip) is fixed to the end of a bar or a cantilever which press the tip on the sample during the measurement process. At a close observation, the tip of any AFM is of rounded form. The radius of curvature of the terminal (end radius) constitutes an important parameter for the resolution of the instrument. The realization of tips with smaller radii of curvature always constitutes one of the main limitations to the development of atomic force microscopy. The magnitude of the deflection of the bar, ascertained by detecting the tunnel current that is created between the bar and a second tip placed above the bar, is a measure of the force acting between the sample surface and the tip (Figure III.2). The first model of AFM allowed a lateral resolution of 30 nm. In modern AFM bars have silicon tip and are covered with a material with high reflectivity (e.g. gold).

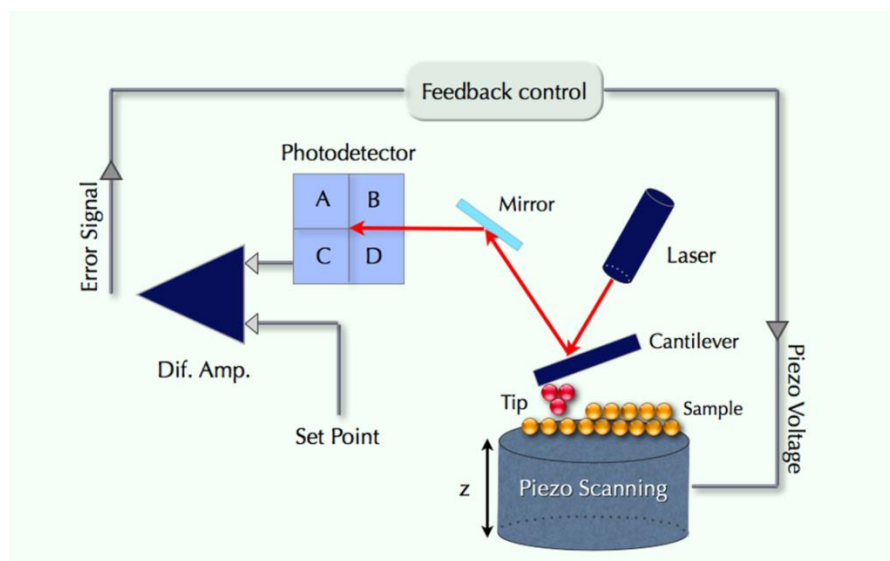


Figure III.2: Atomic force microscope (AFM) diagram of operation: The AFM consists of a cantilever, the end of which is fitted with a tip, typically composed of silicon or silicon nitride, which has a radius of curvature on the order of nanometers. Attraction and repulsion forces between the tip and the sample depend on Van der Waals forces, which cause a deflection of the cantilever (the elastic constant of which is known), in accordance with Hooke's Law. The deflection is measured using a laser light reflected from the top of the micro-lever, which will be detected by a four-quadrant photodiode. A feedback loop adjusts the distance between the tip and the sample in order to keep the force acting between them constant, which in turn allows for perfect scanning of all the surface asperities. The sample is placed on a piezo-electric tube that can move it perpendicularly (z direction) to maintain a constant force in the plane (x and y directions) to analyze the surface. The resulting map (x, y) represents the topography of the surface sample.

III.1.1 Working Principle

In the AFM the tip (the size of a few μm) slides on the surface of a sample that moves along the three Cartesian axes by means of a movement induced by a piezoelectric mechanism. A servo control system (feedback) allows holding the tip in conditions of "constant force" (to acquire information on the strength of interaction between the sample surface and the tip) or "constant height" (to acquire information on the variations in height of the sample). The oscillations of the cantilever are detected by an optical system that registers even very slight cantilever movements that supports the tip. A diode laser is focused on the rear reflective cantilever. In the measure at "constant force", during the scanning movement of the sample surface, the variations in height cause the deflection of the laser beam. A photo-analyzer measures the differences in light intensity between the two components of the binary photodiode that collects the beam deflected and converts them into a voltage that represents the result of the measurement. In the measure at "constant height" the measured voltage is proportional to the necessary strength to the distance between the sample surface and the tip is always constant. This method of use involves the knowledge of calibration parameters that must be entered before the measurement. The piezoelectric system of most SPM uses cylinders of piezoceramics as generators of the scan surface. With small displacements of the sample these microscopes are able to measure quantitatively the microtopography of the surfaces, with a lateral resolution of 5 nm and 0.01 nm vertical. The result of the observation consists in the production of a three-dimensional matrix (x, y, z) of the surface that was the subject of the scan. The first two coordinates provide one-dimensional information of the object; the third gives the measure of the heights (distances between the sample surface and tip).

The microtopography actual of the sample is reconstructed by processing

information about: the method of relative movement between the tip and the sample and the point by point results on the tip-sample distance. The forces acting between tip and sample typically range between 10^{-11} and 10^{-6} N. Considering that between two atoms joined by covalent bond at a distance of ~ 0.1 nm acts a force of about 10^{-9} N, it is understood that measurements made with the use of AFM are non-destructive.

III.1.2 Methods of Use

Depending on the mode of interaction of the tip with the surface of the sample, the AFM can be used in mode: repulsive or contact (if the tip touches the sample effectively, i.e. the distance between tip and sample is less than the average size of an atomic beam), attractive or no contact, if, while being close to the surface of the sample, the tip does not touch it actually, and tapping in the case where the tip explores the sample in order to obtain a discontinuous contact determined by a regular sequence of oscillatory movements (i.e. passing continuously from the contact condition to no contact). In the AFM different types of forces that are established between the sample and the tip can be used to produce images. In the mode no contact (with distances between tip and sample more than 1 nm) images are produced by van der Waals forces, electrostatic or magnetic or capillaries forces. In contact mode, ionic repulsion forces prevail. In addition to these forces is particularly important for the purposes of a complete and detailed of the sample is the friction force acting between the tip and the surface. In addition to being an indicator of the properties of the sample, the friction or "lateral force" or "lateral deflection" provides information about the mode of interaction between the tip and the surface.

III.1.2.i Contact mode

It's the most commonly used methods of use. The electrostatic forces acting on the tip are repulsive and have an average value of 10^{-9} N. In contact mode the tip rests on the sample following the action exerted by the piezoelectric system, on the lever which houses the tip. The deflection of the cantilever is measured and compared with the expected value. If the deflection measured is different from the expected value, the servo control system exerts a strain on the piezoelectric system so that,

moving away or approaching the tip from the surface, restores the expected value of the deflection. The voltage applied to the piezoelectric system is a measure of the profile of the sample surface. The final image is obtained by expressing this voltage as a function of the relative position of the sample (image deflection). Only a small number of AFM work in ultra-high vacuum. Most work in ambient atmosphere or with the system tip/sample immersed in a liquid with the great advantage of being able to observe the samples without the need for pretreatment. The frictional force seems to be the main cause of damage that may occur during the measurement on both the sample and measuring instruments (tip and cantilever), as well as, of the creation of artifacts in terms of distortion of the measured data. The attractive forces can be neutralized by operating with the system tip / sample immersed in a liquid. This configuration eliminates the forces of capillary action and reduces forces of van der Waals forces. It also allows the use of AFM in the study of processes occurring at the solid / liquid interface. The main limitations on the use of this configuration lie in the possible reaction between liquid and samples to be observed.

III.1.2.ii Non-contact mode

The non-contact mode provides that between the tip and the sample surface always remains a distance ranging between 5 and 15 nm. The van der Waals forces acting between the tip and the sample are quantitatively evaluated, and based on this measure a micro-topographic image of the sample is produced. The forces measured in this mode are substantially weaker than those measured in contact mode. For this reason a small oscillation is applied to the tip and weak forces are measured by analyzing the changes in amplitude, phase and frequency of the tip oscillations. In general, the production of images using the non-contact mode may be inadequate

both in consequence of the thickness of the fluid that surrounds the surface of the samples, that could be more extended of the spatial region of effectiveness of the forces that must be measured, and in the case of moving away from the sample, the action of the forces of van der Waals decays.

III.1.2.iii Tapping mode

The tapping mode represents an improvement of the non-contact mode in which it is refined the oscillation applied to the cantilever that supports the tip. This mode allows producing high resolution micro-topographic images even for samples whose surfaces can be easily damaged or cannot be analyzed using the methods discussed above. The tapping mode overcomes the problems related to the forces of friction, adhesion and electrostatic established between the tip and the surface. The tapping mode is normally used in ambient atmosphere, by applying to the cantilever an oscillation close to that of resonance by a piezoelectric system. The amplitude of the oscillation of the tip, in this way, is about 20 nm. The frequency with which the tip moves during scanning of the sample surface varies between 50 and 500 kHz. The measurement starts with the tip in no contact with the sample. Once set into oscillation, the tip gradually approaches to the surface until it starts the cyclic contact. From that moment onwards, the measurement of the variations of the oscillation, induced by the properties of the sample surface, allows to produce the image of the surface. During the measurement, the oscillation amplitude of the cantilever is kept constant by a servo control system. The oscillation frequency is selected by using an appropriate optimum calculation procedure according to the type of the sample and of the measurement configuration.

III.2 Scanning Electron Microscope (SEM)

The SEM is an electro-optical instrument, which allows, following the issue of a beam of electrons, to analyse the various signals produced by the interaction of the electrons of the beam with the test sample. The processing of these signals makes it possible to obtain a wide range of morphological, compositional and structural information relating to the various parts of the sample. The SEM in fact, despite being born with a vocation as a high-resolution three-dimensional, in recent years it has also proved to be very effective in the analysis of the chemical composition and crystallographic orientation of a sample, allowing accurate analysis both qualitative and quantitative. The extreme versatility of this tool is also guaranteed by the variety of types of samples that can be analyzed, both in terms of their nature (only materials containing fluids are not analyzable) and their shape and size (of whatever form, up to about a cubic decimeter), and for the easy preparation of the samples, which, if they are not naturally conductive (metal) should only be covered with a thin layer of a conductive element (graphite or gold).

III.2.1 Working Principle

The SEM (Figure III.3) is constituted by an electron gun, which creates the electron beam, a vacuum chamber, where is placed the sample to be examined by interacting with the electron beam, various types of detectors, which acquire the signals of beam-sample interaction and transfer them to the computer, and a screen, which reconstructs the image signal. The electronic source at the top of column generates the electron beam producing electrons by the thermionic effect by means of a filament (usually tungsten), which is led to a high temperature. The electrons are then made to accelerate energy between few hundreds and some tens of thousands of eV (typically from 200 eV to 30 keV) thanks to an anode placed under the filament. The beam from the source is divergent, but is converged and is focused by a series of electromagnetic lenses and fissures within the column.

At the lower end of the column, a series of scan coils deflects the beam by providing an alternating movement along parallel and equidistant lines, so that, once it reaches the surface of the sample, go to cover a predefined area.

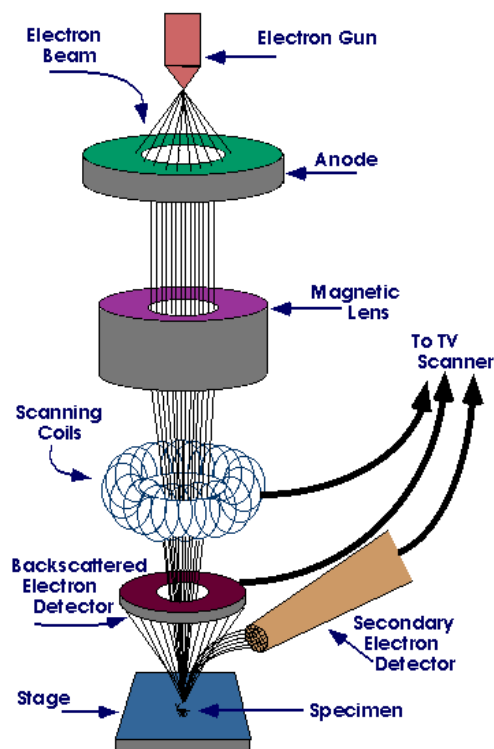


Figure III.3: SEM layout. The SEM uses a beam of high energy electrons generated by an electron gun, processed by magnetic lenses, focused at the specimen surface and systematically scanned (rastered) across the surface of a specimen. Unlike the light in a light microscope (LM), the electrons in a scanning electron microscope (SEM) never form a real image of the sample. The SEM image is in the form of a serial data stream i.e. it is an electronic image. It is a result of the beam probe illuminating the sample one point at a time in a rectangular scanning pattern (raster), with the strength of the signal generated from each point being a reflection of differences (e.g. topographical or compositional) in the sample. The screen is scanned in synchrony with the beam on the specimen in a one-to-one relationship between points on the specimen and points on the image viewing screen i.e. a point-by-point translation. Increased magnification is produced by decreasing the size of the area scanned.

The beam, finally, focused by the final lens, leaves the column and hits the sample within the vacuum chamber. As the beam electrons penetrate the sample, they lose energy, which is re-emitted from the sample in various forms. Each type of emission is potentially a signal from which to create an image.

When the electron beam hits the surface of the sample, the electrons of the beam begin to interact with the nuclei and the electron clouds of the atoms of which is constituted the sample, through two main mechanisms: elastic scattering and inelastic scattering. The result of these processes is the production of a considerable variety of signals: secondary electrons, backscattered electrons, absorbed electrons, transmitted electrons, Auger electrons, electron-hole pairs, electromagnetic radiation (UV-IR spectrum) and the radiation X. The region of the sample from which originate the signals of interaction with the beam and from which they exit to be detected is known as the volume of interaction.

The shape and size of this volume depend on the characteristics of the incident beam and by the composition of the sample and, in many cases, are more extensive in the diameter of the beam thereby determining the limit of resolution. Unlike the optical microscope, which provides a real image of the preparation in question, the SEM, thanks to the scanning of the electron beam, returns a virtual image from the signals emitted from the sample. The scan, in fact, allows the beam to hit the surface of the sample line by line, to cover the area to be examined, and the signals so generated vary in intensity, point by point, as a function of the morphological, chemical and structural properties of the sample. These signals are collected by appropriate detectors, and in order to be processed are converted from analog to digital signals. To view the signals into an image through a screen cathode ray tube (CRT), the deflection of the beam occurs in synchrony with brush deflection of the CRT, which is modulated by the signal intensity. In this way, the system reports the

signal point by point on the monitor, by matching for each point a pixel, thereby creating the image. With the exception of a few operations that can be performed mechanically by the operator (e.g. movement of the sample) the control of the instrument is fully automated and is done through some special software installed on different computers. The most intuitive of these operations are directly related to the sample: its position, then its lateral and vertical movement, its focus and the choice of magnification to use. Other fundamental functions concern the electron beam, which can be properly configured according to the type of analysis to be performed. The parameters that can be modified are substantially two: the acceleration (acting on the potential difference, between a few hundred volts to 30 kV) and the final diameter or spot-size (which may vary from about one micron to a few microns, intervening on electromagnetic lenses). The SEM provides information on the morphology of the sample surface, chemical and physical composition, electrical defects, surface contamination, and measurement of surface potentials.

The combination of high magnification, high resolution, large-amplitude field and easy preparation and observation of the sample makes the SEM one of the most reliable and easiest instrument to use.

III.3 Universal Testing Machine Instron

The Universal Testing Machine (UTM) (Figure III.4) allows the study of a wide range of physical properties such as tensile, bending, compression and fracture mechanics for any material. Moreover these machines allow quantifying exactly the coefficients of friction and possibly creeping of the sample.

UTM can perform many standard tensile and compression tests on materials, components, and structures. One kind of UTM is the Instron electromechanic system. The Instron electromechanical load frames are designed to apply a load to a specimen through a moving crosshead. The drive system moves the crosshead upwards to apply a tensile load on the specimen or downward to apply a compressive load on the specimen. A load transducer (load cell), mounted in series with respect to the specimen, measuring the load applied. The load cell converts the load into an electrical signal that is measured and displayed by the control system. The load cells are interchangeable with others of a different capacity, providing a range of possibilities of load measurements limited only by the maximum capacity of the load frame. It is also possible to use strain transducers (strain gauges) for measuring the deformation.

The main components of an electromechanical system for testing include:

- Frame load
- Command and Control Software
- Controller
- Load cell



Figure III.4: UTM Instron. The specimen is fixed in special clamps for tensile testing, or is placed on plates for compression tests. Special devices are available for individual applications, such as bending tests and peel. If you require strain measurement, an optional extensometer is attached to the specimen.

III.3.1 Working Principle

The test system operates according to the principle of closed loop servo control. The control can be based on the position of the crosshead, on the load or on the deformation.

Using the position of the cross as an example, when a trial begins, the computer sends a command to the controller, which in turn sends a control signal to a servo amplifier requiring a certain position of the crossbar. The servo amplifier receives a feedback signal of the current position of the crosshead by an encoder that is driven by the transmission system of the frame. The servo amplifier compares the command signal and the feedback signal and, if there is a difference between the two, generates an error signal that causes the engine speed to move the crosshead and in the direction that reduces the error. With the Instron two kinds of tests can be performed: “at load control”, i.e. keeping constant the load and investigating the displacement; “at displacement control”, where according to the movement changes in the load are monitored.

All the UTM are closely controlled for sensitivity, accuracy and calibration during every stage of manufacture. Every machine is then calibrated over each of its measuring ranges in accordance with the procedure laid down in British Standards 1610:1964 and IS 1828. An accuracy of $\pm 1\%$ is maintained from 20% of the load range selected to full load.

III.4 Retrieval Analysis

Although many researches have been focused on detailed studies of the mechanical and chemical properties of wires there is a lack of information on the effects of the environment on the structure and intraoral changes in surface composition. The lack of relevant evidence can be derived from the known difficulty of in vitro research to actually simulate in vivo conditions because of the multiplicity of factors present in the oral cavity such as changes in pH and temperature, the complex bacterial flora and its byproducts. In in vivo studies on orthodontic wires focuses more on the corrosion resistance of the alloy to find information regarding hypersensitivity to materials released by the wire and then to the biocompatibility of the same. Even today we are not able to successfully replicate in vivo conditions, but the retrieval analysis can be useful to see how the archwires interacts with the oral environment (Bourauel et al., 2008). The retrieval analysis has recently gained a special interest in the study of dental materials, because it provides useful data for the analysis of the performance of the material in the environment in which it was intended to work. This type of analysis has been used for years in other branches of medical research, such as in orthopedics. Furthermore, the development of standards for retrieval materials analysis is strongly indicative of the importance of this method in the study of the functionality of the materials. The main disadvantages of this type of analysis are the lack of a sequential description of the alteration produced and the inability to obtain quantitative data (Eliades et al., 2000).

Chapter IV

Evaluation of Surface Roughness of Orthodontic Wires by means of Atomic Force Microscopy

IV.1 Abstract

Objective: To compare the surface roughness of different orthodontic archwires. **Materials and Methods:** Four nickel-titanium wires (Sentalloy, Sentalloy High Aesthetic, Titanium Memory ThermaTi Lite, and Titanium Memory Esthetic), three β -titanium wires (TMA, Colored TMA, and Beta Titanium), and one stainless-steel wire (Stainless Steel) were considered for this study. Three samples for each wire were analysed by atomic force microscopy (AFM). Three-dimensional images were processed using Gwiddion software, and the roughness average (R_a), the root mean square (R_{ms}), and the maximum height (M_h) values of the scanned surface profile were recorded. Statistical analysis was performed by one-way analysis of variance (ANOVA) followed by Tukey's post hoc test ($P < 0.05$). **Results:** The R_a , R_{ms} , and M_h values were expressed as the mean \pm standard deviation. Among as-received archwires, the Stainless Steel ($R_a = 36.6 \pm 5.8$; $R_{ms} = 48 \pm 7.7$; $M_h = 328.1 \pm 64$) archwire was less rough than the others (ANOVA, $P < 0.05$). The Sentalloy High Aesthetic was the roughest ($R_a = 133.5 \pm 10.8$; $R_{ms} = 165.8 \pm 9.8$; $M_h = 949.6 \pm 192.1$) of the archwires. **Conclusions:** The surface quality of the wires investigated differed

significantly. Ion implantation effectively reduced the roughness of TMA. Moreover, Teflon-coated Titanium Memory Esthetic was less rough than was ion-implanted Sentalloy High Aesthetic.

IV.2 Introduction

The availability of different alloys for orthodontic archwires has been one of the main breakthroughs in orthodontic materials research, leading to key improvements in the field of mechanotherapy (Eliades, 2007). New materials are constantly being proposed to the orthodontists, and this sometimes increases confusion about the actual characteristics of the wires. In fact, the ubiquitous claims of improved performance are not always supported by accurate information. Thus, the characterization of archwire alloys can be considered an initial step in understanding wire behaviour in the clinical context (Krishnan and Kumar, 2004). Several properties should be considered in the search for the ideal archwire: aesthetics, biostability, friction, formability, weldability, resilience, and springback (Kusy and Whitley, 1997). Moreover, among the alloys' characteristics that alter the behaviour of the archwires, the surface roughness plays an important role. Studies (Wichelhaus et al., 2005) have shown that the surface characteristics influence both the performance and the biocompatibility of orthodontic archwires. In addition, surface topography can critically modify the aesthetics, corrosion, and efficiency of orthodontic components (Kusy et al., 1988). Furthermore, plaque accumulation is affected by surface roughness variation, and this, in turn, has a key role on the other properties previously described (Wichelhaus et al., 2005). Above all, surface roughness may modify the friction coefficient (Tselepis et al., 1994; Downing et al., 1994; Bazakidou et al., 1997). Friction is a dissipative force that resists the relative motion of two objects in contact (Rossouw, 2003). In orthodontics it interferes with the correct sliding of the bracket along the wire (Kusy et al., 1988). Friction depends on the following factors: (1) molecular adhesion (i.e., the electromagnetic forces between atoms), (2) the interlocking produced by surface roughness, and (3)

the plowing effect (Jastrebski, 1987). It is interesting to note that if the surface can be deformed plastically the coefficient of friction (μ) is independent from the contact visible area, as determined by the second law of friction (Jastrebski, 1987; Saunders and Kusy, 1994). Nevertheless, a basic premise of the theory of friction is that apparently flat and smooth surfaces are not smooth when analysed on a microscopic scale. The surface of metals is actually rough, and the asperities determine this roughness (Rossouw et al., 2003). Microscopically, the effective interface area (Σ_{eff}) between two solids is a very small part of the nominal interface area Σ_0 . The effective area is defined as the summed area of contact between the microscopic irregularities of surfaces (Bowden and Tabor, 1950); these points, called asperities, bear the entire load between the surfaces (Rossouw et al., 2003). Therefore, a critical step in the evaluation of archwire performance is the analysis of the surface roughness of different wires available in the market. In past years, the main technique with which to determine surface roughness was the surface profilometry (Bourauel et al., 1998) in which a thin tip was used to scan the topography in a single line of a preselected area. The main drawback of this method was the impossibility of measuring surface defects adjacent to the scan line; furthermore, the profilometry was invasive, and damage to the surface was possible during scanning. Thus, the increasing demand for non-destructive and non-invasive techniques has enhanced new methods of analysis, based on optical methods (Vorburger and Teague, 1981) on a developed scanning tunnelling microscope (Binning et al., 1982). With these methods it is possible to scan a preselected surface area of a model without direct interaction. The scanning probe microscopy includes different types of scanning tunnelling microscopes, the atomic force microscope (AFM) (Binning et al., 1986) and the magnetic force microscope. The AFM is considered the most appropriate tool for measuring surface topography

because it can provide three-dimensional information on surface morphology (Wennerberg et al., 1996). The aims of this study were to compare the surface roughness of eight types of as-received archwires by means of AFM and to evaluate the advantages of AFM in the analysis of orthodontic materials.

IV.3 Materials and Methods

Three orthodontic archwire alloys were considered for this study: stainless-steel (SS), β -titanium (β -Ti), and nickel-titanium (NiTi) alloys. In order to ensure wide availability of data, four NiTi round wires (0.016 inches; Sentalloy and Sentalloy High Aesthetic, GAC International, Bohemia, NY; Titanium Memory ThermaTi Lite and Titanium Memory Esthetic, AO, Sheboygan, Wisc); three β -Ti rectangular wires (0.016x0.022 inches; TMA and Colored TMA,Ormco, Glendora, Calif; Beta Titanium, AO); and one SS rectangular wire (0.016x0.022 inches; Stainless Steel, AO) were selected. In order to analyse approximately straight specimens, three samples of each wire product (5 mm) were cut from the end of three different preformed archwires and were observed with an AFM (AFM Perception, Assing, Italy) operating in contact mode under ambient conditions. The samples were attached to a metal holder using a rapid-drying cyanoacrylate glue, and then, for each specimen, 20 areas (15x15 μm) of the surface were randomly selected and analysed (N=60). AFM probes (curvature radius<10 nm) mounted on cantilevers (250 μm), with a spring constant of 0.1 N/m, were used. Three-dimensional images (400x400 lines) were processed using Gwyddion software 2.9 (<http://www.gwyddion.net>), and average roughness (R_a), mean square roughness (R_{ms}), and maximum value height (M_h) were recorded. The R_a and R_{ms} represent the arithmetical mean of the absolute values and the root mean square value of the scanned surface profile, respectively; M_h is the maximum height of a profile peak. Statistical analysis of the data was performed by means of one-way analysis of variance (ANOVA) followed by a Tukey's post hoc test. The level of significance was set at $P<0.05$.

IV.4 Results

Topographic irregularities were observed in all of the wires tested. Figure IV.1 shows representative three-dimensional AFM topography images (15x15 mm) of the eight wires analysed, while Figure IV.2 shows the two-dimensional images in order to better evaluate the dimension of nanodomains. As shown in Figures IV.1 and IV.2, the surface morphologies of the archwires differed from one another based on their composition. The three roughness parameters were used to quantitatively evaluate the surface topography of each archwire and are shown in Table IV.1 as mean \pm standard deviation in nanometres. Statistically significant differences between different types of alloys were found (Table IV.2). Among the NiTi archwires, Titanium Memory Esthetic was determined to be the least rough (ANOVA, $P < 0.05$), followed by Sentalloy and ThermaTi. Sentalloy High Aesthetic, an ion-implanted wire, was the roughest (ANOVA, $P < 0.05$). Among the β -Ti archwires, Colored TMA showed the lower parameter values, while no treated Beta Titanium and TMA presented a rougher surface. Stainless Steel ($R_a = 36.6 \pm 5.8$; $R_{ms} = 48 \pm 7.7$; $M_h = 328.1 \pm 64$) was determined to be significantly less rough than the other alloys (ANOVA, $P < 0.05$).

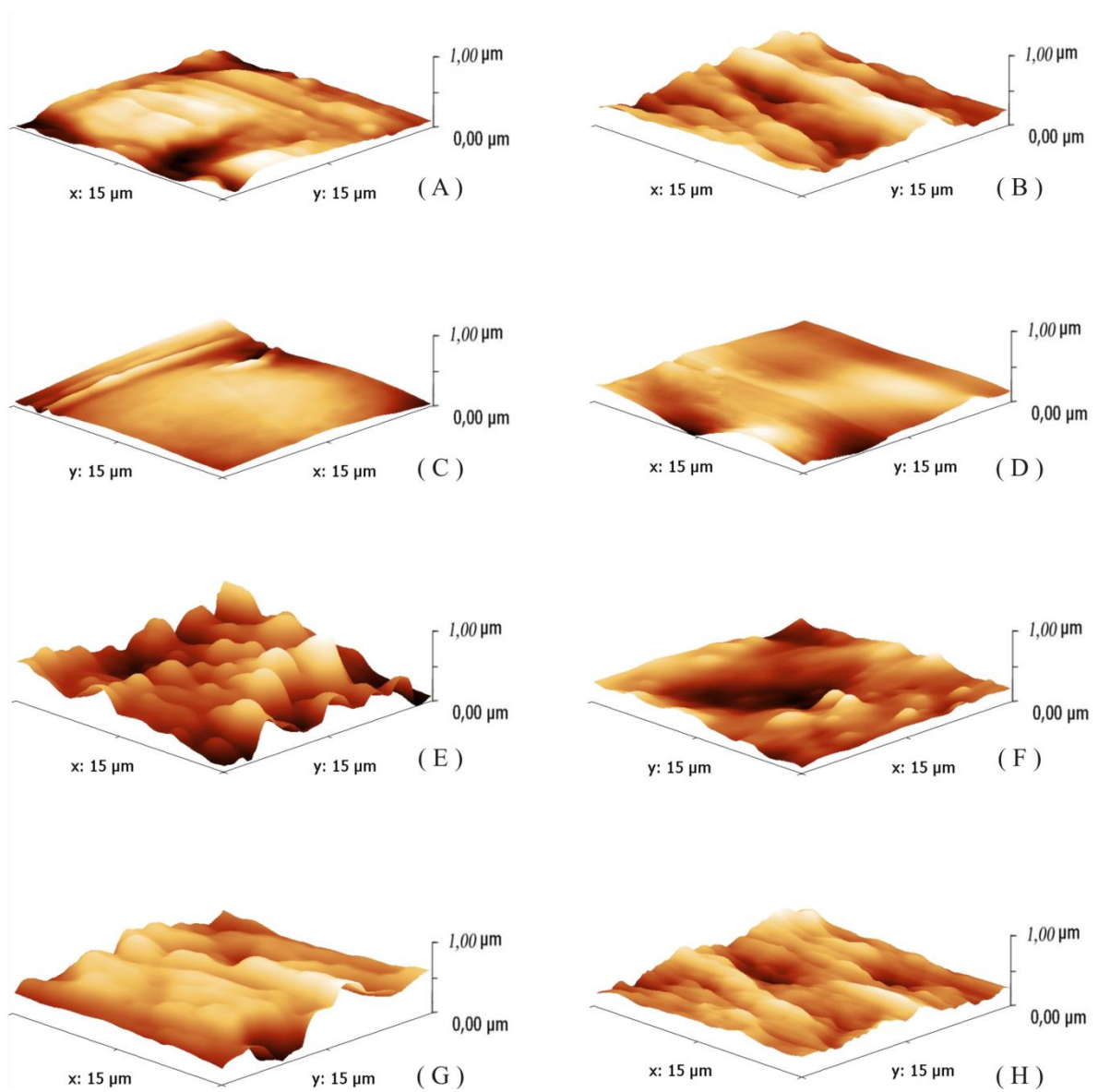


Figure IV.1: Representative three-dimensional AFM topography images (15x15 μm) of the eight samples of orthodontic archwires: Stainless Steel (A), Beta-Titanium (B), Titanium Memory Esthetic (C), Titanium Memory ThermaTi Lite (D), Sentalloy High Aesthetic (E), Sentalloy (F), TMA (G), and Colored TMA (H).

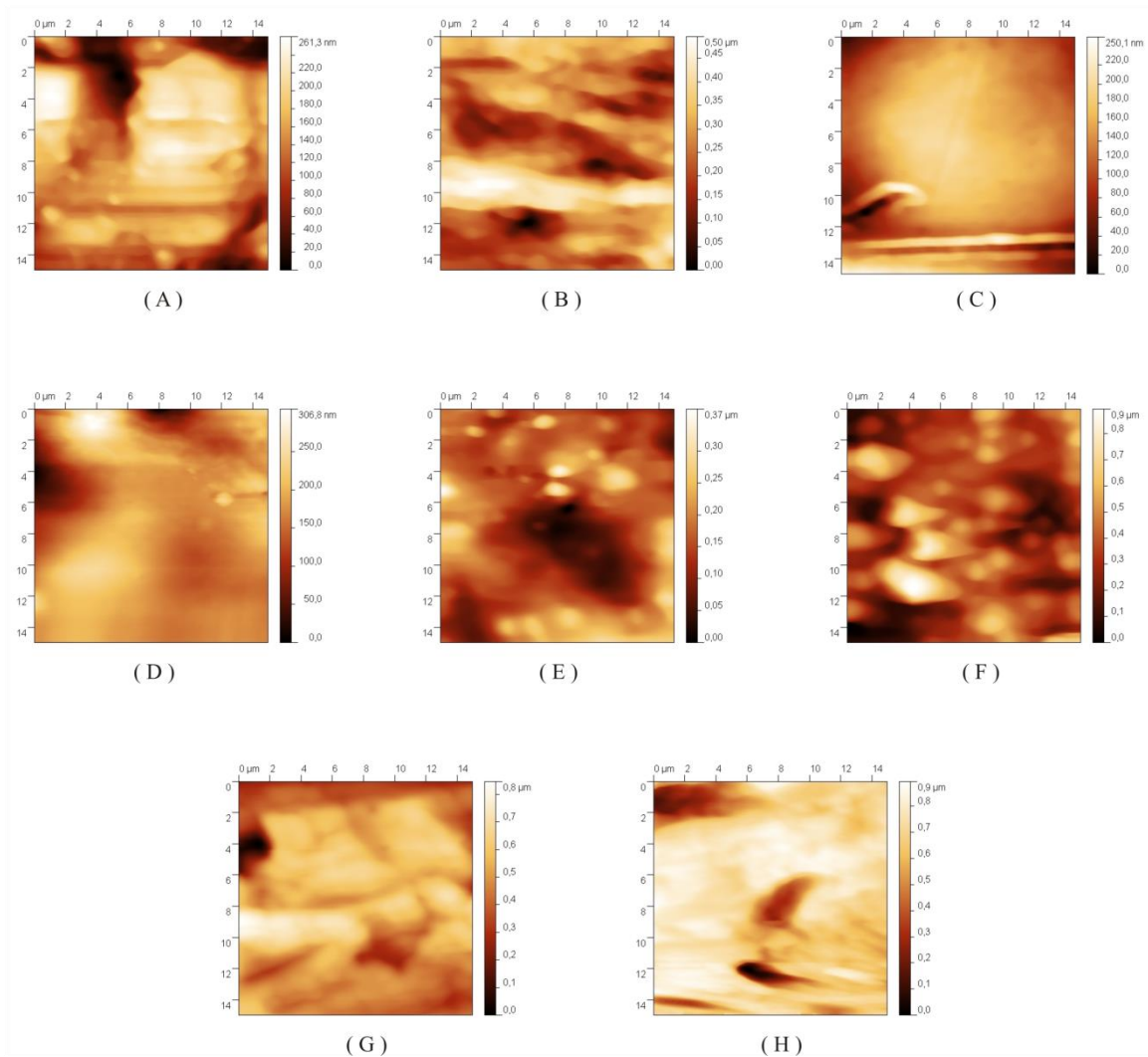


Figure IV.2: Representative AFM topography images (15x15 μm) of the eight samples of orthodontic archwires: Stainless Steel (A), Beta-Titanium (B), Titanium Memory Esthetic (C), Titanium Memory ThermoTi Lite (D), Sentalloy High Aesthetic (E), Sentalloy (F), TMA (G), and Colored TMA (H).

Tested archwires	R_a (mean±SD)	R_{ms} (mean±SD)	M_h (mean±SD)
Sentalloy	71.1±15.4	86.9±18.4	497.3±142.8
Sentalloy High Aesthetic	133.5±10.8	165.8±9.8	949.6±192.1
Titanium Memory ThermaTi Lite	82±27.3	115.5±40.5	727.5±256.8
Titanium Memory Esthetic	44.9±17	55.3±20.6	306.7±130.2
Stainless Steel	36.6±5.8	48±7.7	328.1±64
TMA	120±38.7	155.1±46.9	876.6±401
Colored TMA	69.5±25.1	88.8±33.2	540.9±118
Beta Titanium	77.9±22.4	95.7±26.4	580.4±286.3

Table IV.1: R_a , R_{ms} and M_h of AFM topography images.

Tukey's Multiple Comparison Test	R _a	R _{rms}	M _h
Sentalloy vs. Sentalloy High Aesthetic	***	***	***
Sentalloy vs. Titanium Memory Esthetic	**	*	ns
Sentalloy vs. TMA	***	***	***
Sentalloy vs. Colored TMA	ns	ns	ns
Sentalloy vs. Beta Titanium	ns	ns	ns
Sentalloy vs. Stainless Steel	***	**	ns
Sentalloy vs. Titanium Memory ThermaTi Lite	ns	ns	ns
Sentalloy High Aesthetic vs. Titanium Memory Esthetic	***	***	***
Sentalloy High Aesthetic vs. TMA	ns	ns	ns
Sentalloy High Aesthetic vs. Colored TMA	***	***	***
Sentalloy High Aesthetic vs. Beta Titanium	***	***	***
Sentalloy High Aesthetic vs. Stainless Steel	***	***	***
Sentalloy High Aesthetic vs. Titanium Memory ThermaTi Lite	***	**	ns
Titanium Memory Esthetic vs. TMA	***	***	***
Titanium Memory Esthetic vs. Colored TMA	*	*	**
Titanium Memory Esthetic vs. Beta Titanium	***	***	**
Titanium Memory Esthetic vs. Stainless Steel	ns	ns	ns
Titanium Memory Esthetic vs. Titanium Memory ThermaTi Lite	***	***	***
TMA vs. Colored TMA	***	***	*
TMA vs. Beta Titanium	***	***	***
TMA vs. Stainless Steel	***	***	***
TMA vs. Titanium Memory ThermaTi Lite	**	*	ns
Colored TMA vs. Beta Titanium	ns	ns	ns
Colored TMA vs. Stainless Steel	**	**	*
Colored TMA vs. Titanium Memory ThermaTi Lite	ns	ns	ns
Beta Titanium vs. Stainless Steel	***	***	*
Beta Titanium vs. Titanium Memory ThermaTi Lite	ns	ns	ns
Stainless Steel vs. Titanium Memory ThermaTi Lite	***	***	***

Table IV.2: P-values from statistical analysis of archwires roughness parameters (ANOVA with Tukey's post hoc test). * (P<0.05), ** (P<0.01) and * (P<0.001) indicate significant statistically differences between the two archwires.**

IV.5 Discussion

In the present study, topographic surface characteristics of orthodontic as-received archwires were evaluated by means of AFM. The AFM belongs to the family of scanning probe microscopes, a class of tools that, using interatomic interactions, acquires information on detected surfaces; this microscope obtains the images by sensors, consisting of sharp points interacting with the specimen surface. The AFM is considered a promising technique for the evaluation of surface qualities of dental materials (Silikas et al., 2001; Kakaboura et al., 2007; Lee et al., 2010). Our results showed that the least rough wire was the Stainless Steel wire. It has been demonstrated that SS shows the lowest frictional coefficient and the lowest sliding resistance, when used in passive configuration, because of its combination of low roughness, high hardness, and high strength (Kusy et al., 2004). β -Ti archwires were the roughest, which could be associated with the great friction generated by this material (Kapila and Sachdeva, 1989; Burstone and Goldberg, 1980). These data are consistent with those from the study of Doshi and Bhad-Patil (2011), which showed higher values of surface roughness for TMA, but they are in contrast with the results of several studies (Kusy et al., 1988) in which NiTi wires were considered the roughest. Titanium Memory Esthetic, a Teflon-coated wire, was the least rough among the NiTi archwires, being slightly rougher than Stainless Steel. On the other hand, the Sentalloy High Aesthetic, which is produced by ion implantation of rhodium, showed the highest values of roughness. The ion implantation and the Teflon coating are the most common archwire surface treatments (Husmann et al., 2002; Elayyan et al., 2010). These procedures should decrease the surface roughness of the materials and should improve the sliding of the wire (Wichelhaus et al., 2005; Husmann et al., 2002; Neumann et al., 2002).

Although further studies should be conducted to assess the deterioration of the coating during clinical practice, in evaluating the properties of Teflon-coated as-received archwires Husmann and coll. (2002) and Farronato and coll. (2012) found that in vitro, the coating reduced the friction between wires and brackets. Furthermore, our study showed that not only did ion implantation of rhodium fail to drastically reduce the surface roughness of NiTi wires it even increased it (Wichelhaus et al., 2005; Bourauel et al., 1998). Ion implantation decreased the roughness of β -Ti alloy. Colored TMA was less rough than were no treated β -Ti wires. Burstone and Franzin-Nia (1995) stated that ion implantation increased archwire hardness, reduced flexibility, and improved surface finish; to obtain the maximum reduction on frictional force, ion implantation should be used on brackets and on archwires over and over again (Doshi and Bhad-Patil, 2011). An important factor that influences the surface topography of orthodontic wires is, therefore, the production technique; this hypothesis was confirmed by the fact that the roughness measured for various products from the same batch was quite homogeneous. Opposite opinions exist about the influence of surface quality of wires and bracket slots on the production of friction. Frictional force between wires and brackets is considered a harmful factor that influences the normal movement of the teeth during sliding mechanics (Frank and Nikolay, 1980) Many studies (Tselepis et al., 1994; Downing et al., 1994; Bazakidou et al., 1997; Nanda, 2005) confirm that a correlation exists between surface roughness and friction, but tooth orthodontic movement is a very complex process, correlated with a number of critical factors. In fact, Kusy and coll. (1988) Prosocki and coll. (1991) and Ghafari (1992) found that low wire-surface roughness is not a sufficient condition for low frictional coefficients. Among the selected alloys, TMA generally exhibits maximum frictional force, probably as a result of the adhesive and abrasive wear produced

with the slot of the bracket as a result of the high reactivity of the wire's surface (Kusy et al., 1991; Kusy et al., 2004) The NiTi wire, on the other hand, creates lower friction than do the SS and β -Ti wires; in fact, its stiffness and flexibility improve the performance of the archwire (Kusy et al., 1988; Matarese et al., 2008). The first law of friction, the Amontons-Coulomb Law, states that $F_r = \mu \times F_n$, where μ (friction coefficient) depends on the roughness of the wires and on its physical characteristics (Jastrebski, 1987; Huang, 2007) and where F_n (normal force) is the force that keeps adhering the two surfaces (wire and bracket). In active configuration (Kusy and Whitley, 1997) normal force, which binds the two surfaces, is greater for the stiffer wires, like SS wires, which are less flexible and impact hard against the bracket, developing a stronger contact force. In contrast, more flexible wires like NiTi wires, although more wrinkled, impact less on the surface of the bracket and develop a lighter normal force. Finally, it should be noted that surface roughness also modifies other characteristics of the wires in addition to friction: the aesthetics of the product, the corrosion, the biocompatibility, and the performance (Kusy et al., 1988; Bourauel et al., 1998; Husmann et al., 2002; Wichelhaus et al., 2005). In conclusion, our investigation demonstrated the potential use of an AFM for the study of surface properties of orthodontic materials. In particular, the AFM has many advantages, such as the production of topographical three-dimensional images in real space with a very high resolution ($<10 \text{ \AA}$). The samples do not require any special treatment, such as metallization, and the AFM can provide quantitative values for the investigated parameters. The most important AFM drawback is the small scan size, which, in association with the slow velocity of scanning, often impedes a complete analysis of the sample (Braga and Ricci, 2004) Therefore, there might be some unselected regions with surface defects, thus with very rough, that would be of clinical importance.

IV.6 Conclusions

This study showed great variability in the surface roughness of wires, with Stainless Steel turning out to be the least rough. The ion-implantation technique was advantageous for β -Ti wires.

The clinical relevance of this study should be considered in light of all the other factors that contribute to sliding resistance, and further studies must be undertaken to assess the variation of surface roughness that follows the clinical use and its correlation with the friction.

Chapter V

Effects of Intraoral Aging on Surface Properties of Coated Nickel-Titanium Archwires

V.1 Abstract

Objective: To evaluate the effects of intraoral aging on surface properties of aesthetic and conventional nickel-titanium (NiTi) archwires. **Materials and Methods:** Five NiTi wires were considered for this study (Sentalloy, Sentalloy High Aesthetic, Superelastic Titanium Memory Wire, Esthetic Superelastic Titanium Memory Wire, and EverWhite). For each type of wire, four samples were analysed as received and after 1 month of clinical use by an atomic force microscope (AFM) and a scanning electron microscope (SEM). To evaluate sliding resistance, two stainless steel plates with three metallic or three monocrystalline brackets, bonded in passive configuration, were manufactured; four as-received and retrieved samples for every wire were pulled five times at 5 mm/min for 1 minute by means of an Instron 5566, recording the greatest friction value (N). Data were analysed by one-way analysis of variance and by Student's t-test. **Results:** After clinical use, surface roughness increased considerably. The SEM images showed homogeneity for the as-received control wires; however, after clinical use aesthetic wires exhibited a heterogeneous surface with craters and bumps. The lowest levels of friction were

observed with the as-received Superelastic Titanium Memory Wire on metallic brackets. When tested on ceramic brackets, all the wires exhibited an increase in friction (t-test; $P < 0.05$). Furthermore, all the wires, except Sentalloy, showed a statistically significant increase in friction between the as-received and retrieved groups (t-test; $P < 0.05$). Conclusion: Clinical use of the orthodontic wires increases their surface roughness and the level of friction.

V.2 Introduction

In recent decades, progress in the technology of orthodontic materials has resulted in a large variety of wires with a wide range of properties. Nickel-titanium (NiTi) is one of the most commonly used alloys to manufacture archwires because of its good mechanical and clinical properties (Brantley, 2001; Cioffi et al., 2012). The most important advantages of NiTi wires are their springback and pseudoelasticity, which allows a wide deflection and activation range by delivering low forces (Kusy, 1997). The growing demand of aesthetic appliances led to the introduction of coated NiTi archwires into the orthodontic market. There are two main techniques to modify the wire's surface: ion implantation and coating with polymeric resins composed mainly of polytetrafluoroethylene.

Ion implantation is a permanent modification of the surface composition by inserting ionized atoms (Husmann et al., 2002). In contrast, tooth-colored coatings, with a 20–25 μm thick layer, are usually applied in an atomizing process by using purpose-cleaned compressed air as a transport medium for the atomized particles (Husmann et al., 2002). Coating or refining the wire's surface influences the aesthetic, mechanical, and biological properties of the wires (Wichelhaus et al., 2005). Furthermore, many studies have shown that surface characteristics may directly influence the efficiency of archwire-guided tooth movement (Kusy et al., 2008; Bourauel et al., 1998). Recently, there has been growing interest in the evaluation of aesthetic, mechanical, structural, and surface properties of tooth-colored archwires. It has been reported that coating may or may not increase unloading forces and surface roughness of as-received wires, depending on the technique used for surface treatment (Wichelhaus et al., 2005; Elayyan et al., 2008; D'Antò et al., 2012; Iijima et al., 2012). Loss of a significant amount of coating

(Elayyan et al., 2008; Bradley et al., 2013), poor colour stability (da Silva et al., 2013^a), change of mechanical behaviour and force values (Bradley et al., 2013) and increase in surface roughness (Elayyan et al., 2008; da Silva et al., 2013^c) have all been reported after clinical use. Therefore, the hypothesis tested in this study is that oral environment exposure affects the surface of ion implanted and polymer-coated aesthetic archwires. Furthermore, we evaluated how these surface modifications affect friction between archwires and brackets in passive configuration, which is the component of sliding resistance that may be directly affected by an increase in surface roughness.

V.3 Materials and Methods

Five superelastic round 0.016-inch NiTi archwires were used in this study: Esthetic Superelastic Titanium Memory Wire (Polymer Coated), EverWhite (Polymer Coated), and the uncoated control Superelastic Titanium Memory Wire (American Orthodontics, Sheboygan, Wis); Sentalloy High Aesthetic (ion implanted) and the uncoated control Sentalloy (GAC International, Islandia, NY). The archwires were divided in two groups: the first group (as-received) was formed by the as-received wires; the second group (retrieved) consisted of archwires used for 1 month of treatment on Radiance brackets, slot size 0.022x0.028 inch (American Orthodontics), and ligated with elastomeric modules (colored ligatures, American Orthodontics). These NiTi wires were retrieved during the regular treatment visits of patients. The NiTi archwire insertion and retrieval were performed according to the procedure reported by Eliades and coll. (2000). Ethical approval was obtained by the Ethical Committee of Bambino Gesù` Hospital, Rome, Italy. All the retrieved samples were cleaned with 95% ethanol to remove any precipitation. To investigate wire surface morphology on the micrometer scale, a scanning electron microscope (SEM) was used. Four samples of each wire were observed. For this purpose the polymer-coated Esthetic Superelastic Titanium Memory Wire and Ever-White wire specimens were vacuum-coated with a thin layer of gold-platinum. The samples were attached to a metal holder using rapid-drying cyanoacrylate glue. The morphology surface analysis was performed by an SEM (FEI, Eindhoven, The Netherlands); the images were recorded at x200, x500, and x1000 magnification. To analyse approximately straight specimens, four samples of each wire product (5 mm) were cut from the end of four different preformed archwires and were observed by means of an atomic force microscope (AFM Perception, Assing, Italy) operating in contact mode under ambient conditions, as previously reported

(D'Antò et al., 2012; Ametrano et al., 2011). A standard statistical software package (SPSS version 20.0, SPSS IBM, New York, NY) was used for data analysis. The Kolmogorov-Smirnov test was applied to verify the normality of the data and one-way analysis of variance (ANOVA) followed by Tukey's post hoc test or t-test for unpaired data were performed. The level of significance was set at $P < 0.05$. In addition, the frictional properties of the archwires were evaluated. Two stainless steel plates were manufactured to obtain the best adaptation with an Instron 5566 (Instron Corporation, Canton, Mass), and on these plates two kinds of brackets were bonded. Every archwire was coupled with each type of bracket, a metallic bracket Mini Master Series (American Orthodontics) and an aesthetic bracket Radiance (American Orthodontics). Three metallic and three aesthetic brackets (upper right lateral incisor, canine, and first premolar brackets) were bonded on the two different stainless plates with an orthodontic composite (Transbond XT Light Cure Adhesive, 3M Unitek). To avoid binding, the brackets were positioned aligned, in a perfect passive configuration, at an interbracket distance of 7.5 mm. Bracket alignment was tested using a straight stainless steel arch 0.021x0.025 inch. The archwires were settled with elastomeric modules to avoid the strength variability of metallic ligatures. The experiment was conducted in a dry state. The base was fixed to the machine through a vise, and four samples for each wire typology were subjected to tensile tests with a dynamometer Instron 5566 with a load cell of 50N. The friction produced by the archwires was recorded at a rate of 5 mm/minute for 1 minute. Each sample was assessed five times for types of bracket, and the friction for every couple archwire-bracket was recorded with a total six hundreds value for a minute. For each test the greatest friction value expressed in Newton (N) (Figure V.1-5) was recorded. The Kolmogorov-Smirnov test was applied to verify the normality of the data, and ANOVA followed by Tukey's post hoc test or t-test were performed. The level of significance was set at $P < 0.05$.

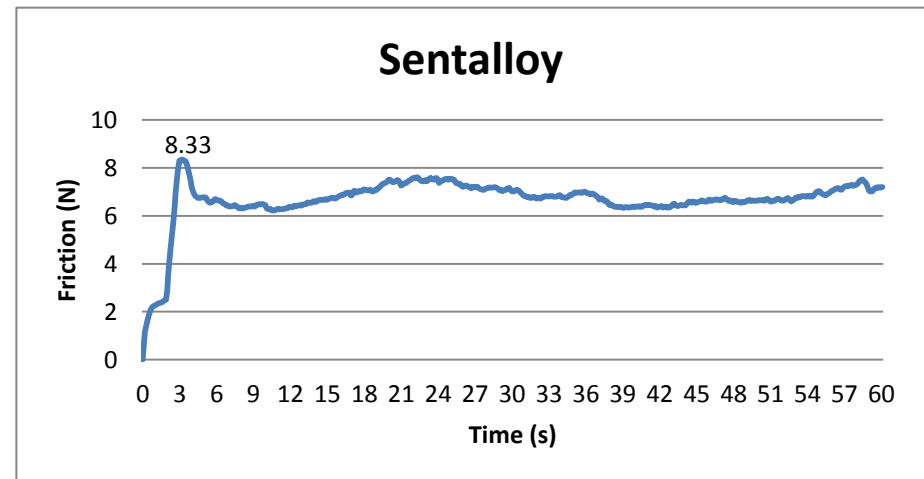
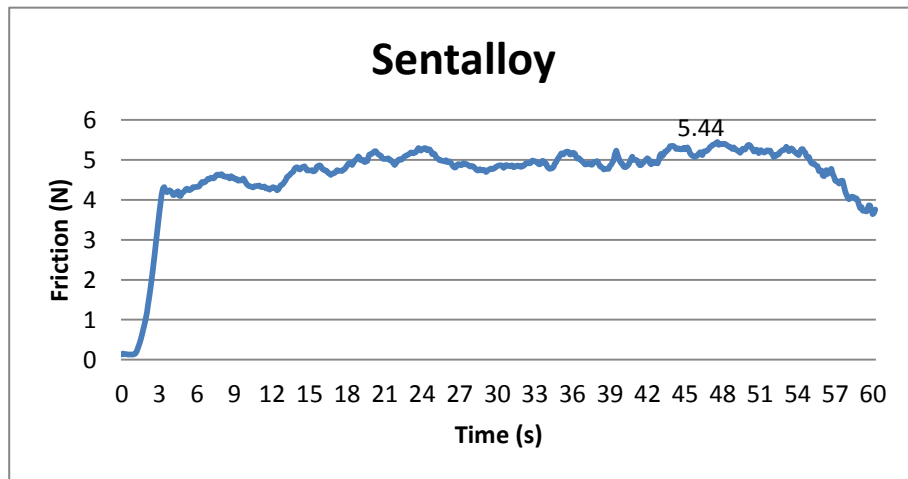
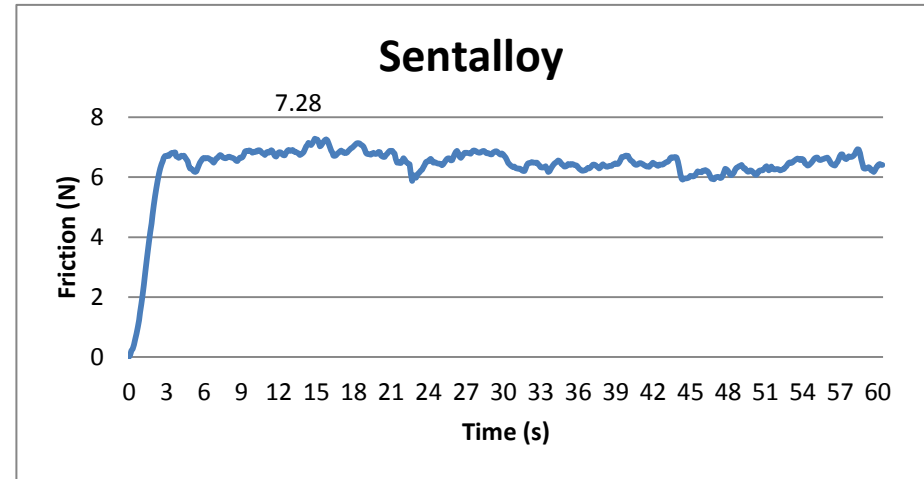
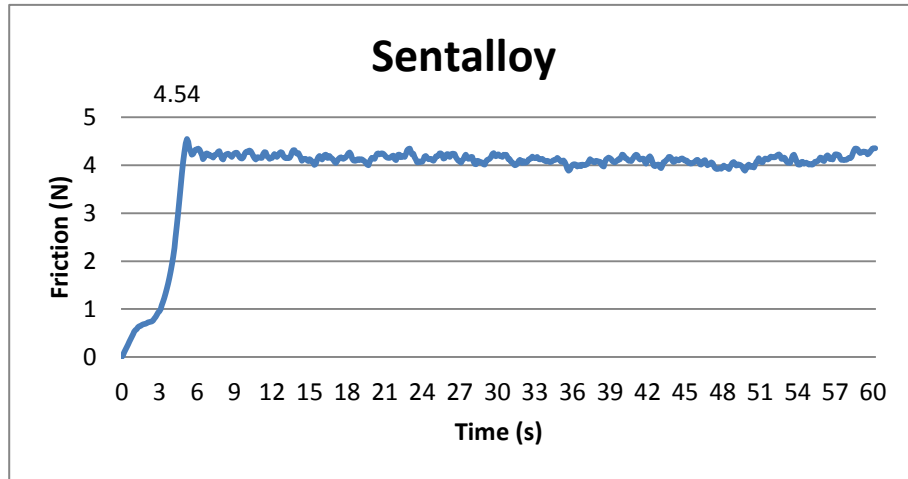


Figure V.1: Representative Time-Friction graphs for Sentalloy on metal brackets (left column) and ceramic brackets (right column), before (upper row) and after (lower row) the clinical use. In evidence the maximum peak.

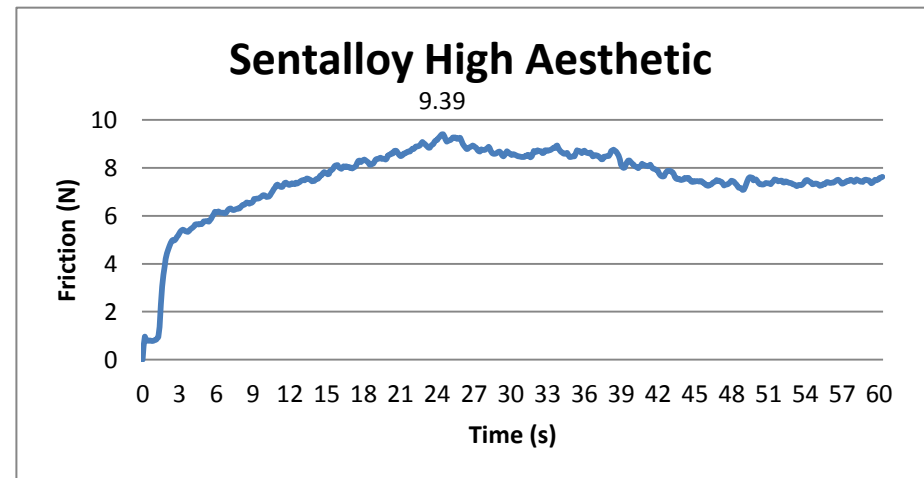
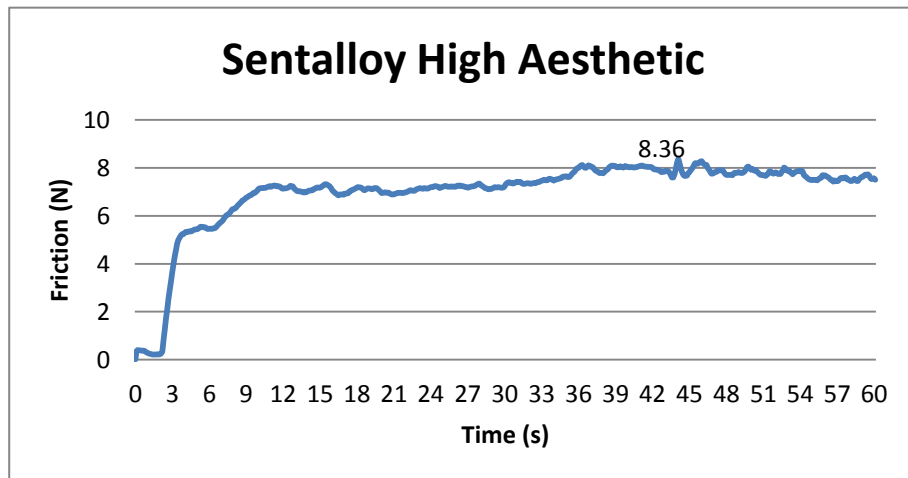
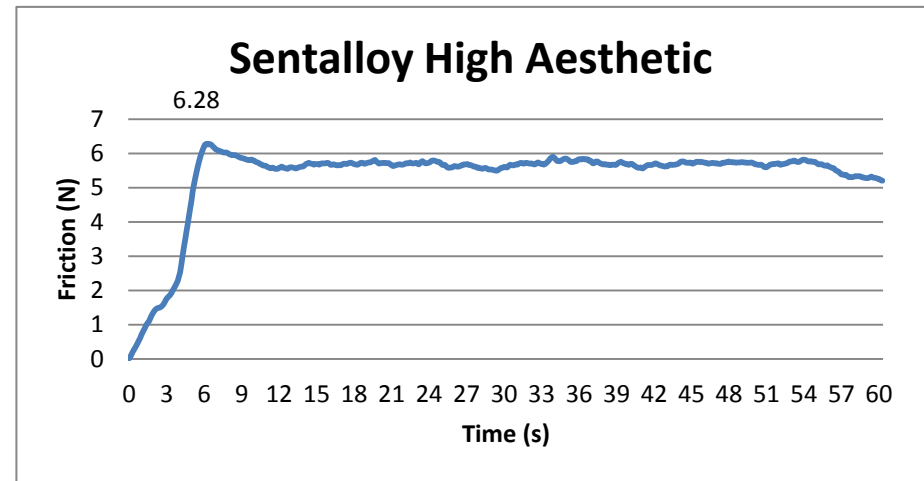
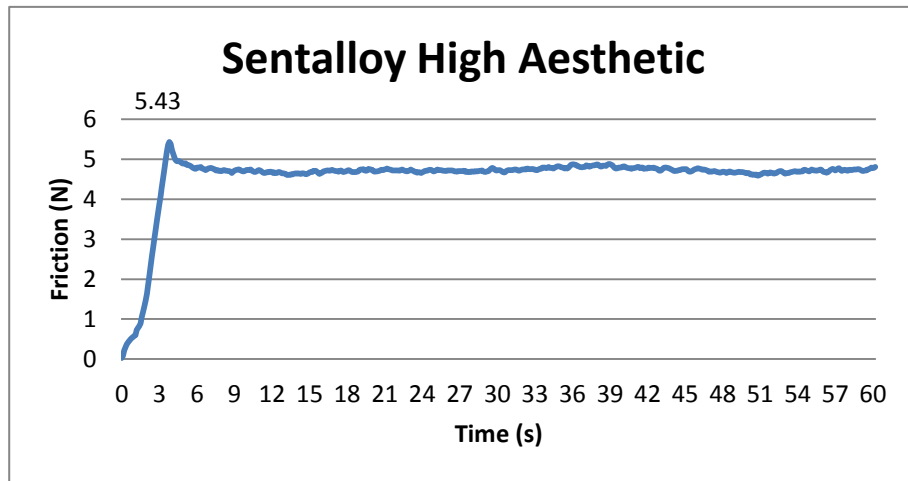


Figure V.2: Representative Time-Friction graphs for Sentalloy High Aesthetic on metal brackets (left column) and ceramic brackets (right column), before (upper row) and after (lower row) the clinical use. In evidence the maximum peak.

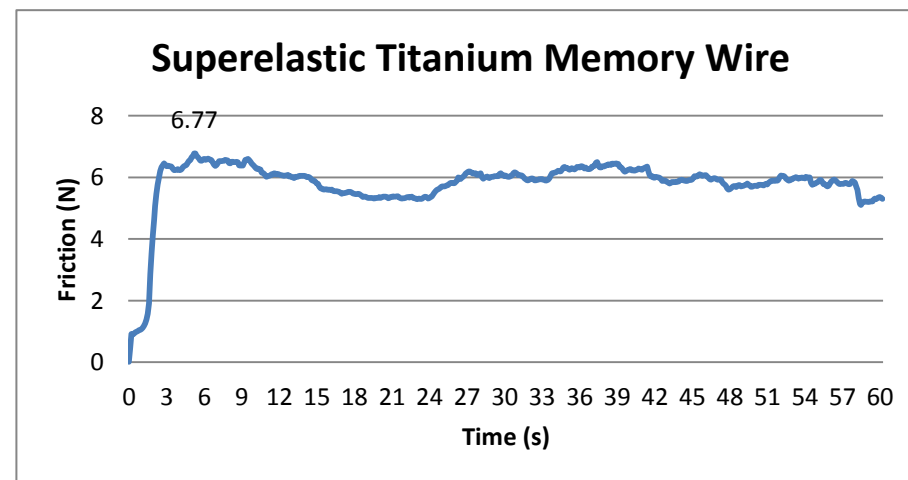
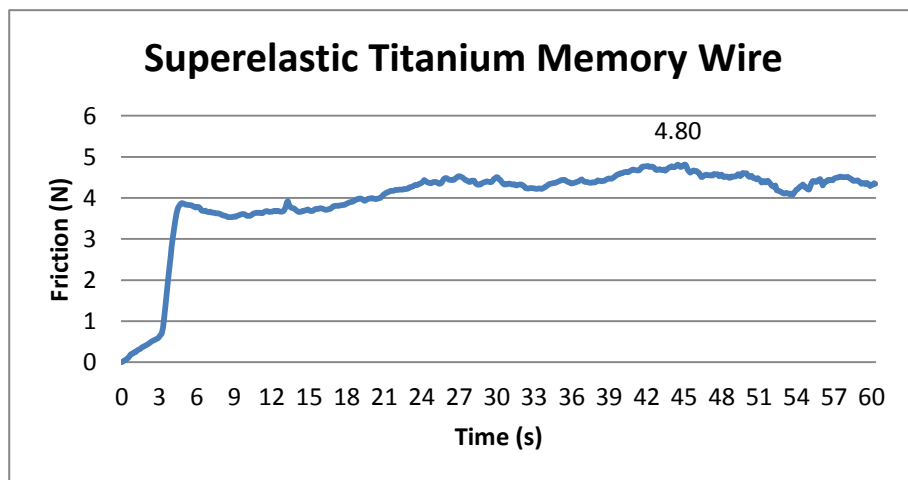
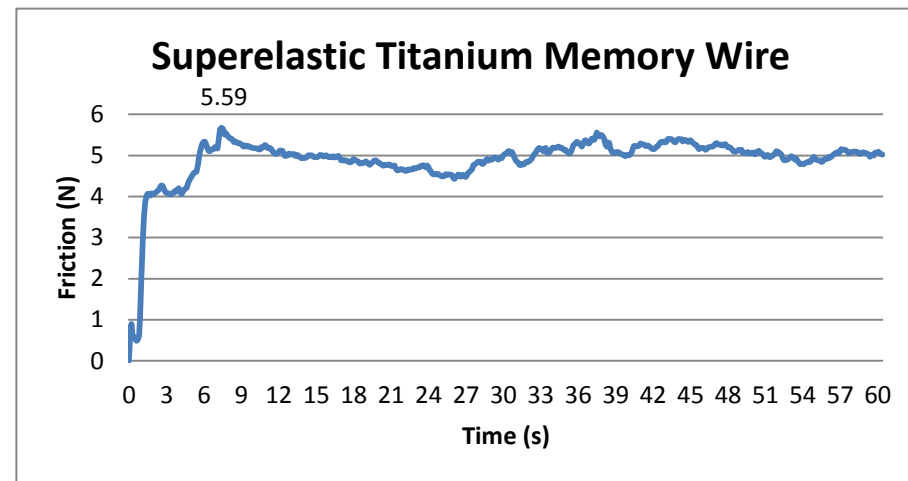
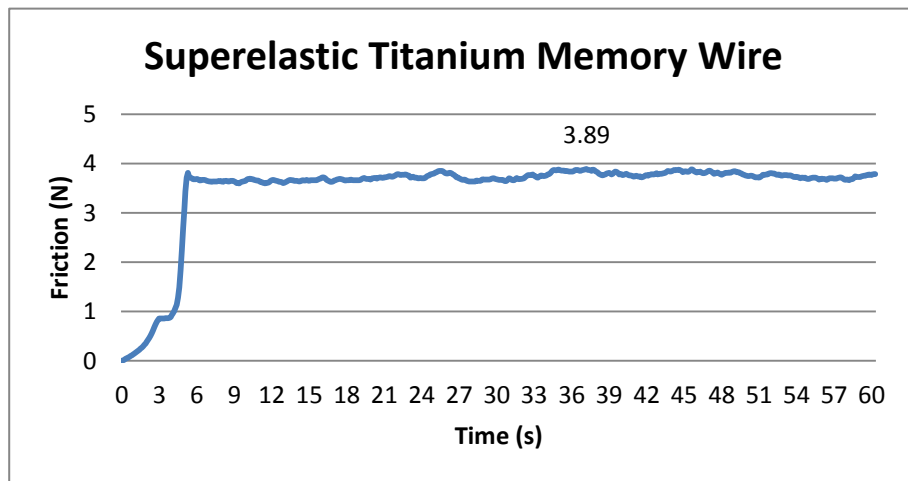


Figure V.3: Representative Time-Friction graphs for Superelastic Titanium Memory Wire on metal brackets (left column) and ceramic brackets (right column), before (upper row) and after (lower row) the clinical use. In evidence the maximum peak.

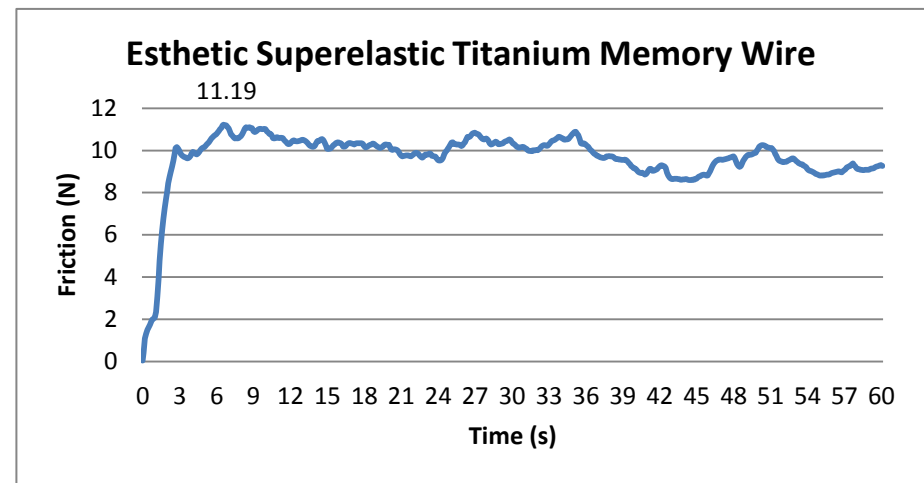
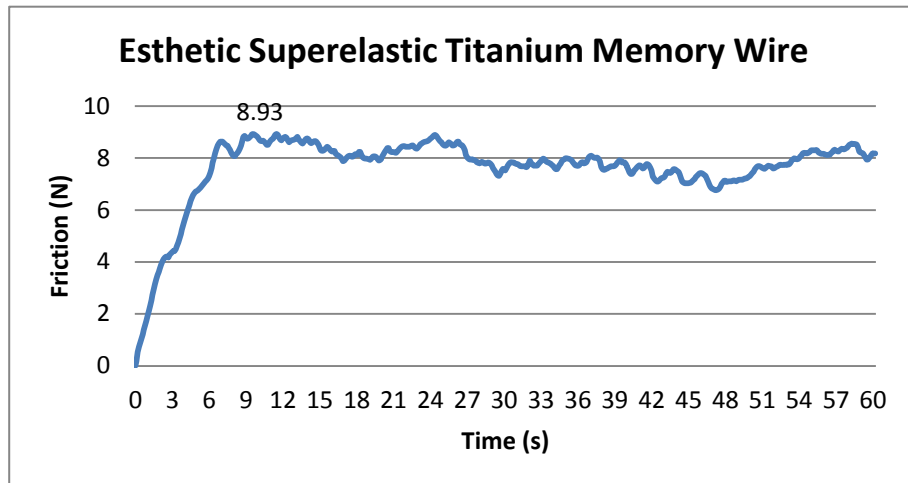
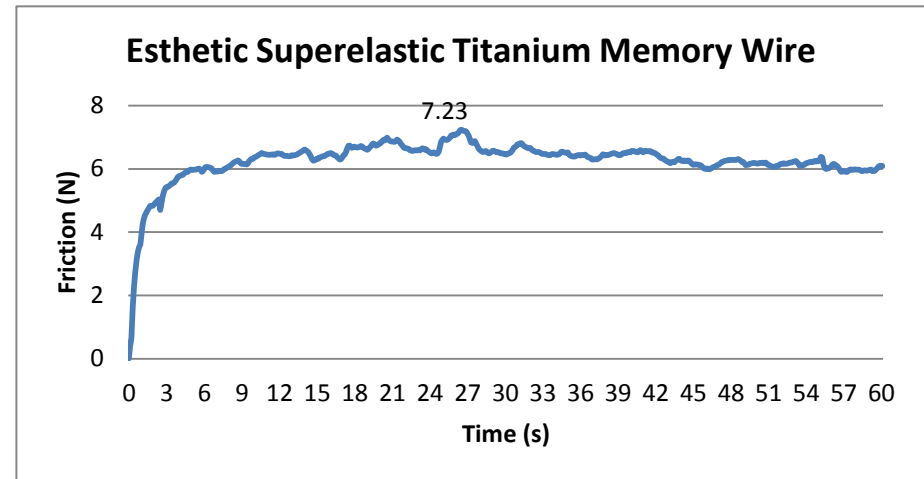
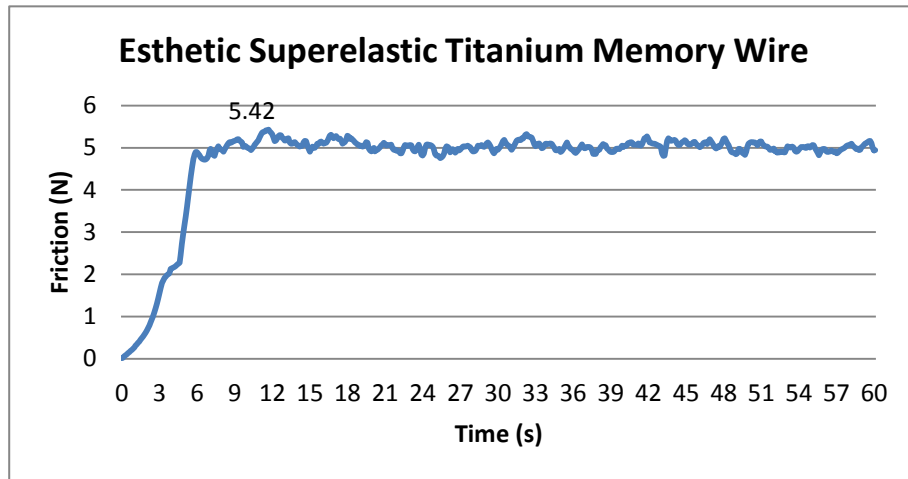


Figure V.4: Representative Time-Friction graphs for Esthetic Superelastic Titanium Memory Wire on metal brackets (left column) and ceramic brackets (right column), before (upper row) and after (lower row) the clinical use. In evidence the maximum peak.

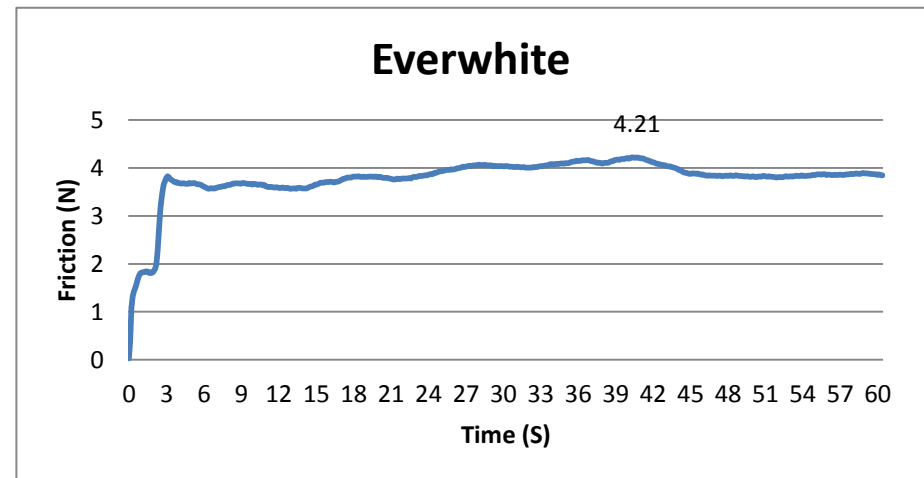
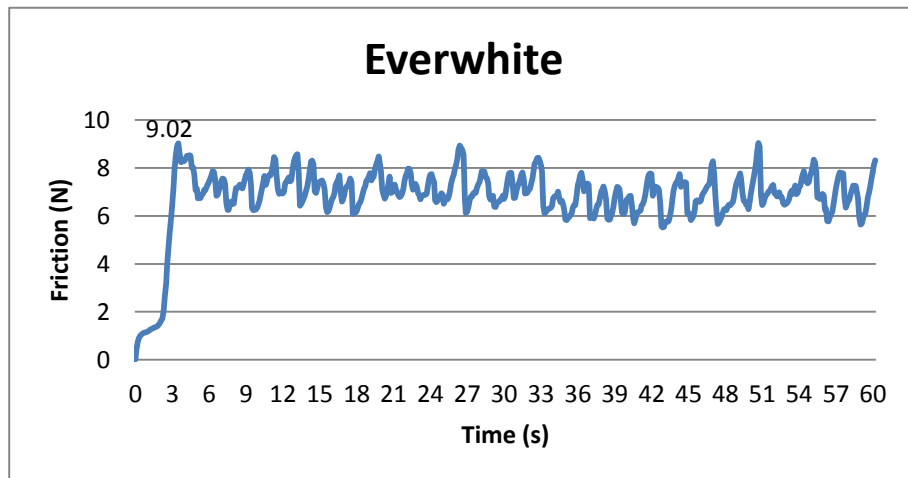
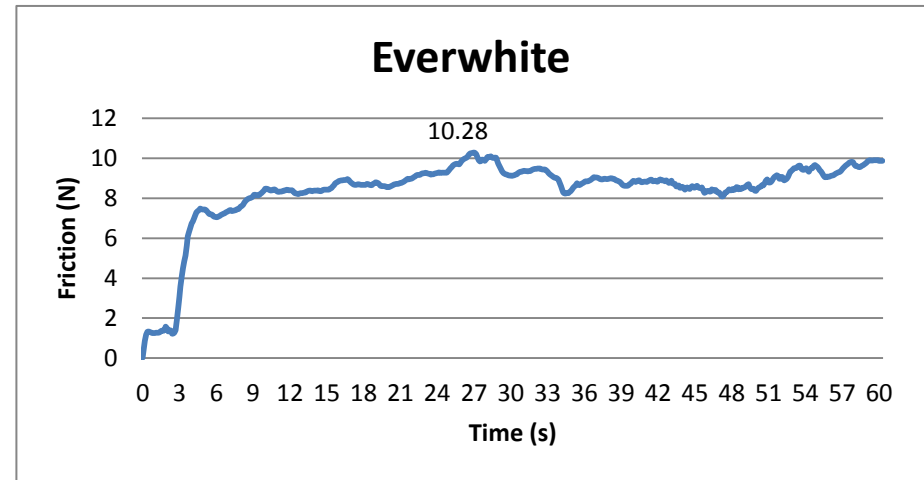
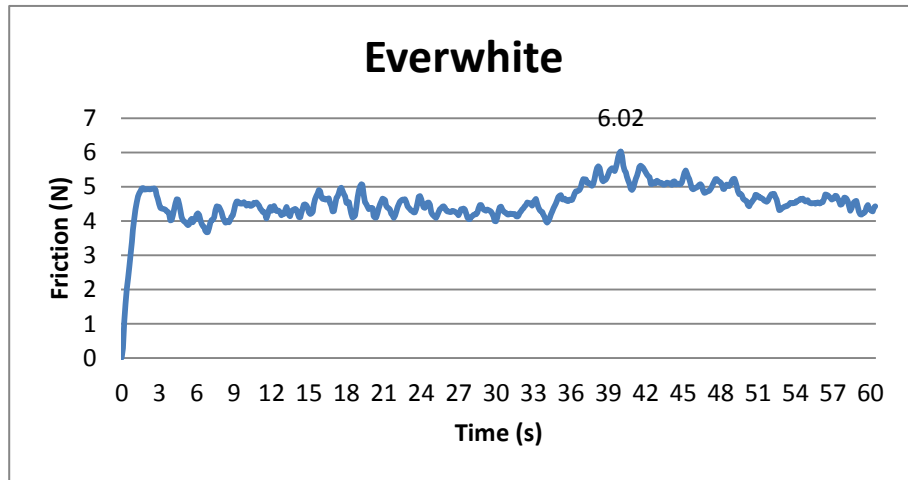


Figure V.5: Representative Time-Friction graphs for EverWhite on metal brackets (left column) and ceramic brackets (right column), before (upper row) and after (lower row) the clinical use. In evidence the maximum peak.

V.4 Results

The SEM micrographs of as-received uncoated superelastic wires showed a regular surface (Figure V.6-10, left). Some anomalies due to inconsistent coating distribution were present on polymer-coated wires, and small depressions and bumps were found along the entire surface of the ion-implanted Sentalloy High Aesthetic (Figure V.7, left). For all the wires considered in this study, SEM images showed a certain amount of surface modifications due to clinical use. Although the retrieved samples showed an extremely variable surface, with holes, ridges, and cracks (Figure V.6-10, right), the two uncoated archwires revealed less surface modification due to intraoral aging. The Esthetic Superelastic Titanium Memory Wire and the EverWhite suffered from coating delamination; the metal below that appeared smooth (Figure V.9-10). The Sentalloy High Aesthetic exhibited deep cracks and loss of its normal morphology (Figure V.7, right). Three-dimensional and two-dimensional images of archwire surfaces, obtained by means of AFM, are shown in Figure V.11-12.

Sentalloy

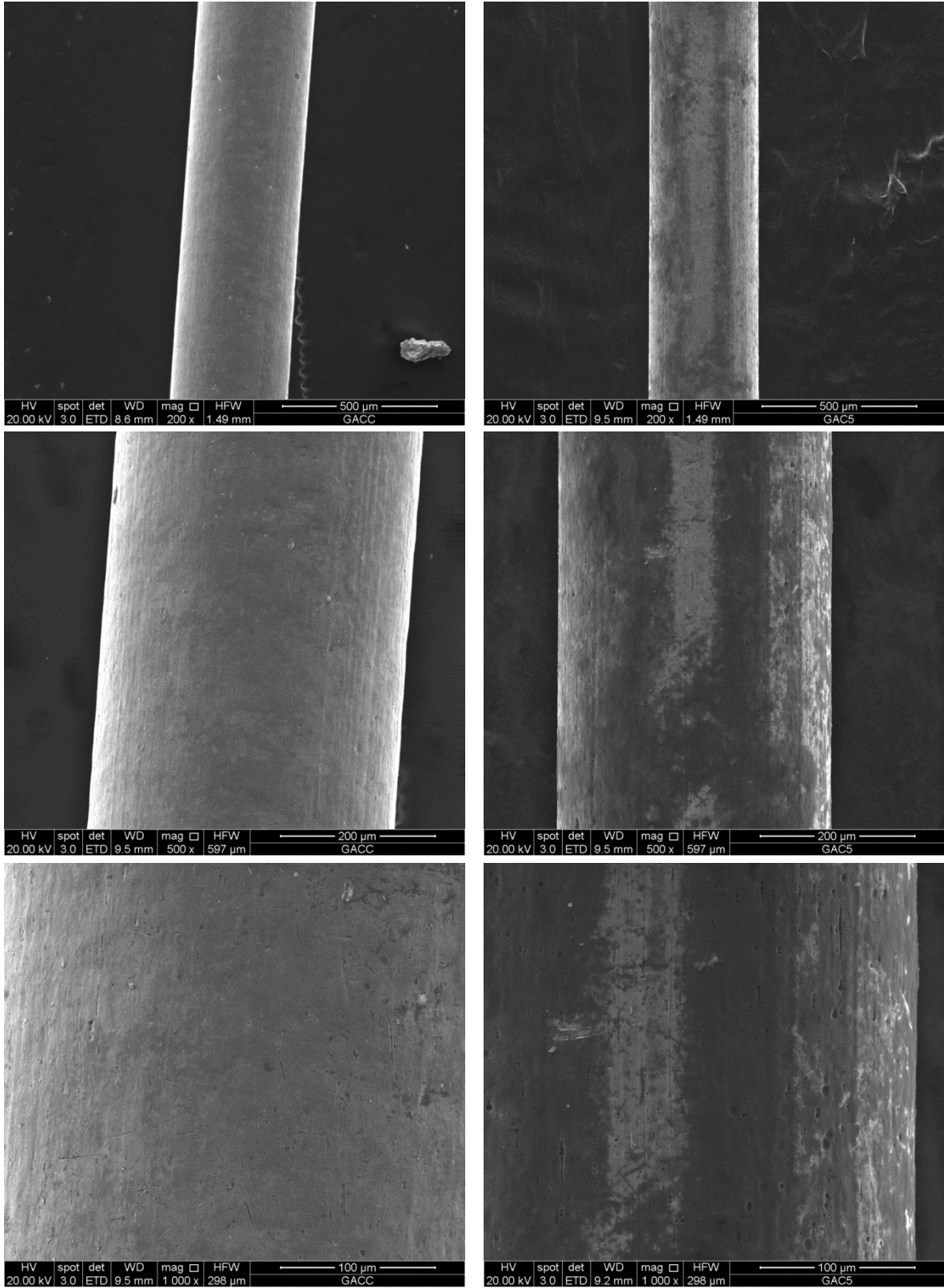


Figure V.6: Sentalloy SEM images at three magnifications x200, x500, x1000, before (left column) and after (right column) the clinical use.

Sentalloy High Aesthetic

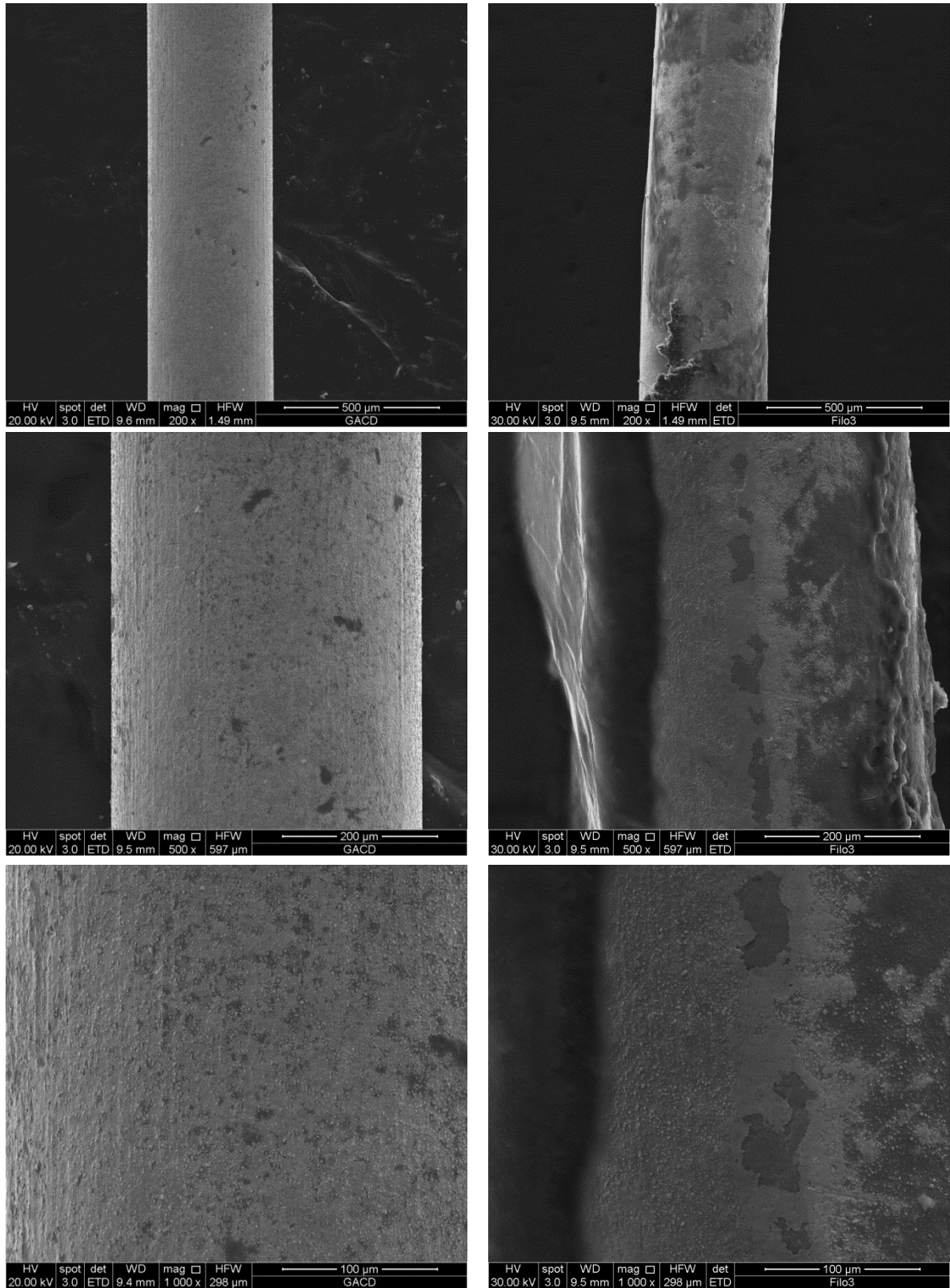


Figure V.7: Sentalloy High Aesthetic SEM images at three magnifications x200, x500, x1000, before (left column) and after (right column) the clinical use.

Superelastic Titanium Memory Wire

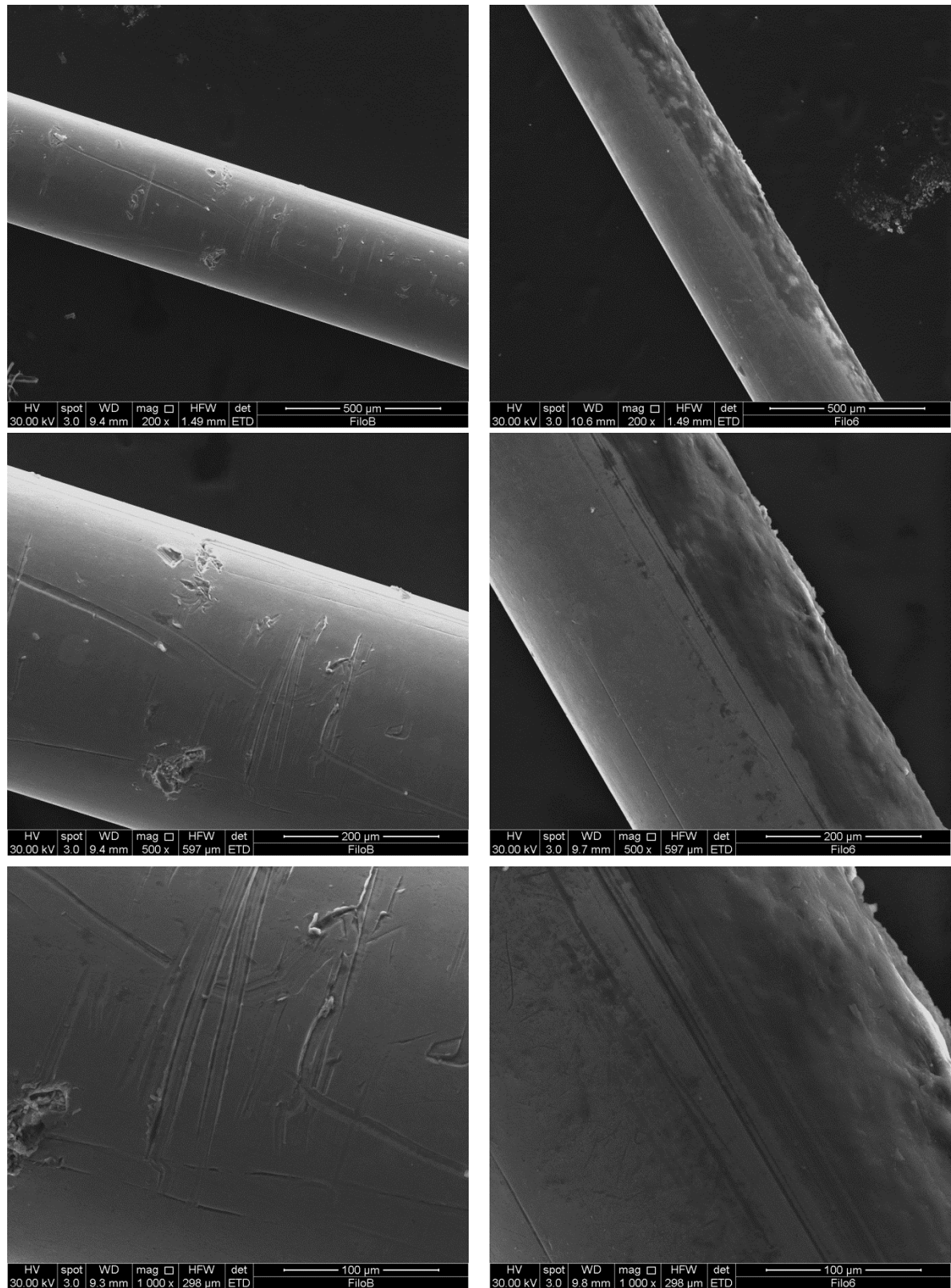


Figure V.8: Superelastic Titanium Memory Wire SEM images at three magnifications x200, x500, x1000, before (left column) and after (right column) the clinical use.

Esthetic Superelastic Titanium Memory Wire

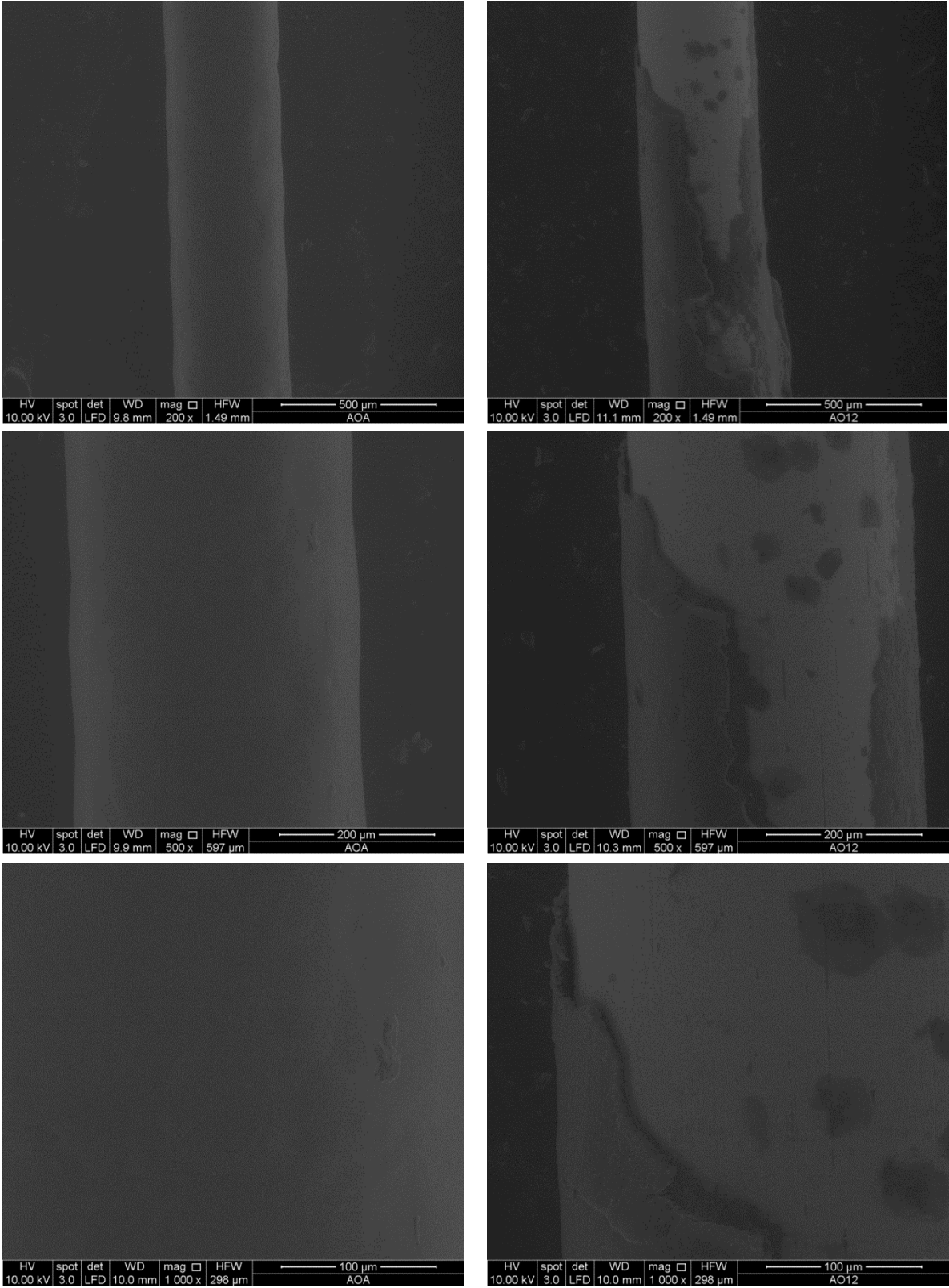


Figure V.9: Esthetic Superelastic Titanium Memory Wire SEM images at three magnifications x200, x500, x1000, before (left column) and after (right column) the clinical use.

EverWhite

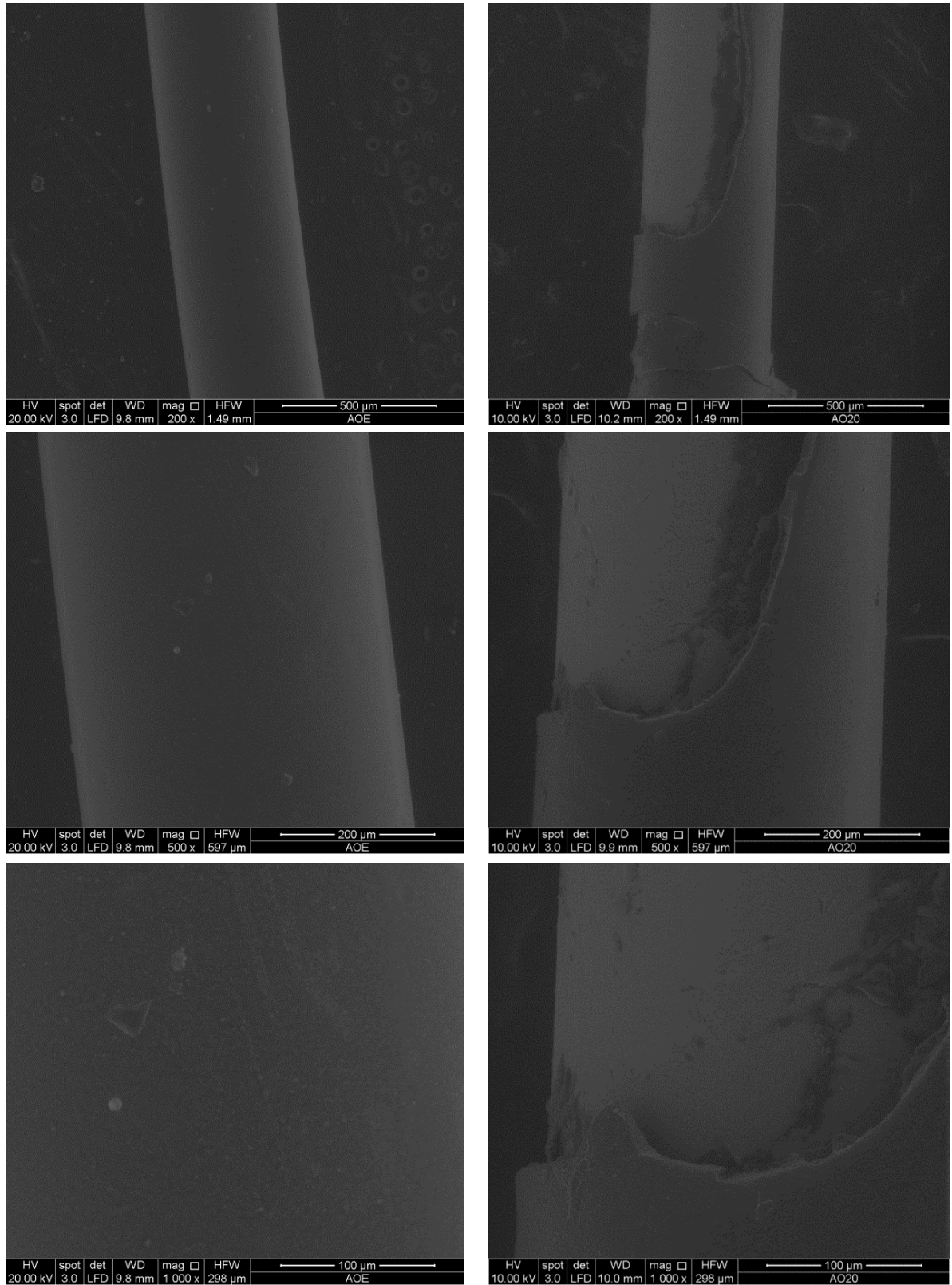
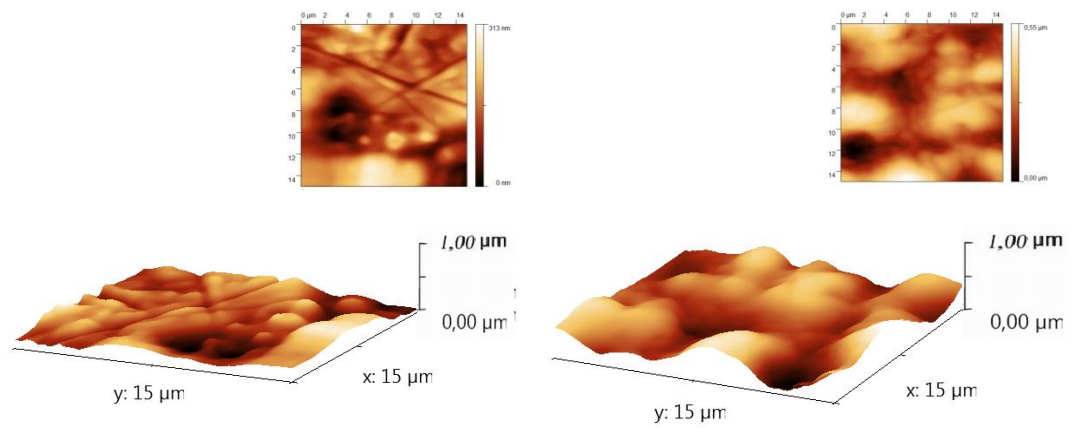
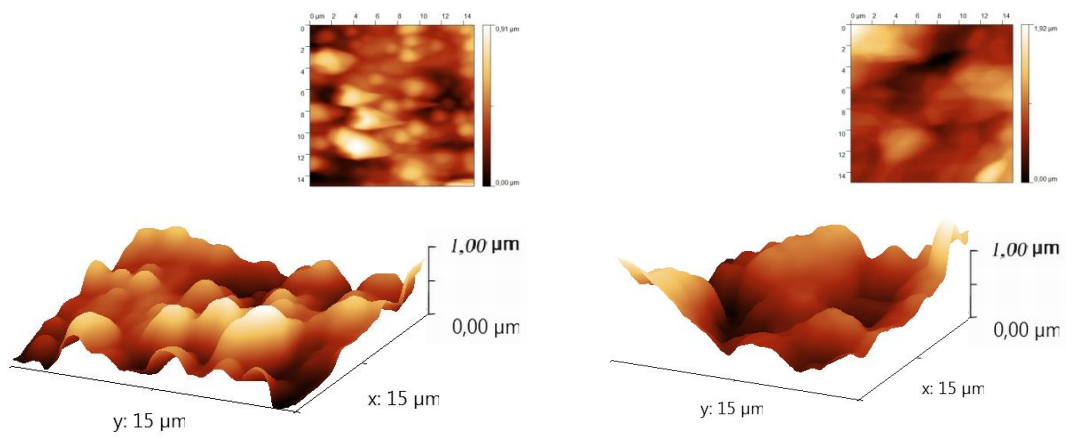


Figure V.10: EverWhite SEM images at three magnifications x200, x500, x1000, before (left column) and after (right column) the clinical use.

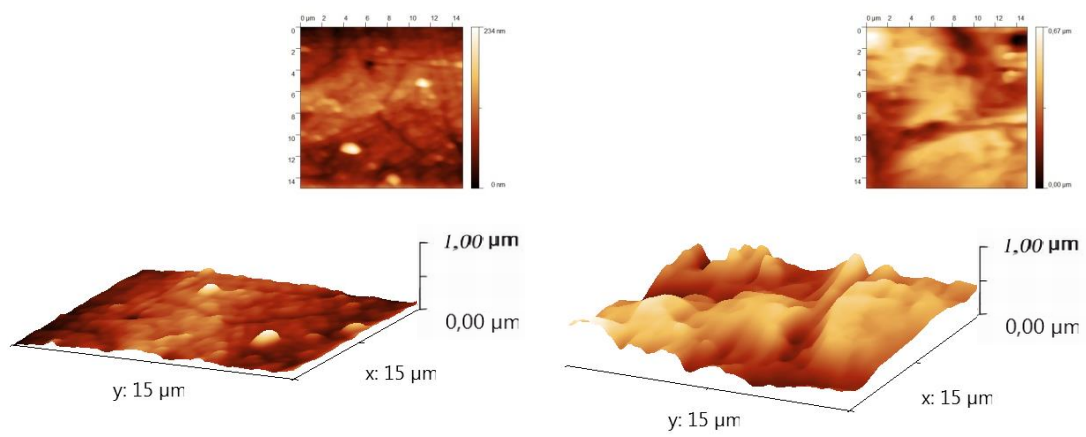


Sentalloy

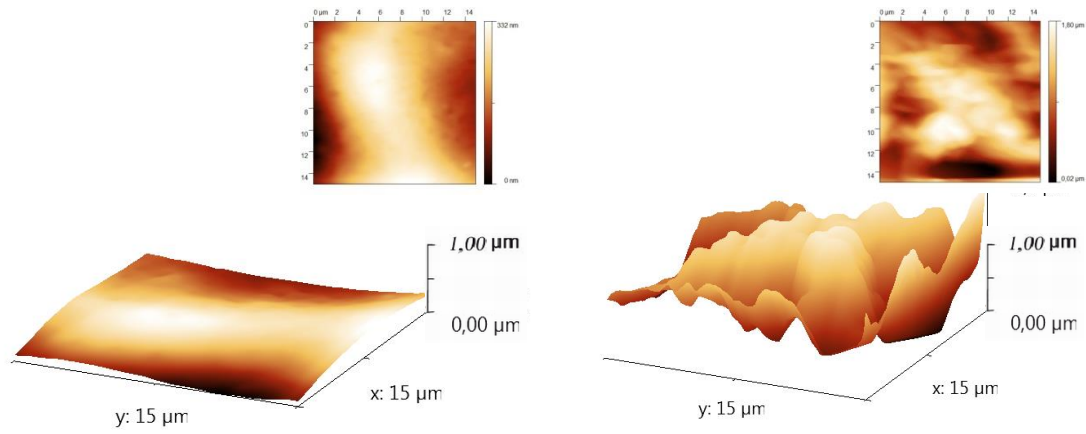


Sentalloy High Aesthetic

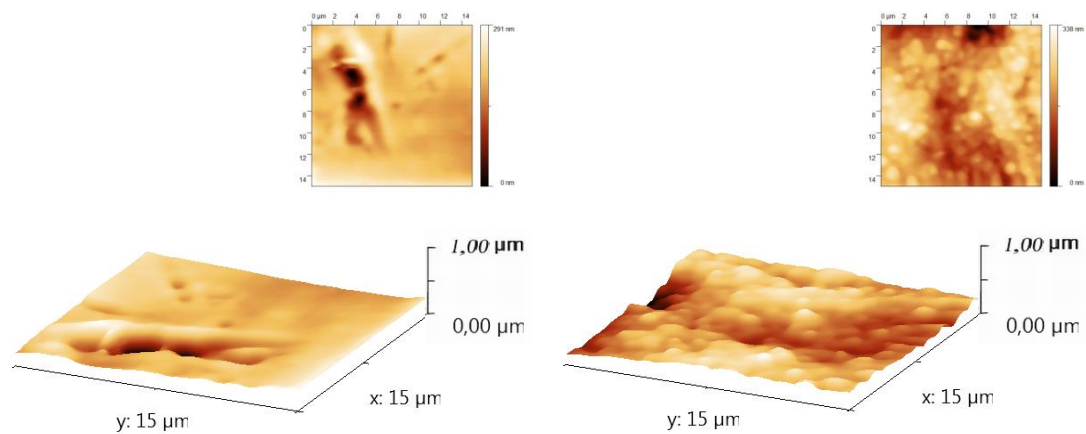
Figure V.11: Representative AFM images of Sentalloy and Sentalloy High Aesthetic before (left column) and after (right column) the clinical use.



Superelastic Titanium Memory Wire



Esthetic Superelastic Titanium Memory Wire



EverWhite

Figure V.12: Representative AFM images of Superelastic Titanium Memory Wire, Esthetic Superelastic Titanium Memory Wire and EverWhite before (left column) and after (right column) the clinical use.

The roughness average, root mean square, and maximum height values were used to quantitatively evaluate the surface topography of each archwire and are shown in Table 1 as mean±standard deviation in nanometres. Among as-received materials, EverWhite showed the lowest values of surface roughness, followed by the Superelastic Titanium Memory Wire and the Esthetic Superelastic Titanium Memory Wire. Furthermore, all the wires suffered a statistically significant increase in surface roughness due to intraoral aging (Tables V.1-2). The Esthetic Superelastic Titanium Memory Wire showed the greatest increase in roughness after clinical use. The roughest wire, in both the as-received and retrieved groups, was the Sentalloy High Aesthetic (ANOVA, $P<0.05$). The sliding resistance (classical friction), in passive configuration, for each bracket-archwire combination is reported in Tables V.3-4. The Superelastic Titanium Memory Wire (ANOVA, $P<0.05$) showed the lowest friction on metallic and aesthetic brackets, both in the as-received and retrieved groups (Tables V.3-4). For all the wires, an increase in friction due to the use of aesthetic brackets and retrieved archwires was recorded (Table V.3). Compared with Superelastic Titanium Memory Wire, all the aesthetic wires showed a significant increase in friction, especially when used on clear brackets after intraoral aging. The Sentalloy was the only archwire that did not show a statistically significant increase in friction between the as-received group and the retrieved group on both bracket types.

Archwires	$R_a(\text{mean}\pm\text{SD})$		$R_{ms}(\text{mean}\pm\text{SD})$		$M_h(\text{mean}\pm\text{SD})$	
	As-received	Retrieved	As-received	Retrieved	As-received	Retrieved
Sentalloy	62.9±14.5	131.3±65.6**	80.7±20	160.8±78.3*	519.3±179.4	906.2±428.1*
Sentalloy High Aesthetic	135.5±10.8	175.8±35.1**	167.6±9.9	220.2±45.5**	982.5±194.6	1227±310.1*
Superelastic Titanium Memory Wire	34.0±12.8	74.0±30.1**	43.5±15.6	92.9±37.3**	306.5±77.9	581.2±241.5***
Esthetic Superelastic Titanium Memory Wire	50.3±15.2	167.2±94.5***	61.7±18.4	210.6±116.3***	354.8±125.1	1298.2±683.3***
EverWhite	28.0±13	68.1±45.5*	38.0±19	86.6±52.2*	327.2±193.2	572.2±229.7*

Table V.1: Roughness Average (R_a), Root Mean Square (R_{ms}), and Maximum Height (M_h) values (mean±SD) of Atomic Force Microscope (AFM) images of orthodontic archwires before (As-received) and after (Retrieved) the clinical use. ^{ns} (not significant) * (P<0.05), ** (P<0.01) and * (P<0.001) indicate significant statistically differences between As-received and Retrieved (Student's t test for unpaired data).**

<i>Tukey's Multiple Comparison Test</i>	As-received			Retrieved		
	R _a	R _{ms}	M _h	R _a	R _{ms}	M _h
Sentalloy vs Sentalloy High Aesthetic	***	***	***	ns	ns	ns
Sentalloy vs Superelastic Titanium Memory Wire	***	***	*	**	*	ns
Sentalloy vs Esthetic Superelastic Titanium Memory Wire	ns	ns	ns	ns	ns	**
Sentalloy vs EverWhite	***	***	ns	*	*	ns
Sentalloy High Aesthetic vs Superelastic Titanium Memory Wire	***	***	***	***	***	***
Sentalloy High Aesthetic vs Esthetic Superelastic Titanium Memory Wire	***	***	***	ns	ns	ns
Sentalloy High Aesthetic vs EverWhite	***	***	***	***	***	***
Superelastic Titanium Memory Wire vs Esthetic Superelastic Titanium Memory Wire	*	ns	ns	***	***	***
Superelastic Titanium Memory Wire vs EverWhite	ns	ns	ns	ns	ns	ns
Esthetic Superelastic Titanium Memory Wire vs EverWhite	**	*	ns	***	***	***

Table V.2: P-values from statistical analysis of archwires roughness parameters (ANOVA with post hoc Tukey's test). ns indicates not significant. * P<0.05; ** P<0.01; and * P<0.001 indicate statistically significant differences between two archwires.**

Archwires	Metallic Brackets		Ceramic Brackets	
	Friction (mean±SD)		Friction (mean±SD)	
	As-received	Retrieved	As-received	Retrieved
Sentalloy	4.5±0.4	5.0±1.1 ^{ns}	7.7±1.2 ^b	8.0±0.9 ^{nsb}
Sentalloy High Aesthetic	4.8±1.0	5.9±1.3 ^{**}	8.2±0.3 ^b	9.1±1.2 ^{**b}
Superelastic Titanium Memory Wire	3.9±0.5	4.6±1.0 [*]	5.1±1.1 ^b	5.6±1 ^{nsa}
Esthetic Superelastic Titanium Memory Wire	5.1±0.7	8.4±0.8 ^{***}	7.2±0.9 ^b	9.1±2.6 ^c
EverWhite	4.3±0.5	6.3±1.0 ^{***}	6.8±1.2 ^b	9.7±2.1 ^{***b}

Table V.3: Friction (N) values (mean±SD) on metallic and ceramic brackets of orthodontic archwires before (As-received) and after (Retrieved) the clinical use. ns (not significant) * (P<0.05), ** (P<0.01) and * (P<0.001) indicate significant statistically differences between As-received and Retrieved (Student's T test for unpaired data). a (P<0.05), b (P<0.001), c (not significant) indicate significant statistically differences between ceramic brackets and metallic brackets (Student's t-test for paired data).**

<i>Tukey's Multiple Comparison Test</i>	Metallic Brackets		Ceramic Brackets	
	As-received	Retrieved	As-received	Retrieved
Sentalloy vs Sentalloy High Aesthetic	ns	ns	ns	ns
Sentalloy vs Superelastic Titanium Memory Wire	*	ns	***	***
Sentalloy vs Esthetic Superelastic Titanium Memory Wire	ns	***	ns	ns
Sentalloy vs EverWhite	ns	**	ns	*
Sentalloy High Aesthetic vs Superelastic Titanium Memory Wire	**	**	***	***
Sentalloy High Aesthetic vs Esthetic Superelastic Titanium Memory Wire	ns	***	*	ns
Sentalloy High Aesthetic vs EverWhite	ns	ns	***	ns
Superelastic Titanium Memory Wire vs Esthetic Superelastic Titanium Memory Wire	***	***	***	***
Superelastic Titanium Memory Wire vs EverWhite	ns	***	***	***
Esthetic Superelastic Titanium Memory Wire vs EverWhite	**	***	ns	ns

Table V.4: P-values from statistical analysis of archwires friction parameters (ANOVA with post hoc Tukey's test): ns (not significant) * (P<0.05), ** (P<0.01) and * (P<0.001) indicate significant statistically differences between the archwires on the two brackets typology.**

V.5 Discussion

The present study focuses on the evaluation of intraoral aging of five different NiTi archwires; the aim was to compare the behaviour of aesthetic and uncoated superelastic wires. There is still a lack of studies concerning the intraoral aging of wires and the associated phenomena, such as variation of mechanical properties and surface alterations (Eliades and Bourauel, 2005). Therefore, retrieval analyses conducted on dental materials are receiving growing interest because of the critical information provided (Eliades, 2000; Eliades et al., 1999) Recent *ex vivo* studies showed that intraoral aging might compromise the aesthetic properties of tooth-colored wires (Elayyan et al., 2008; Bradley et al., 2013; da Silva et al., 2013^e). Mechanical properties, with a decrease of delivered forces, are affected as well (Elayyan et al., 2008; Bradley et al., 2013). Moreover, it has been proposed that intraoral aging influences surface roughness of polymer-coated wires (Elayyan et al., 2008; da Silva et al., 2013^e). In this study, the AFM and SEM were used to establish the topographic alterations of the archwires, evaluating polymer-coated and ion-implanted materials and their uncoated counterparts. The AFM was found to be an excellent tool to determine numeric values that describe the surface roughness, even if it presents some drawbacks, such as small scan size (Braga and Ricci, 2004; Spagnuolo et al., 2012; D'Antò et al., 2012). Therefore, the SEM was used for qualitative evaluation of the surface at a micrometer scale. The SEM analysis of as-received wires presented different surface images depending on the manufacturing process. The uncoated samples showed the typical characteristics of the superelastic archwires and had a regular surface; the polymer coated wires exhibited some anomalies, mainly regarding coating layers, and the rhodium-implanted Sentalloy High Aesthetic showed a peculiar highly rough surface. In the

retrieved group, a certain degree of corrosion and a large amount of debris were present on the uncoated wires, as might be expected (Huang, 2005). Polymer-coated archwires revealed a considerable amount of coating delamination, consistent with findings of previous studies (Elayyan et al., 2008; da Silva et al., 2013^c). This deterioration may impair the aesthetic properties, thereby affecting patient satisfaction (Bradley et al., 2013). Even if multiple areas of the polymer layer peeled off, no defects were found on the naked surface, probably because of the manufacturing process, as suggested by previous studies that found controversial results on polymer-coated wires of different manufacturers (Elayyan et al., 2008; da Silva et al., 2013^c). A relation between bracket imprints and delamination areas was notable in several specimens. It must be emphasized that the irregular surfaces may lead to plaque accumulation, and tooth movement may be affected because of the entrapment of bracket edges inside these defects (Postlethwaite, 1992; Bourauel et al., 1998; Neumann et al., 2002). After clinical use, the ion-implanted Sentalloy High Aesthetic also lost its typical surface characteristics. This study was the first to assess changes in surface roughness due to intraoral aging of an ion-implanted wire. In a previous study, the corrosion resistance of nitrogen-implanted Neo Sentalloy Longuard in fluoride mouth rinse solutions was tested. These results were similar to classic Neo Sentalloy (Iijima et al., 2010) but are not comparable to our results because of the different materials and conditions of the experiment. The quantitative surface analysis performed by means of the AFM showed significant differences among the tested wires. Our findings suggest a different effect of the surface treatments of the two aesthetic wires. EverWhite and Superelastic Titanium Memory Wire were the least rough wires in the as-received group; Sentalloy High Aesthetic was the roughest. This increase in surface roughness due to ion implantation was confirmed by a previous study (Bradley et al., 2013). After clinical

use there was an increase in the roughness parameters for all the wires. Among retrieved samples, the Sentalloy High Aesthetic was the roughest wire, and the greatest increase in roughness was observed on the Teflon-coated Esthetic Superelastic Titanium Memory Wire. These data are consistent with the results of other studies that report a surface roughness increase after clinical use (Elayyan et al., 2008) and should be evaluated in light of the key role of surface roughness on wire performance, in terms of corrosion aging, plaque accumulation, biocompatibility, and sliding resistance (Bourauel et al., 1998; Wichelhaus et al., 2005; D'Antò et al., 2009). Sliding resistance is the result of the additive effects of three phenomena: classical friction, binding, and notching (Kusy and Whitley, 1997). In our study the frictional behaviour of five different NiTi wires were assessed in vitro, in a passive bracket configuration. The decision to use the brackets in passive configuration was determined by the necessity to evaluate only simple friction, avoiding binding and notching components of the sliding resistance (Kusy and Whitley, 1997). In all four tested scenarios, the wire that exhibited the least amount of friction was the Superelastic Titanium Memory Wire. In the as-received group, aesthetic wires showed a higher level of friction than uncoated controls. Previous studies have shown that polymer coating may decrease the friction produced by wires, in disagreement with our results. Some variables, like the use of different brackets, different dimensions of wires, and different wire brands may explain these differences (Husmann et al., 2002; Farronato et al., 2012). Nevertheless, in the as-received group it was not possible to establish a clear correlation between AFM results and friction analysis. The increase in friction due to surface roughness is a controversial topic discussed in relevant literature (Kusy et al., 1988; Prosocki et al., 1991; Tselepis et al., 1994). Some authors confirm the existence of a close correlation between surface roughness and friction (Prosocki et

al., 1991), but other studies state that a wire's low surface roughness is not a sufficient condition for low frictional coefficients (Kusy et al., 1988). As for surface parameters, all the wires suffered an increase in friction due to intraoral aging. The aesthetic wires were more affected by clinical use in the friction test. In the retrieved group, the Esthetic Superelastic Titanium Memory Wire produced the highest friction on the metallic brackets, and the EverWhite produced the highest values on the ceramic brackets. These results may be due to coating degradation. The clinical relevance of this study is that, despite the vast improvements in manufacturing aesthetic brackets, an adequate aesthetic wire has not been produced yet. Despite the unsatisfying coating durability, coated wires continue to be marketed and used in clinical practices. Orthodontists should be aware that the exposure to the oral environment significantly affects the performances of aesthetic archwires. A limitation of this study was the examination of the wires at only two time intervals. Differences in oral hygiene protocols, pH, fluoride use, and degree of teeth irregularity in the in vivo part of the trial could also have influenced the outcome.

V.6 Conclusions

The clinical use of wires altered their surface properties and increased surface roughness and level of friction. N The SEM images confirmed the heterogeneous surface of the coated wires after clinical use. Even if EverWhite wire overcame some of the disadvantages of the Esthetic Superelastic Titanium Memory Wire, exhibiting a lower and more stable surface roughness, it still suffers coating delamination.

Chapter VI

General Conclusions

In conclusion, aesthetic orthodontic archwires are not considerable at the same level of the metal archwires. Aesthetic archwires mechanical properties are different from the properties of the metallic ones and moreover their aesthetic is affected by the clinical use.

Our investigation demonstrated the potential use of an AFM for the study of surface properties of orthodontic materials. In particular, the AFM has many advantages, such as the production of topographical three-dimensional images in real space with a very high resolution ($<10 \text{ \AA}$). The samples do not require any special treatment, such as metallization, and the AFM can provide quantitative values for the investigated parameters. The most important AFM drawback is the small scan size, which, in association with the slow velocity of scanning, often impedes a complete analysis of the sample.

Aesthetic coated as-received orthodontic archwires showed a lower surface roughness than ion implanted wires and of the respective uncoated wire. Ion implantation seems to have a better effect on TMA wires than on NiTi wires.

Aesthetic archwires properties are altered by the clinical use and an evident increase in surface roughness and level of friction was shown.

The SEM images confirmed the heterogeneous surface of the coated wires after clinical use. Even if EverWhite wire overcame some of the disadvantages of the Esthetic Superelastic Titanium Memory Wire, exhibiting a lower and more stable surface roughness, it still suffers coating delamination.

The clinical relevance of this study is that, despite the vast improvement in manufacturing aesthetic brackets, an adequate aesthetic wire has not been produced yet. Despite the unsatisfying coating durability, coated wires continue to be marketed and used in clinical practices. Orthodontists should be aware that the exposure to the oral environment significantly affects the performances of aesthetic archwires.

References

Adler RJ, Picraux ST. Repetitively pulsed metal ion beams for ion implantation. *Nucl. Instrum. Meth. Phys. Res. B.* 1985;6:123-8.

Alavi S, Hosseini N. Load-deflection and surface properties of coated and conventional superelastic orthodontic archwires in conventional and metal-insert ceramic brackets. *Dent Res J (Isfahan).* 2012;9:133-8.

Alcock JP, Barbour ME, Sandy JR, Ireland AJ. Nanoindentation of orthodontic archwires: The effect of decontamination and clinical use on hardness, elastic modulus and surface roughness. *Dent Mater.* 2009;25:1039-43.

Ametrano G, D'Antò V, Di Caprio MP, Simeone M, Rengo S, Spagnuolo G. Effects of sodium hypochlorite and ethylenediaminetetraacetic acid on rotary nickel-titanium instruments evaluated using atomic force microscopy. *Int Endod J.* 2011; 44:203-9.

Amini F, Rakhshan V, Pousti M, Rahimi H, Shariati M, Aghamohamadi B. Variations in surface roughness of seven orthodontic archwires: an SEM-profilometry study. *Korean J Orthod.* 2012;42:129-37.

Andreasen GF, Morrow RE. Laboratory and clinical analyses of nitinol wire. *Am J Orthod.* 1978;73:142-51.

Articolo LC, Kusy K, Saunders CR, Kusy RP. Influence of ceramic and stainless steel brackets on the notching of archwires during clinical treatment. *Eur J Orthod.* 2000;22:409-25.

Articolo LP, Kusy RP. Influence of Angulation on the Resistance to Sliding in Fixed Appliances. *Am J Orthod Dentofacial Orthop* 1999;115:39-51.

Baldwin PD, Pender N, Last KS. Effects on tooth movement of force delivery from nickel-titanium archwires. *Eur J Orthod.* 1999;21:481-9.

Ballard RW, Sarkar NK, Irby MC, Armbruster PC, Berzins DW. Three-point bending test comparison of fiber-reinforced composite archwires to nickel-titanium archwires. *Orthodontics (Chic.).* 2012;13:46-51.

Bandeira AM, dos Santos MP, Pulitini G, Elias CN, da Costa MF. Influence of thermal or chemical degradation on the frictional force of an experimental coated NiTi wire. *Angle Orthod.* 2011;81:484-9.

Bass JK, Fine H, Cisneros GJ. Nickel hypersensitivity in the orthodontic patient. *Am J Orthod Dentofacial Orthop.* 1993;103:280-5.

Bazakidou E, Nanda RS, Duncanson MG Jr, Sinha PE. Valuation of frictional resistance in esthetic brackets. *Am J Orthod Dentofacial Orthop.* 1997;112:138-44.

Beer FP, Johnston ER. *Mechanics of Materials.* New York, NY:McGraw-Hill; 1981.

Benz M, Rosenberg KJ, Kramer EJ, Israelachvili JN. The deformation and adhesion of randomly rough and patterned surfaces. *J Phys Chem B.* 2006;110:11884-93.

Binnig G, Quate CF, Gerber C. Atomic force microscope. *Phys Rev Lett.* 1986;56:930-3.

Binnig G, Rohrer H, Gerber C, Weibel E. Tunneling through a controllable vacuum gap. *Appl Phys Lett.* 1982;40:178-86.

Bourauel C, Fries T, Drescher D, Plietsch R. Surface roughness of orthodontic wires via atomic force microscopy, laser specular reflectance and profilometry. *Eur J Orthod.* 1998;20:79-92.

Bourauel C, Scharold W, Jäger A, Eliades T. Fatigue failure of as-received and retrieved NiTi orthodontic archwires. *Dent Mater.* 2008;24:1095-101.

Bowden FP, Tabor D. *The friction and lubrication of solids.* 5th ed. Oxford University Press; 2001.

Bowden FP, Tabor D. *The friction and lubrication of solids.* 1st ed. Oxford, UK: Clarendon Press; 1950.

Bradley TG, Berzins DW, Valeri N, Pruszynski J, Eliades T, Katsaros C. An investigation into the mechanical and esthetic properties of new generation coated nickel-titanium wires in the as-received state and after clinical use. *Eur J Orthod.* 2013. doi: 10.1093/ejo/cjt048.

Bradley TG, Brantley WA, Culbertson BM. Differential scanning calorimetry (DSC) analyses of superelastic and nonsuperelastic nickel-titanium orthodontic wires. *Am J Orthod Dentofacial Orthop.* 1996;109:589-97.

Braga PC, Ricci D. *Atomic Force Microscopy: Biomedical Methods and Applications.* Totowa, NJ: Humana Press; 2004.

Brantley WA. Orthodontic wires. In: Brantley WA, Eliades T, eds. *Orthodontic Materials: Scientific and Clinical Aspects.* Stuttgart, Germany: Thieme; 2001.

Braun S, Bluestein M, Moore BK, Benson G. Friction in perspective. *Am J Orthod Dentofacial Orthop.* 1999;115:619-27.

Bravo LA, de Cabañes AG, Manero JM, Rúperez E, Gil FJ. NiTi superelastic orthodontic

archwires with polyamide coating. *J Mater Sci Mater Med.* 2014;25:555-60.

Burstone CJ, Frazin-Nia F. Production of low-friction and colored TMA by ion implantation. *J Clin Orthod.* 1995;29: 453-61.

Burstone CJ, Goldberg AJ. Beta titanium: a new orthodontic alloy. *Am J Orthod.* 1980;77:121-32.

Burstone CJ, Liebler SA, Goldberg AJ. Polyphenylene polymers as esthetic orthodontic archwires. *Am J Orthod Dentofacial Orthop.* 2011;139:e391-8.

Caroli C, Nozieres P. Hysteresis and elastic interactions of microasperities in dry friction. *Eur. Phys. J. B.* 1998;4:233-46.

Cash A, Curtis R, Garrigia-Majo D, McDonald F. A comparative study of the static and kinetic frictional resistance of titanium molybdenum alloy archwires in stainless steel brackets. *Eur J Orthod.* 2004;26:105-11.

Chang JH, Berzins DW, Pruszyński JE, Ballard RW. The effect of water storage on the bending properties of esthetic, fiber-reinforced composite orthodontic archwires. *Angle Orthod.* 2013 doi: 10.2319/061213-443.1

Chern Lin JH, Lo SJ, Ju CP. Bio corrosion study of titanium–nickel alloys. *J Oral Rehabil* 1996;23:129-34.

Cioffi I, Piccolo A, Tagliaferri R, Paduano S, Galeotti A, Martina R. Pain perception following first orthodontic archwire placement—thermoelastic vs superelastic alloys: a randomized controlled trial. *Quintessence Int.* 2012;43:61-9.

Conrad JR, Radtke JL, Dodd RA, Worzala FJ, Tran NC. Plasma source ion implantation technique for surface modification of materials. *J. Appl. Phys.* 1987;62:4591-6.

D'Antò V, Eckhardt A, Hiller KA, Spagnuolo G, Valletta R, Ambrosio L, Schmalz G, Schweikl H. The influence of Ni(II) on surface antigen expression in murine macrophages. *Biomaterials.* 2009;30:1492-501.

D'Antò V, Rongo R, Ametrano G, Spagnuolo G, Manzo P, Martina R, Paduano S, Valletta R. Evaluation of surface roughness of orthodontic wires by means of atomic force microscopy. *Angle Orthod.* 2012;82:922-8.

da Silva DL, Mattos CT, de Araújo MV, de Oliveira Ruellas AC. Color stability and fluorescence of different orthodontic esthetic archwires. *Angle Orthod.* 2013;83:127-32.^a

da Silva DL, Mattos CT, Sant'Anna EF, Ruellas AC, Elias CN. Cross-section dimensions and mechanical properties of esthetic orthodontic coated archwires. *Am J Orthod Dentofacial Orthop.* 2013;143:S85-91.^b

da Silva DL, Mattos CT, Simão RA, de Oliveira Ruellas AC. Coating stability and surface characteristics of esthetic orthodontic coated archwires. *Angle Orthod.* 2013;83:994-1001.^c

Doshi UH, Bhad-Patil WA. Static frictional force and surface roughness of various bracket and wire combinations. *Am J Orthod Dentofacial Orthop.* 2011;139:74-9.

Downing A, McCabe J, Gordon P. A study of frictional forces between orthodontic brackets and archwires. *Br J Orthod.* 1994;21:349-57.

Drake SR, Wayne DM, Powers JM, Asgar K. Mechanical properties of orthodontic wires in tension, bending, and torsion. *Am J Orthod.* 1982;82:206-10.

Elayyan F, Silikas N, Bearn D. Ex vivo surface and mechanical properties of coated orthodontic archwires. *Eur J Orthod.* 2008;30:661-7.

Elayyan F, Silikas N, Bearn D. Mechanical properties of coated superelastic archwires in conventional and selfligating orthodontic brackets. *Am J Orthod Dentofacial Orthop.* 2010;137:213-17.

Eliades T, Bourauel C. Intraoral aging of orthodontic materials: the picture we miss and its clinical relevance. *Am J Orthod Dentofacial Orthop.* 2005;127:403-12.

Eliades T, Eliades G, Athanasiou AE, Bradley TG. Surface characterization of retrieved NiTi orthodontic archwires. *Eur J Orthod.* 2000;22:317-26.

Eliades T, Eliades G, Watts DC. Structural conformation of in vitro and in vivo-aged orthodontic elastomeric modules. *Eur J Orthod.* 1999;6:649-58.

Eliades T. Orthodontic materials research and applications: part 2. Current status and projected future developments in materials and biocompatibility. *Am J Orthod Dentofacial Orthop.* 2007;31:253-62.

Es-Souni M, Es-Souni M, Fischer-Brandies H. On the properties of two binary NiTi shape memory alloys. Effects of surface finish on the corrosion behavior and in vitro biocompatibility. *Biomaterials.* 2002;23:2887-94.

Farronato G, Maijer R, Caria MP, Esposito L, Alberzoni D, Cacciatore G. The effect of Teflon coating on the resistance to sliding of orthodontic archwires. *Eur J Orthod.* 2012;34:410-7.

- Filho HL, Maia LH, Araújo MV, Eliast CN, Ruellas AC. Colour stability of aesthetic brackets: ceramic and plastic. *Aust Orthod J*. 2013.
- Fillmore GM, Tomlinson JL. Heat treatment of cobalt-chromium alloys of various tempers. *Angle Orthod*. 1979;49:126-30.
- Frank CA, Nikolai RJ. A comparative study of frictional resistances between orthodontic bracket and arch wire. *Am J Orthod*. 1980;78:593-609.
- Ghafari J. Problems associated with ceramic brackets suggest limiting use on selected teeth. *Angle Orthod*. 1992;62:145-52.
- Goldberg AJ, Burstone CJ. Status report on beta-titanium orthodontic wires. Council on Dental Materials, Instruments and Equipment. *J Am Dent Assoc*, 1982;684-5.
- Goldberg AJ, Burstone CJ. The use of continuous fiber reinforcement in dentistry. *Dent Mater*. 1992;8:197-202.
- Goldberg AJ, Liebler SA, Burstone CJ. Viscoelastic properties of an aesthetic translucent orthodontic wire. *Eur J Orthod*. 2011;33:673-8.
- Hammad SM, Al-Wakeel EE, Gad el-S. Mechanical properties and surface characterization of translucent composite wire following topical fluoride treatment. *Angle Orthod*. 2012;82:8-13.
- Hiroce M, Fernandes DJ, Elias CN, Miguel JA. Sliding resistance of polycarbonate self-ligating brackets and stainless steel esthetic archwires. *Prog Orthod*. 2012;13:148-53.
- Huang HH. Variation in corrosion resistance of nickeltitanium wires from different manufacturers. *Angle Orthod*. 2005;75:661-5.
- Huang HH. Variation in surface topography of different NiTi orthodontic archwires in various commercial fluoridecontaining environments. *Dent Mater*. 2007;23:24-33.
- Huang ZM, Gopal R, Fujihara K, Ramakrishna S, Loh PL, Foong WC, Ganesh VK, Chew CL. Fabrication of a new composite orthodontic archwire and validation by a bridging micromechanics model. *Biomaterials*. 2003;24:2941-53.
- Hunt NP, Cunningham SJ, Golden CG, Sheriff M. An investigation into the effects of polishing on surface hardness and corrosion of orthodontic archwires. *Angle Orthod*. 1999;69:433-40.
- Husmann P, Bourauel C, Wessinger M, Jäger A. The frictional behavior of coated guiding archwires. *J Orofac Orthop*. 2002;63:199-211.

- Iijima M, Muguruma T, Brantley W, Choe HC, Nakagaki S, Alapati SB, Mizoguchi I. Effect of coating on properties of esthetic orthodontic nickel-titanium wires. *Angle Orthod.* 2012;82:319-25.
- Iijima M, Yuasa T, Endo K, Muguruma T, Ohno H, Mizoguchi. Corrosion behavior of ion implanted nickel-titanium orthodontic wire in fluoride mouth rinse solutions. *Dent Mater J.* 2010;29:53-58.
- Iwasaki LW, Beatty MW, Nickel JC. Friction and Orthodontic Mechanics: Clinical Studies of Moment and Ligation Effects. *Semin Orthod.* 2003;9:290-7.
- Jang TH, Kim SC, Cho JH, Chae JM, Chang NY, Kang KH. The comparison of the frictional force by the type and angle of orthodontic bracket and the coated or non-coated feature of archwire *Korean J Orthod.* 2011;41:399-410
- Jastrebki ZB. *The Nature and Properties of Engineering Materials*, 3rd ed. New York, NY: Wiley; 1987.
- Kakaboura A, Fragouli M, Rahiotis C, Silikas N. Evaluation of surface characteristics of dental composites using profilometry, scanning electron, atomic force microscopy and gloss-meter. *J Mater Sci Mater Med.* 2007;18:155-63.
- Kaphoor AA, Sundareswaran S. Aesthetic nickel titanium wires--how much do they deliver? *Eur J Orthod.* 2012;34:603-9.
- Kapila S, Sachdeva R. Mechanical properties and clinical applications of orthodontic wires. *Am J Orthod Dentofacial Orthop.* 1989;96:100-09.
- Katić V, Curković HO, Semenski D, Baršić G, Marušić K, Spalj S. Influence of surface layer on mechanical and corrosion properties of nickel-titanium orthodontic wires. *Angle Orthod.* 2014. doi: 10.2319/090413-651.1
- Kim H, Johnson JW. Corrosion of stainless steel, nickel-titanium, coated nickel-titanium, and titanium orthodontic wires. *Angle Orthod.* 1999;69:39-44.
- Krim J, Heyvaert II, Van Haesendonck C, Bruynseraede Y. Scanning tunnelling microscopy observation of self-affine fractal roughness in ion-bombarded film surfaces. *Phys Rev Lett.* 1993;70:57-60.
- Krishnan M, Saraswathy S, Sukumaran K, Abraham KM. Effect of ion-implantation on surface characteristics of nickel titanium and titanium molybdenum alloy arch wires. *Indian J Dent Res.* 2013;24:411-7.

Krishnan M, Seema S, Kumar AV, Varthini NP, Sukumaran K, Pawar VR, Arora V. Corrosion resistance of surface modified nickel titanium archwires. *Angle Orthod.* 2014;84:358-67.

Krishnan V, Kumar KJ. Mechanical properties and surface characteristics of three archwire alloys. *Angle Orthod.* 2004; 74:825-31.

Kusy RP, Whitley JQ, de Araújo Gurgel J. Comparisons of surface roughnesses and sliding resistances of 6 titanium based or TMA-type archwires. *Am J Orthod Dentofacial Orthop.* 2004;126:589-603.

Kusy RP, Whitley JQ, Mayhew MJ, Buckthal JE. Surface roughness of orthodontic archwires via laser spectroscopy. *Angle Orthod.* 1988;58:33-45.

Kusy RP, Whitley JQ, Prewitt MJ. Comparison of the frictional coefficients for selected archwire-bracket slot combinations in the dry and wet states. *Angle Orthod.* 1991;61:293-302.

Kusy RP, Whitley JQ. Coefficients of friction for arch wires in stainless steel and polycrystalline alumina bracket slots. I. The dry state. *Am J Orthod Dentofacial Orthop.* 1990;98:300-12..

Kusy RP, Whitley JQ. Friction between different wirebracket configurations and materials. *Semin Orthod.* 1997; 3:166-77.

Kusy RP, Whitley JQ. Influence of archwire and bracket dimensions on sliding mechanics: derivations and determinations of the critical contact angles for binding. *Eur J Orthod.* 1999;21:199-208.

Kusy RP, Whitley JQ. Resistance to sliding of orthodontic appliances in the dry and wet states: influence of archwire alloy, interbracket distance, and bracket engagement. *J Biomed Mater Res.* 2000;52:797-811.

Kusy RP. A review of contemporary archwires: their properties and characteristics. *Angle Orthod.* 1997;67:197-207.

Lee GJ, Park KH, Park YG, Park HK. A quantitative AFM analysis of nano-scale surface roughness in various orthodontic brackets. *Micron.* 2010;41:775-82.

Matarese G, Nucera R, Militi A, et al. Evaluation of frictional forces during dental alignment: an experimental model with 3 nonleveled brackets. *Am J Orthod Dentofacial Orthop.* 2008;133:708-15.

Murayama M, Namura Y, Tamura T, Iwai H, Shimizu N. Relationship between friction force and orthodontic force at the leveling stage using a coated wire. *J Appl Oral Sci.* 2013;21:554-9.

- Nakano H, Satoh K, Norris R, Jin T, Kamegai T, Ishikawa F, Katsura H. Mechanical properties of several nickel-titanium alloy wires in three-point bending tests. *Am J Orthod Dentofacial Orthop.* 1999;115:390-5.
- Nanda RS. *Biomechanics and Esthetic Strategies in Clinical Orthodontics.* St Louis, Mo: Elsevier; 2005.
- Nelson KR, Burstone CJ, Goldberg AJ. Optimal welding of beta titanium orthodontic wires. *Am J Orthod Dentofacial Orthop.* 1987;92:213-9.
- Neumann P, Bourauel C, Jäger A. Corrosion and permanent fracture resistance of coated and conventional orthodontic wires. *J Mater Sci Mater Med.* 2002;13:141-7.
- Normando D, de Araújo AM, Marques Ida S, Barroso Tavares Dias CG, Miguel JA. Archwire cleaning after intraoral ageing: the effects on debris, roughness, and friction. *Eur J Orthod.* 2013;35:223-9.
- Ohtonen J, Vallittu PK, Lassila LV. Effect of monomer composition of polymer matrix on flexural properties of glass fibre-reinforced orthodontic archwire. *Eur J Orthod.* 2013;35:110-4.
- Patir N, Cheng HS. An average flow model for determining effects of three-dimensional roughness on partial hydrodynamic lubrication. *J. Tribol.* 1978;100:12-7
- Persson BNJ, Albohr O, Tartaglino U, Volokitin AI, Tosatti E. On the nature of surface roughness with application to contact mechanics, sealing, rubber friction and adhesion. *J Phys Condens Matter.* 2005;17:R1-R62.
- Persson BNJ, Tosatti E. *Physics of Sliding Friction.* Kluwer, Dordrecht; 1996
- Persson BNJ, Tosatti E. Theory of friction: elastic coherence length and earthquake dynamics. *Solid State Communications.* 1999;109:739-44
- Persson BNJ. *Sliding Friction: Physical Principles and Applications.* Number 2nd Edition. Springer, Heidelberg; 2000.
- Picton DCA Some implications of normal tooth mobility during mastication. *Arch Oral Biol* 1964;9:565-73
- Postlethwaite KM. Advances in fixed appliance design and use: 1. Brackets and archwires. *Dent Update.* 1992;19:276-80.
- Proffit WR, Fields HW, Sarver DM. *Contemporary Orthodontics.* 5th ed. St. Louis, Mo: Mosby Elsevier; 2012.

Prososki RR, Bagby MD, Erickson LC. Friction and roughness of nickel-titanium arch wires. *Am J Orthod Dentofacial Orthop.* 1991;100:341-38.

Rabinowicz E. Friction and wear of materials. 2nd Ed. New York, NY Wiley; 1995.

Rongo R, Ametrano G, Gloria A, Spagnuolo G, Galeotti A, Paduano S, Valletta R, D'Antò V. Effects of intraoral aging on surface properties of coated nickel-titanium archwires. *Angle Orthod.* 2013. doi: 10.2319/081213-593.1

Rossouw PE, Kamelchuk LS, Kusy RP. A fundamental review of variables associated with low velocity frictional dynamics. *Semin Orthod.* 2003;9:223-35.

Rossouw PE. Friction: an overview. *Semin Orthod.* 2003;9: 218-22.

Russell JS. Aesthetic orthodontic brackets. *J Orthod.* 2005 Jun;32(2):146-63.

Saunders CR, Kusy RP. Surface topography and frictional characteristics of ceramic brackets. *Am J Orthod Dentofacial Orthop.* 1994;106:76-87.

Shinjo K, Hirano M. Dynamics of friction: superlubric state. *Surf. Sci.* 1993;283.1: 473-8

Silikas N, Lennie AR, England KER, Watts DC. AFM as a tool in dental research. *Microsc Analysis.* 2001;82:19-21.

Spagnuolo G, Ametrano G, D'Anto` V, et al. Effect of autoclaving on the surfaces of TiN-coated and conventional nickel-titanium rotary instruments. *Int Endod J.* 2012;45:1148-55.

Sridharan K, Anders S, Nastasi M, Walter KC, Anders A, Monterio OR, Ensinger W. Nonsemiconductor application of PIII&D. In: Anders A, (ed.) *Handbook of Plasma Immersion Ion Implantation and Deposition.* Weinheim, Wiley-VCH; 2004.

Thierry B, Tabrizian M, Trepanier C, Savadogo O, Yahia L. Effect of surface treatment and sterilization processes on the corrosion behaviour of NiTi shape memory alloy. *J Biomed Mater Res* 2000;51:685-93.

Thorstenson GA, Kusy RP. Effects of ligation type and method on the resistance to sliding of novel orthodontic brackets with second-order angulation in the dry and wet states. *Angle Orthod.* 2003;73:418-30.

Tselepis M, Brockhurst P, West VC. Frictional resistance between brackets and archwires. *Am J Orthod Dentofacial Orthop.* 1994;106:131-8.

Vaughan JL, Duncanson Jr MG, Nanda RS, Currier GF. Relative kinetic frictional forces between

sintered stainless steel brackets and orthodontic wires. *Am J Orthod Dentofac Orthop* 1995;107:20-7.

Volokitin AI, Persson BNJ. Near-field radiative heat transfer and noncontact friction. *Rev. Mod. Phys.* 2007;79:1291-329.

Vorburger TV, Teague EC. Optical techniques for online measurement of surface topography. *Precision Eng.* 1981;3:61-83.

Walton DK, Fields HW, Johnston WM, Rosenstiel SF, Firestone AR, Christensen JC. Orthodontic appliance preferences of children and adolescents. *Am J Orthod Dentofacial Orthop.* 2010;138:698.e1-12.

Watanabe I, Watanabe E. Surface changes induced by fluoride prophylactic agents on titanium-based orthodontic wires. *Am J Orthod Dentofacial Orthop.* 2003;123:653-6.

Wennerberg A, Ohlsson R, Ros'en BG, Andersson B. Characterizing three-dimensional topography of engineering and biomaterial surfaces by confocal laser scanning and stylus techniques. *Med Eng Phys.* 1996;18:548-56.

Whitley JQ, Kusy RP. Influence of interbracket distances on the resistance to sliding of orthodontic appliances. *Am J Orthod Dentofacial Orthop.* 2007;132:360-72.

Wichelhaus A, Geserick A, Hibst R, Sander FG. The effect of surface treatment and clinical use on friction in NiTi orthodontic wires. *Dent Mater.* 2005;21:938-45.

Wichelhaus A, Sander FG, Hempowitz H. The transformation behaviour of wires in elastic and plastic range in dependence upon temperature-treatment. In: Pelton AR, Hodgson D, Duerig T; Proceedings of the international conference on shape memory and superelastic technologies. editors. SMST-97; 1997.

Williams JK, Cook PA, Isaacson KG and Thom AR. *Fixed Orthodontic Appliances: Principles and Practice.* Oxford; Boston: Wright; 1995.

Yang C, Tartaglino U, Persson BNJ. Influence of surface roughness on super- hydrophobicity, *Phys. Rev. Lett.* 2006;97:116103.

Zegan G, Sodor A, Munteanu C. Surface characteristics of retrieved coated and nickel-titanium orthodontic archwires. *Rom J Morphol Embryol.* 2012;53:935-9.

Ziuchkovski JP, Fields HW, Johnston WM, Lindsey DT. Assessment of perceived orthodontic appliance attractiveness. *Am J Orthod Dentofacial Orthop.* 2008;133:S68-78.

Zufall SW, Kennedy KC, Kusy RP. Frictional characteristics of composite orthodontic archwires against stainless steel and ceramic brackets in the passive and active configurations. *J Mater Sci Mater Med.* 1998;9:611-20.

Zufall SW, Kusy RP. Stress relaxation and recovery behaviour of composite orthodontic archwires in bending. *Eur J Orthod.* 2000;22:1-12.^a

Zufall SW, Kusy RP. Sliding mechanics of coated composite wires and the development of an engineering model for binding. *Angle Orthod.* 2000;70:34-47.^b

Curriculum Vitae



Personal information

Surname(s) / First name(s) **Rongo Roberto**
Address(es) Via Kennedy 18, San Nicola la Strada (CE), 81020 ITALY
Telephone(s) 0039-0823423553 Mobile: 0039-3349494549
0039-3282465618
Fax(es) 0039-0823423553
E-mail roberto.rongo@gmail.com
Nationality Italian
Date of birth 25-01-1987
Gender M

Occupational field **Dentistry, Orthodontics, Research**

Education and training

Dates 2011 Master at University of Naples "Federico II" Faculty of Medicine and Surgery in "New approaches in contemporary orthodontics"
2011 PhD students in Oral Sciences at University of Naples "Federico II"
2010 License to Practice Dentistry
2005-2010 Degree in Dentistry at University of Naples "Federico II" Faculty of Medicine and Surgery
Grade 110/110 cum Laude
Thesis: "The surface roughness of orthodontic wires after clinical use" (October 2010)

Personal skills and competences

Establishing collaborative relationships and projects, Able to work well in teams, Self-motivated, Able to work under tight deadlines, Able to network effectively

Mother tongue(s) **Italian**

Other language(s)

Self-assessment
European level (*)

English
Spanish

Understanding				Speaking				Writing	
Listening		Reading		Spoken interaction		Spoken production			
	B2		C2		B2		B2		B2
	C1		C1		B2		B2		A2

(*) Common European Framework of Reference for Languages

Annexes Papers:

1. Michelotti A., Cioffi I, **Rongo R**, Borrelli R, Chiodini P, Svensson P.
EFFECTS OF MUSCLE PAIN INDUCED BY GLUTAMATE INJECTIONS DURING SUSTAINED CLENCHING ON THE CONTRACTION PATTERN OF MASTICATORY MUSCLES
J Orofac Pain. Accepted.
2. **Rongo R**, Antoun JS, Lim YX, Dias G, Valletta R, Farella M.
THREE-DIMENSIONAL EVALUATION OF THE RELATIONSHIP BETWEEN JAW DIVERGENCE AND FACIAL SOFT TISSUE DIMENSIONS.
Angle Orthod. 2014 Feb 21. doi 10.2319/092313-699.1
3. **Rongo R**, Ametrano G, Gloria A, Spagnuolo G, Galeotti A, Paduano S, Valletta R, D'Antò V.
EFFECTS OF INTRAORAL AGING ON SURFACE PROPERTIES OF COATED NICKEL-TITANIUM ARCHWIRES.
Angle Orthod. 2013 Dec 5 doi 10.2319/081213-593.1
4. D'Antò V, **Rongo R**, Valletta R, Martina R
BONDAGGIO CON I SISTEMI ADESIVI EAGLE: RISULTATI DI 5 ANNI DI RICERCA
Professione Ortodonzia 2013
5. D'Antò V, **Rongo R**, Ametrano G, Spagnuolo G, Manzo P, Martina R, Paduano S, Valletta R.
EVALUATION OF SURFACE ROUGHNESS OF ORTHODONTIC WIRES BY MEANS OF ATOMIC FORCE MICROSCOPY.
Angle Orthod. 2012;82:922-8.
6. Valletta R, D'Antò V, Manzo P, **Rongo R**.
VARIAZIONE DELLA RUGOSITÀ DEI FILI ESTETICI IN SEGUITO ALL'UTILIZZO CLINICO
Professione Ortodonzia 2011

Oral Communications:

1. **Rongo R.**, Michelotti A., Farella M.
VALUTAZIONE TRIDIMENSIONALE DELLA DIVERGENZA MANDIBOLARE: ANALISI DEI TESSUTI MOLLI
International meeting SIDO 2014 Torino
2. D'Antò V., Bucci R., **Rongo R**.
CLASS II ORTHOPEDIC TREATMENT: QUALITY ASSESSMENT OF SYSTEMATIC REVIEWS
International Congress SIDO 2013 Roma
3. **Rongo R.**, Manfredonia A., D'Antò V.
REPRODUCIBILITY OF CERVICAL VERTEBRAE MATURATION METHOD
International Congress SIDO 2013 Roma
4. **Rongo R**, D'Albenzio L, Antoun JS
THREE-DIMENSIONAL EVALUATION OF THE RELATIONSHIP BETWEEN JAW DIVERGENCE AND TRANSVERSAL CRANIOFACIAL TRAITS
International Congress SIDO 2012 Firenze
5. **Rongo R**, Paduano S, Manzo P, Galeotti A, Valletta R, D'Antò V
COMPARISON OF MECHANICAL FEATURES AND SURFACES MODIFICATIONS OF RETRIEVED ESTHETIC AND METALLIC NITI ARCHWIRES
International Congress SIDO 2012 Firenze

Annexes

6. **Rongo R**
OPZIONI ESTETICHE DI TRATTAMENTO IN ORTODONZIA VESTIBOLARE
Formazione Straight Wire Advancement In Orthodontics 2012 Roma
7. **Rongo R, Cioffi A, Valletta R**
EVALUATION OF THE PSYCHOSOCIAL IMPACT OF DENTAL AESTHETIC DUE TO
MALOCCLUSION/ORTHODONTIC TREATMENT NEED, ON QUALITY OF LIFE
International Congress SIDO 2011 Roma
8. **Rongo R, Borrelli R, D'Antò V**
HOW CAN WE EVALUATE THE IMPACT OF DENTAL AESTHETICS
International Congress SIDO 2011 Roma
9. **Rongo R, Valletta R**
RETRIEVED NITI ORTHODONTIC ARCHWIRES BY ATOMIC FORCE MICROSCOPY
(AFM)
International Congress SIDO 2010 Firenze

Poster

1. **Rongo R, Lim, YX Antoun, J.S. Dias, G. Farella, M.**
EVALUATING THE EFFECT OF JAW DIVERGENCE ON THE FACE'S TRANSVERSAL
DIMENSIONS
International Congress EOS 2013 Reykjavik
2. **Rongo R, Lim, YX Antoun, J.S. Dias, G. Farella, M.**
SOFT TISSUE ANALYSIS OF JAW DIVERGENCE USING THREE-DIMENSIONAL
IMAGING
International Congress EOS 2013 Reykjavik
3. Michelotti M, Cioffi I, Borrelli R, **Rongo R**, Chiodini P, Svensson P
INFLUENCE OF GLUTAMATE ON MASTICATORY MUSCLES DURING LOW-LEVEL
SUSTAINED CLENCHING
IADR/AADR/CADR General Session and Exhibition 2013 Seattle
4. **Rongo R, Antoun Js, Farella M**
THREE DIMENSIONAL IMAGING OF SOFT TISSUE TO ANALYSE JAW DIVERGENCE
International meeting SIDO SICOI 2013 Roma Winner Fifth SIDO SICOI price
5. Cioffi A, **Rongo R**, D'Antò V, Martina S, Valletta R,
RELATIONSHIP BETWEEN MALOCCLUSION/ORTHODONTIC TREATMENT NEED AND
ORAL HEALTH RELATED QUALITY OF LIFE
International Congress EOS 2012 Santiago de Compostela
6. **Rongo R, Cioffi A, Paduano S, Franzese G, Valletta R,**
HOW CAN WE ASSESS THE IMPACT OF DENTAL APPEARANCE ON
MALOCCLUSION/ORTHODONTIC TREATMENT NEED
International Congress EOS 2012 Santiago de Compostela
7. **Rongo R, D'Antò V, Cioffi A, Martina S, Valletta R,**
QUALITY OF LIFE IN PATIENTS REQUIRING ORTHODONTIC TREATMENT
International Congress EOS 2012 Santiago de Compostela

Annexes

8. Turco C, **Rongo R**, D'Antò V
VALUTAZIONE DELLE PROPRIETÀ MECCANICHE DI UN DISPOSITIVO ORTOPEDICO-FUNZIONALE: FORSUS FDR.
International Congress SIDO 2011 Roma
9. Borrelli R, Cioffi A, **Rongo R**
RIPRODUCIBILITÀ NELLA VALUTAZIONE DEI SEGNI DI BJÖRK DELLA STRUTTURA MANDIBOLARE
International Congress SIDO 2011 Roma
10. Manzo P, **Rongo R**, D'Antò V, Martina R, Valletta R
ATOMIC FORCE MICROSCOPY (AFM) EVALUATION OF SURFACE ROUGHNESS OF NEW AND RETRIEVED NITI ORTHODONTIC ARCHWIRES.
International Congress EOS 2011 Istanbul
11. D'Antò V, **Rongo R**, Pace M, Manzo P, Valletta R
VALUTAZIONE DEL CAMBIAMENTO DELLA RUGOSITÀ SUPERFICIALE DI ARCHI ESTETICI IN NITI DOPO L'UTILIZZO CLINICO
Simposio delle Scuole ortodontiche 2011 Taormina
12. D'Antò V, **Rongo R**, Panariello G, Manzo P, Valletta R
UTILIZZO DELLA MICROSCOPIA A FORZA ATOMICA (AFM) PER L'ANALISI DELLA RUGOSITA' SUPERFICIALE DEGLI ARCHI ORTODONTICI
Simposio delle Scuole ortodontiche 2011Taormina